Efficient Spectrum Sharing Techniques in Cognitive Radio Network for Full-Duplex Communication

Thesis submitted
by
DIPAK SAMANTA

Doctor of Philosophy (Engineering)

Department of Instrumentation and Electronics Engineering
Faculty Council of Engineering and Technology
Jadavpur University
Kolkata, India
2025

JADAVPUR UNIVERSITY
KOLKATA - 700 032, INDIA

INDEX NO. 85/22/E

Title of the Thesis:

Efficient Spectrum Sharing Techniques in Cognitive Radio Network for Full-Duplex Communication

Name, Designation and Institution of the Supervisors:

1. Dr. Abhijit Chandra
Associate Professor
Department of IEE, Jadavpur University
Sector III, Block LB, Plot No. 8, Saltlake City, Saltlake Bypass, Kolkata-700106

2. Dr. Chanchal Kumar De
Professor
Department of ECE, Haldia Institute of Technology
ICARE, Hatiberia, Haldia, Purba Medinipur, West Bengal, 721657

INDEX NO. 85/22/E

List of Publications

International Journals:

1. **D. Samanta**, J.K. Bag, C.K. De and A. Chandra, "A smart spectrum utilization approach using multiantenna-based cognitive relays in cognitive radio network" *International Journal of Communication Systems*,34,1,e4671,2021,Wiley Online Library. [link]

2. **D. Samanta**, C.K. De and A. Chandra, "Performance analysis of full-duplex multirelaying energy harvesting scheme in presence of multiuser cognitive radio network" *IEEE Transactions on Green Communications and Networking*, 7,2,626–634,2022. [link]

3. **D. Samanta**, C.K. De and A. Chandra, "Performance analysis of NOMA based hybrid cognitive radio network assist by full-duplex relay" *Telecommunication Systems*, 88,1,37,2025. [link]

4. **D. Samanta**, C.K. De and A. Chandra, "Performance Analysis of Full Duplex Relay based Cognitive Radio Assisted by IRS network" *communicated to Wireless Networks*. [link]

List of Presentations in International Conference :

1. **D. Samanta**, J.K. Bag, C.K. De and A. Chandra, "Performance Analysis of Energy Harvesting-Based Relay-Assisted CR Network Under Co-channel Interference Environment" Proc. *4^{th} International Conference on Communication, Devices and Computing (ICCDC)*, Haldia Institute of Technology, West Bengal, India, 685–705, 2023. [link]

2. **D. Samanta**, C.K. De and A. Chandra, "Performance Analysis of Energy Harvesting-Based CR Network Assisted by Full-Duplex Relays Under Joint Underlay/Overlay Mode" Proc. *4^{th} International Conference on Communication, Devices and Computing (ICCDC)*, Haldia Institute of Technology, West Bengal, India, 617–631, 2023. [link]

3. **D. Samanta**, J.K. Bag, C.K. De and A. Chandra, "Performance Analysis of Full-Duplex Relay aided Multi-Primary CR Network under Non-linear Energy-Harvesting Environment" Proc. *2024 IEEE Calcutta Conference (CALCON)*, Jadavpur University, Kolkata, West Bengal, India, 1–6, 2024. [link]

PROFORMA - 1

"Statement of Originality"

I, Dipak Samanta registered on 6^{th} May, 2022, do hereby declare that the thesis entitled "Efficient Spectrum Sharing Techniques in Cognitive Radio Network for Full-Duplex Communication" contains literature survey and original research work done by the undersigned candidate as part of Doctoral studies.

All information in this thesis have been obtained and presented in accordance with existing academic rules and ethical conduct. I declare that, as required by these rules and conduct, I have fully cited and referred all materials and results that are not original to this work.

I also declare that I have checked this thesis as per the "Policy on Anti Plagiarism, Jadavpur University, 2025", and the level of similarity as checked by iThenticate software is 3%.

Signature of Candidate: Dipak Samanta.
Date : 05/12/25

Certified by Supervisor(s):
(Signature with date, seal)

1. Abhijit Chandra 05/12/2025
Associate Professor
Dept. of Inst. & Electronics Engg.
Jadavpur University
Salt Lake Campus
Kolkata-106

2. Chanchal Kumar De 5/12/2025
Prof. (Dr.) Chanchal Kumar De
Head of the Department
Electronics & Communication Engineering
Haldia Institute of Technology, Haldia-721657

PROFORMA- 2

CERTIFICATE FROM THE SUPERVISOR

This is to certify that the thesis entitled "Efficient Spectrum Sharing Techniques in Cognitive Radio Network for Full-Duplex Communication" submitted by Shri Dipak Samanta, who got his name registered on 6^{th} May, 2022 for the award of Ph. D. (Engg.) degree from Jadavpur University is absolutely based upon his own work under the supervision of Dr. Abhijit Chandra, Associate Professor, Department of IEE, Jadavpur University, and Dr. Chanchal Kumar De, Professor, Department of ECE, Haldia Institute of Technology, and that neither his thesis nor any part of the thesis has been submitted for any degree/diploma or any other academic award anywhere before.

1. Dr. Abhijit Chandra
Associate Professor
Department of IEE, Jadavpur University

Abhijit Chandra 05/12/2025

Associate Professor
Dept. of Inst. & Electronics Engg.
Jadavpur University
Salt Lake Campus
Kolkata-106

Signature of the Supervisor and date with Office Seal

2. Dr. Chanchal Kumar De
Professor
Department of ECE, Haldia Institute of Technology

Chanchal kumar De. 5/12/25

Prof. (Dr.) Chanchal Kumar De
Head of the Department
Electronics & Communication Engineering
Haldia Institute of Technology, Haldia-721657

Signature of the Co-supervisor and date with Office Seal

ACKNOWLEDGEMENTS

I am incredibly grateful to my supervisor Prof. Abhijit Chandra, Associate Professor, Department of IEE, Jadavpur University, Kolkata, West Bengal, India, and to my co-supervisor Dr. Chanchal Kumar De, Professor, Department of ECE, Haldia Institute of Technology, Haldia, West Bengal, India, for their valuable comments, suggestions and guidance throughout my research work.

I also express my heartiest graduate to other members of Research Advisory Committee (RAC), Prof. P. Venkateswaran, Professor, Dept. of ETCE, Jadavpur University, Prof. Rajani K Mudi, Professor, Dept. of IEE, Jadavpur University and Head of the Department of IEE, Jadavpur University, for their valuable advice.

I am also thankful to Haldia Institute of Technology, ICARE Complex, Hatiberia, Haldia, West Bengal, for providing me the computing facilities for carrying out my research works even on institute's holidays.

I would also like to give special thanks to Mr. Jayanta Kumar Bag and Mr. Raj Kumar Maity, both from Department of Electronics and Communication Engineering, Haldia Institute of Technology for their valuable cooperation to handle the difficulties faced during my research works.

For their editing assistance and emotional support, I am also appreciative of my colleagues at Department of ECE, Haldia Institute of Technology.

I wish to express my deepest sense of gratitude to my parents, wife, son, sister and relatives. It is their blessings that enable me to complete the task.

Finally, I would like to thank God, for letting me through all the difficulties. I have experienced your guidance day by day. You are the one who let me finish my degree. I will keep on trusting you for my future.

Dipak Samanta
05/12/25

ABSTRACT

Efficient spectrum utilization has emerged as a vital approach to address the underutilization of licensed radio frequency (RF) spectrum in modern wireless communication systems. Cognitive radio networks (CRNs), which enable dynamic spectrum sharing between primary users (PUs) and secondary users (SUs), play a pivotal role in enhancing spectral efficiency. This thesis presents a progressive exploration of multiple CRN architectures, beginning with half-duplex (HD) relay-based systems and advancing toward full-duplex (FD) relay-enabled networks. Each architecture is systematically developed to address evolving communication challenges, focusing on outage performance, throughput analysis, and energy efficiency under various practical constraints.

The investigation begins with an HD-based CRN framework employing a multi-antenna proactive decode-and-forward (DF) relay selection scheme.The architecture employs adaptive spectrum sharing through a hybrid underlay/overlay protocol, where the SU transmitter (SU-Tx) continuously monitors PU activity using energy detection. Based on the sensing outcome, SU-Tx dynamically switches between underlay and overlay modes, allowing maximization of transmission rate while protecting PU transmissions. A comparative analysis demonstrates that, under the same diversity order, increasing the number of relays yields better outage performance than increasing the number of antennas.

Expanding upon this foundation, the next development introduces energy harvesting (EH) and co-channel interference (CCI) into a multi-HD relay CRN. In this model, SU-Tx and secondary relays harvest energy from PU transmissions and ambient interference. An adaptive hybrid relay (AHR) protocol is proposed to switch between amplify-and-forward (AF) and DF relaying based on signal-to-interference-plus-noise ratio (SINR) thresholds. The impact of relay count, energy harvesting efficiency, and decoding thresholds on secondary outage probability is analyzed, showcasing the superiority of the AHR strategy over conventional AF and DF modes.

The thesis subsequently makes a transition to more advanced FD-based CRN architectures. The system model introduces a joint underlay/overlay protocol into an EH-assisted FD CRN. SU transmitters, equipped with RF energy detectors, dynamically switch transmission modes based on PU presence. Power allocation is optimized across all transmitting nodes to enhance end-to-end throughput. The model

accounts for SI and PU-induced interference, and demonstrates significant throughput improvement through the integration of FD relays and joint-mode transmission.

Continuing the exploration of FD systems, a complementary scenario is investigated involving an EH-assisted FD multi-relay network within a multi-user spectrum sharing environment. Analytical expressions for outage probability are derived, incorporating the effects of self-interference (SI) at FD relays and aggregate interference at all receivers. Power control policies are formulated for SU sources and relays. A comparative study confirms the performance gains of FD relaying over traditional HD relaying, particularly in scenarios involving multiple destinations.

Advancing further, the analysis introduces a nonlinear EH model to better mirror real-world energy harvesting behavior. Multiple FD relays support hybrid-mode communication, with SU transmitters dynamically selecting underlay or overlay modes based on sensing results. A closed-form outage analysis is presented, optimizing power allocation under comprehensive interference conditions, thereby enhancing the reliability and energy efficiency of the network.

The next proposed architecture integrates non-orthogonal multiple access (NOMA) into the hybrid FD CRN framework. A base station assisted by FD relays transmits to multiple SU destinations using NOMA principles. SU transmitters, equipped with RF energy harvesting and detection circuitry, operate adaptively in underlay or overlay modes. An analytical model is developed to derive closed-form outage probabilities under SI and imperfect successive interference cancellation (i-SIC), highlighting improvements in spectral efficiency and system throughput.

Finally, the architecture introduces an intelligent reflecting surface (IRS) to assist FD relaying in an m-Nakagami fading environment. Information is transmitted from the SU source to the destination via both an IRS and FD relay using the DF protocol. The IRS supports interference management to ensure PU protection while enhancing the received signal strength at the SU receiver. Performance comparisons reveal that IRS-assisted FD relaying provides significant gains over conventional FD setups.

This thesis presents rigorous mathematical analyses and closed-form derivations to evaluate outage probability and throughput. The progression from HD to FD relaying, integration of energy harvesting, dynamic modes, and the use of NOMA and IRS together reflect a holistic approach to improving cognitive radio performance in complex, resource-limited environments.

Contents

List of Figures

List of Tables

List of Abbreviations

5G	**Fifth Generation**
AF	**Amplify-and-Forward**
AHR	**Adaptive Hybrid Relay**
AWGN	**Additive White Gaussian Noise**
BER	**Bit Error Rate**
BS	**Base Station**
CCI	**Co-channel Interference**
CDMA	**Code Division Multiple Access**
CNOMA	**Cooperative Non-Orthogonal Multiple Access**
CR	**Cognitive Radio**
CR-NOMA	**Cognitive Radio and Non-Orthogonal Multiple Access**
CRN	**Cognitive Radio Network**
CSI	**Channel State Information**
CDF	**Cumulative Distribution Function**
D	**Destination**
D2D	**Device-to-Device**
DF	**Decode-and-Forward**
ED	**Energy Detection**
EGC	**Equal Gain Combining**
EH	**Energy Harvesting**
eMBB	**Enhanced Mobile Broadband**
FCC	**Federal Communications Commission**

FD	**Full Duplex**
FDMA	**Frequency Division Multiple Access**
GPS	**Global Positioning System**
HD	**Half Duplex**
IBFD	**In-band Full-Duplex**
IoT	**Internet of Things**
i-CSI	**Imperfect Channel State Information**
IRS	**Intelligent Reflecting Surfaces**
IRS-CRNs	**IRS-assisted Cognitive Radio Networks**
LTE	**Long Term Evolution**
mMTC	**Massive Machine Type Communications**
MIMO	**Multiple-Input Multiple-Output**
MISO	**Multiple Input Single Output**
MRC	**Maximal Ratio Combining**
NOMA	**Non-Orthogonal Multiple Access**
OFDM	**Orthogonal Frequency-Division Multiplexing**
OFDMA	**Orthogonal Frequency Division Multiple Access**
OMA	**Orthogonal Multiple Access**
OP	**Outage Performance**
PRS	**Partial Relay Selection**
PSD	**Power Spectral Density**
PU	**Primary User**
PU-Rx	**Primary User Receiver**
QoS	**Quality of Service**
RF	**Radio Frequency**
RIS	**Reconfigurable Intelligent Surface**
RVs	**Random Variables**
SC	**Selection Combining**
SE	**Spectral Efficiency**

SIC	**Successive Interference Cancellation**
SI	**Self Interference**
SIS	**Self-Interference Suppression**
SINR	**Signal-to-Interference-plus-Noise Ratio**
SMSE	**Spectrally Modulated Spectrally Encoded**
SNR	**Signal-to-Noise Ratio**
SR	**Secondary Relay**
SU	**Secondary User**
SU-Rx	**Secondary User Receiver**
SU-Tx	**Secondary User Transmitter**
SWIPT	**Simultaneous Wireless Information and Power Transfer**
TDMA	**Time Division Multiple Access**
TSR	**Time Switching Relay / Time Switching Relaying**
UAV	**Unmanned Aerial Vehicle**
URLLC	**Ultra-Reliable Low-Latency Communications**
VFD	**Virtual Full-Duplex**

List of Symbols

$\mathrm{F_x}(\cdot)$	: Cumulative Distribution Function (CDF)
$\mathrm{f_x}(\cdot)$	: Probability Density Function (PDF)
$\mathrm{G}_{p\ q}^{m\ n}[\cdot]$	: Meijer's G function
$\Gamma(\cdot)$	: Gamma function
$\prod_{k=n}^{m} f(k)$	: Product-function
$\mathcal{N}(\cdot)$	: Normal distribution
$\sum(\cdot)$	: Summation of the all variables
H_0	: Null Hypothesis
H_1	: Alternative Hypothesis
ε	: outage constraint at primary receiver

Chapter 1

Introduction

Cognitive radio (CR) is an innovative method for dynamically accessing the radio spectrum, helping to mitigate the scarcity of available frequency spectrum caused by the surge in wireless users. The invention of the cognitive radio framework in wireless communication networks requires extensive research focused on utilizing the unused radio spectrum. The improper management of licensed spectrum plays the key role in inefficient spectrum usage. In the conventional approach, particular users are granted exclusive access to designated frequencies. In case, these licensed users do not use their assigned spectrum, others without a license are prohibited from using it, resulting in resource waste. As a result of this restrictions, a certain frequency band has traffic congestion in dynamic frequency allocation, whereas other bands operate sparingly. Cognitive radio uses the spectrum resources effectively and efficiently by allocating frequencies in a dynamic and adaptable manner to operate wireless devices across several spectra. In this regard, the CR network plays a crucial role by constantly identifying spectrum holes and choosing the appropriate frequency to prioritize client access to the spectrum. The critical role of CR is specifically described by spectrum sensing and decision-making, followed by spectrum management, sharing and allocation. CR must develop various spectrum

access strategies through suitable adaptive spectrum allocation that supports effective and efficient spectrum sharing procedures in order to evolve into more adaptable to the changing spectrum environment.

1.1 Architecture of a cognitive radio network

The demand for additional spectrum is continuously rising due to the introduction of new wireless applications, which has caused the available spectrum for communication to become overcrowded. Researchers are investigating contemporary technologies for spectrum sensing and dynamic spectrum sharing using a unique cognitive radio network strategy to address the problem of spectrum shortage.

Based on cognitive radio network (CRN) infrastructure, a basic network is divided

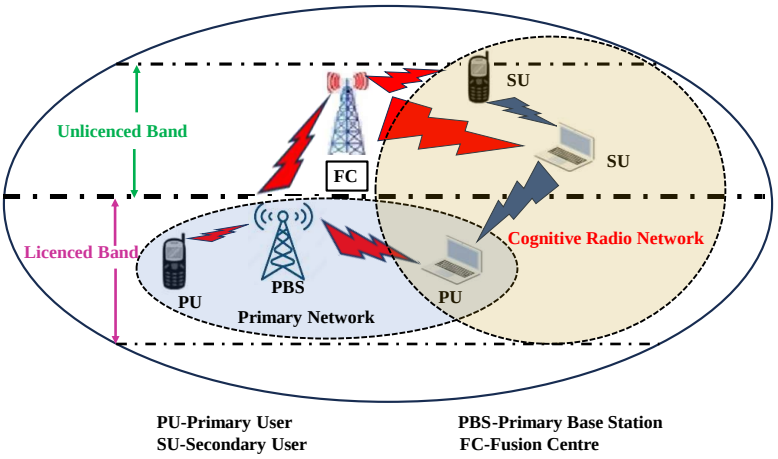

FIGURE 1.1: Basic cognitive radio network

into two groups namely, the primary network and the cognitive radio network or secondary network. A specific frequency band can only be used by the primary user. This access can only be managed by the primary base station, while other users should not interfere with it. On the other hand, secondary users, secondary base stations, and secondary relays are the elements of a cognitive radio network.

These users do not have direct access to the prime users' licensed frequency bands. Essentially cognitive radio networks (CRNs) incorporate intelligent wireless communication system protocols in which the secondary users (SUs) are provided to use the licensed channels of primary users (PUs) in an efficient manner, ensuring a better model in its approach [1].

1.2 Operational principles of cognitive radio network

With the proliferation of wireless devices and services, the demand for radio spectrum has increased tremendously. And yet, vast tracts of this precious resource lie idle due to inflexible licensing policies. That is where CRNs enter the scene. They are communication systems which can intelligently adjust to their environment and utilize available spectrum — particularly the unused gaps between licensed users. At the center of CRNs, we have five central capabilities: spectrum sensing, decision making, spectrum management, spectrum sharing, and spectrum allocation. Let's deconstruct these in a manner that is easy to understand but remains technically accurate [2].

1.2.1 Spectrum sensing

Spectrum sensing is analogous to a secondary user entering a frequency band and first performing signal detection to determine if a primary user is already transmitting before initiating its own communication. A cognitive radio "hears" the wireless world to see whether a licensed (primary) user is already occupied with a frequency. If the channel is clear — even briefly — the CR can use it.

The challenge is that it's not so simple to detect weak signals in noisy environments. Methods such as energy detection and more advanced cooperative sensing (where

several radios collaborate to make a better call) enhance accuracy. This approach is analogous to multiple nodes performing spectrum sensing collaboratively to ensure the channel is idle before initiating transmission.

Spectrum sensing is a fundamental function of cognitive radio networks. It enables secondary users (SUs) to detect unused spectrum without causing interference to primary users (PUs). Various sensing mechanisms exist, with different complexity and performance under noise, fading, and interference conditions.

1.2.1.1 Energy detection (ED)

Energy detection works by measuring the energy of the received signal and comparing it to a predefined threshold. If the energy exceeds the threshold, it is assumed that a primary user is present. Energy detection is the most widely used technique due to its simplicity and low computational requirements.

The received signal $y(t)$ is modeled as:

$$\begin{aligned} H_0 &: y(t) = n(t),\ \textit{only noise} \\ H_1 &: y(t) = s(t) + n(t),\ \textit{signal and noise} \end{aligned} \tag{1.1}$$

Here, n(t) is white Gaussian noise and s(t) is the primary user signal.

The test statistic is:

$$T = \frac{1}{N} \times \sum |y(i)|^2 \tag{1.2}$$

Compare T with a threshold λ:

If $T > \lambda$, decide in favor of H_1 (signal present)

If $T \leq \lambda$, decide in favor of H_0 (signal absent)

Advantages and disadvantages of this mechanism are as follows:

Advantages

(i) No prior knowledge of PU signal is needed.

(ii) Simple to implement in hardware.

Disadvantages

(i) Poor performance at low SNR.

(ii) Cannot differentiate between PU signal and noise/interference.

(iii) Requires accurate estimation of noise power.

1.2.1.2 Cyclostationary feature detection

Cyclostationary feature detection is a more advanced sensing technique that exploits the periodic statistical properties inherent in most modulated signals. Unlike energy detection, which treats all received energy as potentially meaningful, this method differentiates between noise and actual communication signals by identifying periodic features such as cyclic prefixes or pilot signals.

This technique works by analyzing the spectral correlation function of the received signal to detect features that occur at specific cyclic frequencies. These features are characteristic of modulated signals and can be used not only to detect the presence of a primary user but also to identify the type of modulation used. As a result, cyclostationary detection is robust in environments with high noise and interference and can operate effectively even at low SNR levels.

However, the improved performance comes at the cost of increased computational complexity and a need for partial knowledge about the signal characteristics. Implementing cyclostationary detection typically requires advanced signal processing techniques and considerable processing power, making it less suitable for lightweight or resource-constrained devices.

Cyclostationary sensing exploits periodic properties of modulated signals (e.g., cyclic redundancy in symbols). Unlike energy detection, it distinguishes PU signals from noise by detecting spectral correlation.

Advantages

(i) Robust to noise uncertainty.

(ii) Can differentiate between different signal types.

Disadvantages

(i) High computational complexity.

(ii) Requires knowledge of signal characteristics.

1.2.1.3 Matched filtering detection

Matched filtering is considered as an optimal detection technique when the primary user's signal is completely known. This method involves correlating the received signal with a known reference or template of the PU signal. The output of the correlation is maximized when the received signal matches the template, providing highly accurate detection with the shortest possible sensing time. The main advantage of matched filtering is its superior performance in terms of detection speed and accuracy, especially in scenarios where the PU signal is consistent and fully characterized. However, this method demands exact knowledge of the signal's parameters, including modulation type, pulse shape, and timing. Without such information, matched filtering becomes ineffective.

Furthermore, the high computational complexity and power consumption associated with matched filtering limit its practicality, particularly in mobile or power-sensitive applications. It is most commonly used in scenarios where the PU waveform is standardized and accessible, such as certain military or cooperative communication environments.

1.2.1.4 Wavelet-based sensing

Wavelet-based sensing is a modern technique suited for wideband spectrum environments. It utilizes wavelet transforms to analyze the power spectral density (PSD) of the received signal and detect abrupt changes or edges. These changes typically represent transitions between occupied and unoccupied frequency bands. This method does not require any prior knowledge of the primary user's signal and is particularly effective for identifying the boundaries of occupied channels in a wideband spectrum. It enables secondary users to pinpoint which segments of the spectrum are in use and which are available, thus facilitating dynamic access across large frequency ranges.

However, wavelet-based sensing is sensitive to noise and can produce false detections if the noise mimics the edge-like features of legitimate signals. Additionally, it requires high sampling rates, which may be challenging to implement with existing hardware. The complexity of the wavelet transform process also demands substantial computational resources.

Wavelet sensing is used to detect edges in power spectral density (PSD), ideal for wideband spectrum sensing. It detects spectral features without requiring prior signal knowledge.

In conclusion, each spectrum sensing method presents a trade-off between the complexity of implementation, the detection precision, the robustness of the noise and the amount of prior knowledge required about the signal of the primary user. Energy detection remains popular due to its simplicity and low cost, making it suitable for many CRN applications. However, its limitations in low SNR conditions and inability to distinguish interference from legitimate signals make it less effective in challenging environments. More sophisticated methods like cyclostationary feature detection and matched filtering offer greater accuracy but require higher computational power and more detailed knowledge of the signal. Wavelet-based sensing

provides a promising solution for wideband sensing, although its reliance on high sampling rates and sensitivity to noise pose practical challenges. In practice, hybrid approaches that combine multiple techniques are increasingly being explored to leverage the strengths and mitigate the weaknesses of individual methods. In this thesis, all spectrum sensing is carried out via an energy detection approach.

1.2.2 Decision-making

After a cognitive radio identifies the available channels, the subsequent task involves determining the most efficient way to utilize them. This entails real-time selection of the optimal frequency band, transmission power, modulation scheme, and transmission timing. The process is analogous to dynamically choosing the least congested route using a GPS system with live traffic updates.

The cognitive radio system evaluates parameters such as signal strength, user demands, interference levels, and historical performance data. The objective is to maintain seamless and continuous communication while minimizing disruption to other signals. Effective decision-making often necessitates a degree of machine learning. As the system accumulates experience, its ability to make optimal operational decisions improves over time.

1.2.3 Spectrum management

Let us visualize a highly attentive traffic controller controlling dozens of routes and vehicles — that's spectrum management in a CRN. It controls how spectrum is being utilized and makes sure everything goes smoothly. This involves monitoring which channels are available, when they're most likely to be free, and how to change channels if things change.

One of the most important aspects of this is spectrum mobility — when a primary user returns and takes back a frequency, the CR must change rapidly to a different

available channel without losing the connection. It's like lane changing smoothly when someone accelerates up behind you — it must be done fast and without any fuss.

1.2.4 Spectrum sharing

Cognitive radios do not live in a vacuum. There are other devices — primary and secondary — attempting to utilize the same airwaves. Spectrum sharing is all about ensuring everyone receives their fair portion without stomping on each other's signals.
There are primarily two methods available for spectrum sharing, namely

(i) Overlay sharing: where CRs occupy only the unused channels.

(ii) Underlay sharing: where they send at very low power, even if someone else is already occupying the band.

To make this possible, CRNs apply clever coordination techniques — sometimes centralized (like a control tower) and sometimes distributed (like self-gathering crowds). The aim is to prevent conflicts and ensure that everybody may use the spectrum without interfering.

1.2.5 Spectrum allocation

This is where decisions are made regarding who can utilize what slice of spectrum and for how long. It's an instantaneous process that has to balance a variety of factors such as available channels, user demand, fairness, interference avoidance, and quality of service. In a static universe, this would be done once and never remembered. But in CRNs, circumstances are always shifting. So, allocation must be adaptive and accommodating. At times, a centralized authority does it; at times,

devices allocate autonomously. Either way, intelligent algorithms (even machine learning) can provide predictions of future use and better allocations with the passage of time.

Cognitive radio networks (CRNs) are all about smarter but not harder, use of spectrum. They listen first and then speak, they adjust to evolving conditions, and they make smart decisions that legacy networks just can't. By integrating spectrum sensing, real-time decision-making, smart management, cooperative sharing, and adaptive allocation, CRNs are revolutionizing the paradigm of wireless communication. In a world where spectrum is valuable and demand continues to rise, CRNs are like the resourceful multitaskers who ensure each ounce of available airspace is utilized efficiently without being disruptive.

1.3 Hierarchical usage in cognitive radio network

Sensing activity performed by secondary networks is the backbone of dynamic spectrum management, access, and sharing policies in the cognitive radio network. Spectrum sensing enables the identification of vacant frequency bands, and the subsequent processes of appropriate selection and dynamic allocation to users are categorized into three main prototypes. As discussed earlier, various users enjoy different priorities based on their spectrum license agreement policies. The spectrum owner, sometimes referred to as the primary users, is granted the highest level of priority to access the spectrum. Secondary users, also known as unlicensed users, can then opportunistically use the spectrum of licensed users.

Cognitive radio, which enables SUs to access the licensed frequency band occupied by the PUs in an opportunistic or collaborative manner while protecting the PUs' quality of service, also provides an efficient use of the wireless spectrum [3]. CRNs are generally classified into three spectrum access paradigms on the basis of information transmission viz. underlay, overlay and joint underlay/overlay modes.

1.3.1 Underlay mode of cognitive radio network

In underlay mode of communication, as long as they do not significantly interfere with the primary users, unlicensed secondary users are permitted to transmit jointly with licensed primary users. Both primary and secondary users share the same spectrum. Monitoring is done on the channel gain between the primary receiver and the secondary transmitter. In an underlay CR network, SUs are permitted to utilise the busy PU's spectrum with the requirement that the PU's quality of service be preserved by controlling the SU's transmission power below a set threshold or interference temperature [1]. There is an interference temperature limit that limits the secondary user's transmission. Underlay condition can be described as [4]:

$$P_{su} h_{ps} \leq I_{th} \tag{1.3}$$

where, P_{su} stands for transmit power of secondary user, h_{ps} is channel gain from secondary transmitter to primary receiver, I_{th} is interference threshold at the primary receiver.

1.3.2 Overlay mode of cognitive radio network

The overlay mode, sometimes called opportunistic spectrum access, is a CRN operating mode in which secondary users are only permitted to transmit when the primary users, or licensed users, are not using the spectrum. To put it simple, secondary users keep track on the spectrum and make use of unused channels without interfering with primary ones. In overlay mode, the secondary source is allowed only to transmit with the maximum transmit power when the primary user is idle [1]. After sensing the primary users in inactive mode, their is an opportunity on transmit power by the secondary users to transmit information at its desired power.

1.3.3 Joint underlay/overlay mode of cognitive radio network

In contrast to overlay mode, where SUs' transmit power is maximized only during spectrum gaps, underlay operation limits SUs' transmit power by a threshold value to preserve the quality of service of PUs. Each has its own limitations in both situations. A joint underlay/overlay mode combines both these features to increase performance and flexibility.

Joint underlay/overlay mode works on the principle of adaptive switching designed

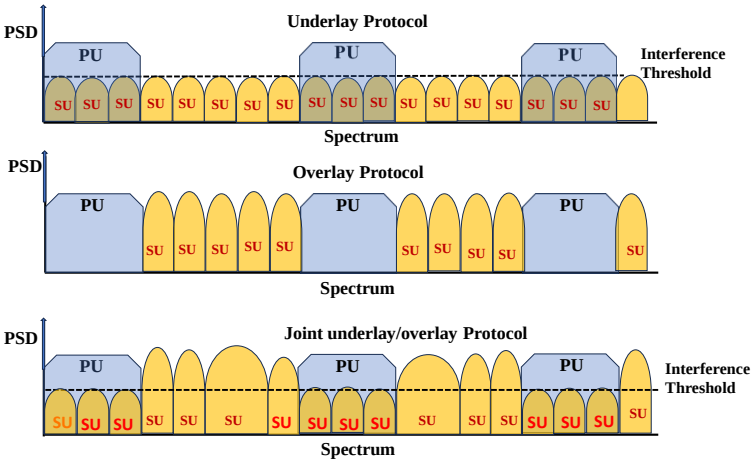

FIGURE 1.2: Underlay, overlay and joint underlay/overlay in cognitive radio network

at secondary user where simultaneous swapping between underlay and overlay mode is decided by SU, which senses the availability of PU information through sensing mechanism. After sensing, if the PU is found busy, SU activates its power restriction mode (i.e., underlay); otherwise, SU operates with its maximum power (i.e., overlay) mode. This thesis highlights the advantages of this opportunistic spectrum use, which include enhanced secondary network throughput performance and maximum spectrum utilization.

1.4 Introduction to relay communication in cognitive radio network

The primary goal of wireless communication is to achieve higher transmission rates with wide coverage, but this is challenged by factors such as attenuation, fading, and shadowing effects. The issue caused by the fading/shadowing effect is resolved by the usage of cooperative relay communication. In order to send an independent duplicate of the same signal, cooperative relay communication requires both the direct source-destination connection and the relay to destination. A total of K+1 copies of the transmitted signal will be received at the destination if a cooperative relay network has K relays.

A secondary transmitter and secondary receiver communicate with each other with

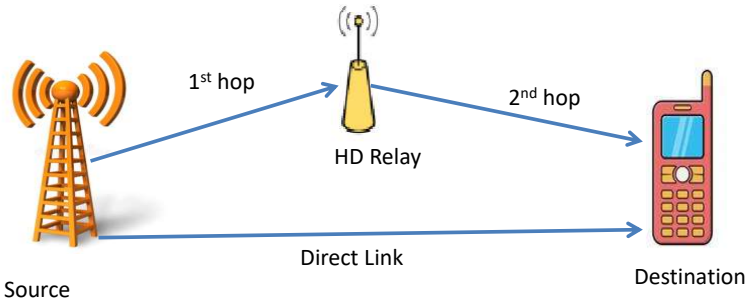

FIGURE 1.3: Relay based secondary network

the help of intermediate relay nodes in a relay-based CRN. Particularly in settings with inadequate direct link quality, these relays can aid in increasing throughput, reliability, and range. A forwarding strategy is required once a relay is implemented in order to assist in moving the message from its source to its destination.

1.4.1 Amplify-and-Forward (AF) protocol

In the **Amplify-and-Forward (AF)** protocol, the relay does not attempt to decode or alter the incoming signal from the source. Instead, it directly amplifies the received signal and transmits it to the destination. This amplification is aimed at mitigating the effects of fading. However, since the relay forwards the signal without decoding, any noise present in the received signal is also amplified, which can degrade the quality of the signal by the time it arrives at the destination [5].

1.4.2 Decode-and-Forward (DF) protocol

In the **Decode-and-Forward (DF)** protocol, the relay first receives and then decodes the incoming data. Before sending it to the destination, the relay re-encodes the information. By decoding and retransmitting the signal, the relay helps minimize the impact of noise and interference, thereby enhancing the reliability of the communication [6].

1.4.3 Adaptive Hybrid Relay (AHR) protocol

Adaptive Hybrid Relay (AHR) protocol technique combines both Amplify-and-Forward (AF) and Decode-and-Forward (DF) strategies, and selects between them based on current channel conditions. Its primary objective is to dynamically select the most suitable relay method—either AF or DF—to improve signal quality, data throughput, and communication reliability. Initially, the relay attempts to decode the received signal. If decoding is successful, it uses the DF protocol to forward the decoded data. However, if decoding fails, the relay switches to the AF mode, amplifies the signal, and transmits it to the destination.

1.4.4 Relay based half-duplex communication

In half-duplex (HD) relay communication, the relay functions on two hops: receives information from the source in the first hop of the cycle and transmits the signal to the receiver in the second hop. As a result, it is unable to transmit and receive both signals simultaneously. The complete transmission via HD relay is accompanied by two phase that in turn reduces spectral efficiency but simpler to integrate into cooperative CRNs to increase coverage.

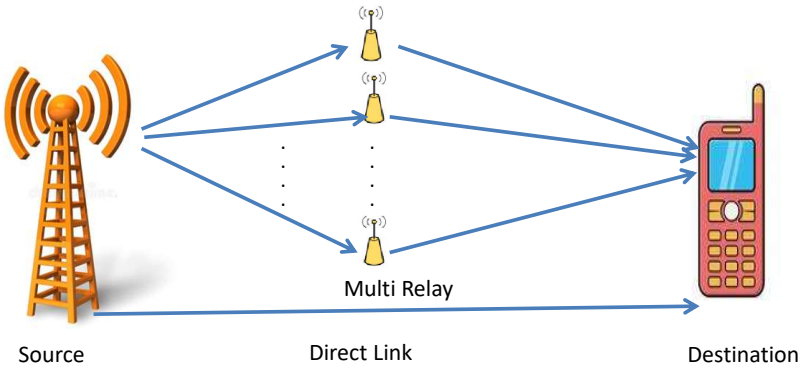

FIGURE 1.4: Multi-relay based secondary network

1.4.5 Relay based full-duplex communication

The relay in the full-duplex (FD) relay communication allows for simultaneous operation by receiving data from the source and sending it to the destination without any transmission delays in a realistic and useful scenario. However, the problem that FD relays faces is self-interference (SI), where the transmitted signal interferes with the received signal. With advancement of technology and beamforming mechanism, the solution to mitigate the SI issue partly can be solved.

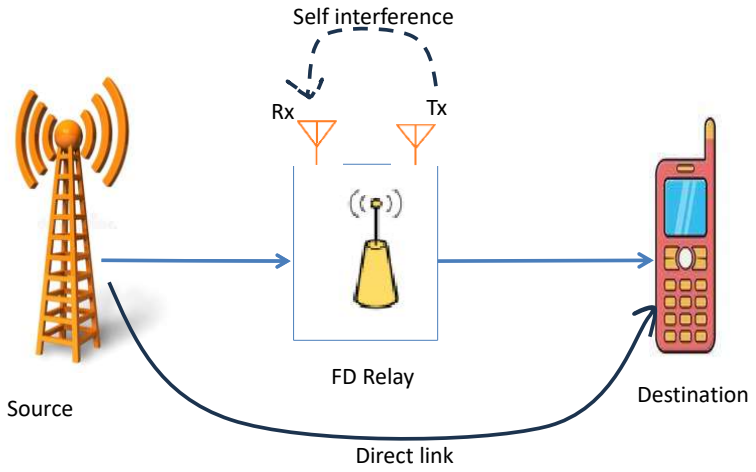

FIGURE 1.5: FD relay based secondary network

1.5 Multiple access in wireless communication system

In communication systems, multiple access is a technique that enables several users to effectively share a single communication channel or spectrum without interfering with one another. Its primary objective is to make use most of the available bandwidth, permit several users to send data at once, reduce minimized collisions and interference, assure equitable and effective distribution of resources.
The event of having only one user broadcasting at a time without various access methods is extremely wasteful and unfeasible for real-world applications. The different classification of multiple access techniques are defined in below sections.

1.5.1 Orthogonal Multiple Access (OMA)

To prevent interference, each user in a pool of many users is given distinct resources (time, frequency, or code) using the well-known classic multiple access mechanism known as orthogonal multiple access (OMA). OMA can be classified into three main types as follows:

1.5.1.1 Frequency Division Multiple Access (FDMA)

Frequency Division Multiple Access or FDMA, is a communication technique that divides the frequency spectrum into distinct bands, with each user being assigned a specific frequency band. The users can transmit simultaneously but operate on different frequencies. To prevent interference, the bandwidth is split into non-overlapping frequency channels. FDMA can be used in analog communication systems and satellite communications. This technique has a drawback in terms of bandwidth utilization, where it can be inefficient, particularly when data transmission requirements vary [7].

1.5.1.2 Time Division Multiple Access (TDMA)

Time Division Multiple Access or TDMA, is a method which segments the time domain and each user gets a turn to transmit within the allocated time slot, sharing the same frequency channel. In this method, no two users can transmit simultaneously. They transmit in sequence, in rapid succession. Each user employs a specific time slot for transmission throughout the available bandwidth sequentially in a cyclic manner with no collision in same time slot. This technique is commonly used in digital cellular systems. Unlike FDMA, this technique enhances bandwidth utilization. This method has limitations as there may exist idle slots when a user has no data to send. It also relies on precise time synchronization [7].

1.5.1.3 Code Division Multiple Access (CDMA)

Code Division Multiple Access or CDMA, is a spread-spectrum approach, where multiple users can transmit simultaneously over the same frequency. In order to distinguish, each user's signal is assigned with a unique code which is mathematically orthogonal to prevent interference. CDMA is implemented in mobile communication systems like 3G. The ability to support numerous users within the same bandwidth,

makes it efficient. CDMA enables several users to use distinct spreading codes to communicate simultaneously on the same frequency. By matching the proper code, the receiver isolates the desired signal and ignores other signals as noise. It is limited to complex decoding [7].

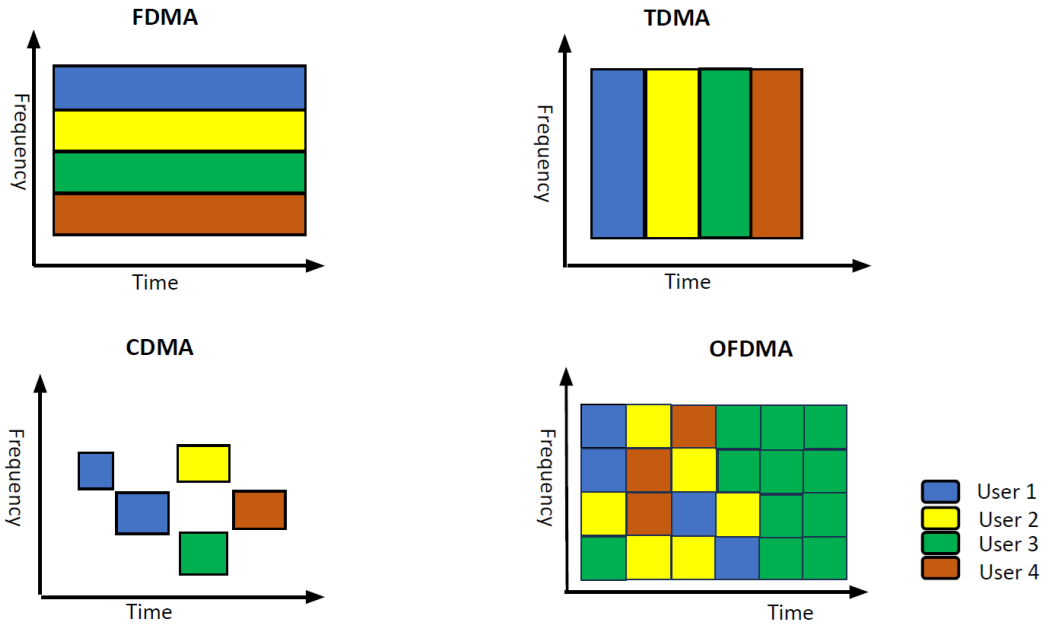

FIGURE 1.6: Orthogonal Multiple Access (OMA) technique

1.5.1.4 Orthogonal Frequency Division Multiple Access

Orthogonal Frequency Division Multiple Access or OFDMA, is a frequency-division-based resource allocation, where the spectrum is divided into subcarriers, which are grouped into resource blocks. Different users are assigned with different subcarriers provided in the same frequency band and timeframe. This allows multiple users to transmit simultaneously without interference. It is widely used in wireless communication system, such as LTE and wi-fi networks. It is highly flexible and suitable for broadband and varying traffic loads. Its limitations comprise of sensitivity to

frequency drift and phase noise. To enable efficiency, OFDMA merges OFDM with multiple user access. Numerous orthogonal subcarriers make up the entire channel bandwidth. One or more subcarriers are allotted to each user for communication within a specific time period. Despite their close spacing, these subcarriers are orthogonal, which means they don't interfere with one another [8].

1.5.2 Non-Orthogonal Multiple Access (NOMA)

Non-Orthogonal Multiple Access (NOMA) is the upcoming cutting-edge technology in the field of multiple access technique in recent wireless communication domain. Inclusion of NOMA technology in this CRN field increases spectral efficiency, connectivity, and improves system performance in dynamic spectrum environments. In NOMA methodology, depending upon the channel quality multiple users can access the same frequency spectrum by employing different power levels for individual users. Thus, the CRNs get facilitate in terms of spectral efficiency with the implementation of NOMA technology by guaranteeing equitable and efficient distribution of power. Key features which are involved in NOMA enabled cognitive radio network are as follows:

Multiplexing via Power Domain: Users are assigned with varying levels of power based on the severity of the channel condition. Furthermore, higher power is assigned to those with poorer channel conditions.

Successive Interference Cancellation (SIC): This is a methodical signal decoding procedure where the receiver receives the composite signal, which consists of data transmitted from multiple users at different power levels and decodes the strongest signal first with the highest power level and moves on to the next strongest signal, and so on [9].

Channel State Information (CSI): By constantly regulating power levels, CSI awareness improves the effectiveness of spectrum sharing.

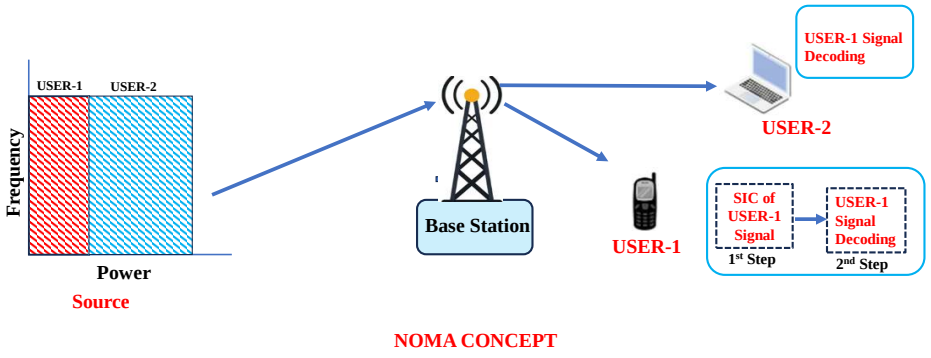

FIGURE 1.7: Non-Orthogonal Multiple Access (NOMA) technique

1.6 Energy harvesting in cognitive radio networks

Energy harvesting (EH) in cognitive radio networks (CRNs) is a wireless communication systems which collects energy from the surrounding environment and also operates without needing frequent battery changes or constant charging, which is especially useful in mobile or remote areas. A cognitive radio network is a type of wireless communication system where radios (smart devices) can automatically detect and adjust to the available radio frequencies. These radios are designed to be flexible and efficient, meaning they can "sense" their environment and decide when and where to transmit or receive data. Cognitive radios improve the use of available radio frequencies, helps to reduce interference and make better use of the wireless spectrum. Energy harvesting is the process of collecting energy from natural sources in the environment to power electronic devices [10].

In traditional wireless networks, devices usually depend on batteries to work. However, cognitive radios in CRNs are continuously scanning the environment and making decisions about frequency use. This can require a lot of power. With energy harvesting, cognitive radios can collect energy from the environment around them, which helps extend their operational time and reduces the need to constantly recharge batteries. For example, if a cognitive radio is located in a place with good

sunlight, it can use solar energy to stay powered.

There are two main types of energy harvesting in CRNs: linear energy harvesting

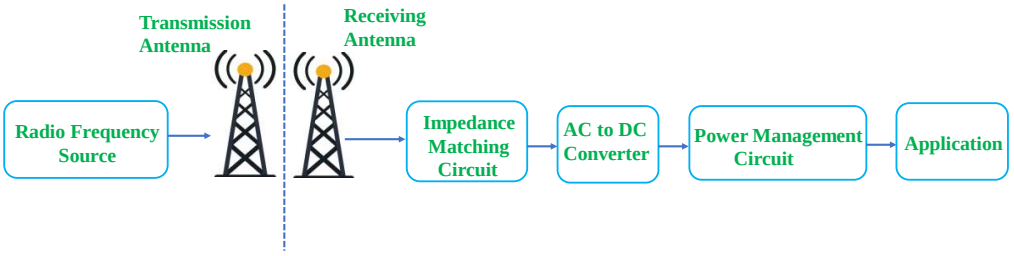

FIGURE 1.8: Block diagram of energy harvesting network

and non-linear energy harvesting. These terms describe how the amount of energy collected changes in relation to the energy source (like sunlight or radio signals).

1.6.1 Linear energy harvesting scenario

In linear energy harvesting, the amount of energy harvested is directly proportional to the energy source. This means that if the energy source increases (like more sunlight or stronger radio waves), the energy harvested also increases in a predictable way.

The harvested energy, E_h in the linear EH model is exactly proportionate to the input radio frequency power [11]:

$$E_h = \eta P_i \tau \tag{1.4}$$

where, η= energy harvesting efficiency factor ($0 < \eta \leq 1$).

P_i is input transmitted RF power.

τ is duration of energy harvesting.

1.6.2 Non-linear energy harvesting scenario

In non-linear energy harvesting, the energy collected does not increase in a simple, straight-line relationship with the energy source. The amount of energy harvested can depend on several factors, and the connection between the energy source and the energy harvested can be more complex.
The nonlinear energy harvesting relation can be expressed as [12, 13]:

$$E_{hn} = \begin{cases} 0, & \text{if } P_i < P_{\text{thresold}} \\ \eta P_i, & \text{if } P_{\text{thresold}} \leq P_i \leq P_{\max} \\ E_{\max}, & \text{if } P_{\text{in}} > P_{\max} \end{cases} \tag{1.5}$$

where, $E_{\max}$ is the maximum energy harvested and P_{thresold} is the minimum power for EH circuit to operate.

1.7 Intelligent reflecting surface assisted wireless communication in cognitive radio network

With more and more gadgets connecting every day, wireless communication is expanding quickly. Additionally, people desire better data speeds. This has made optimal utilization of the radio frequency spectrum more difficult. The spectrum can no longer be effectively divided into definite pieces using the outdated method. The spectrum is congested in certain areas and underutilized in others. Cognitive radio networks were developed as a solution to this issue. CRNs are intelligent systems that let unlicensed users, often known as secondary users, to utilize unused spectrum without interfering with primary users, who are licensed users. Despite this, CRN continues to confront significant challenges, including mistakes in identifying available spectrum, controlling user interference, and adjusting to the dynamic nature of wireless transmissions. These problems can be resolved with the use of

a novel technology known as intelligent reflecting surfaces (IRS). IRS can modify

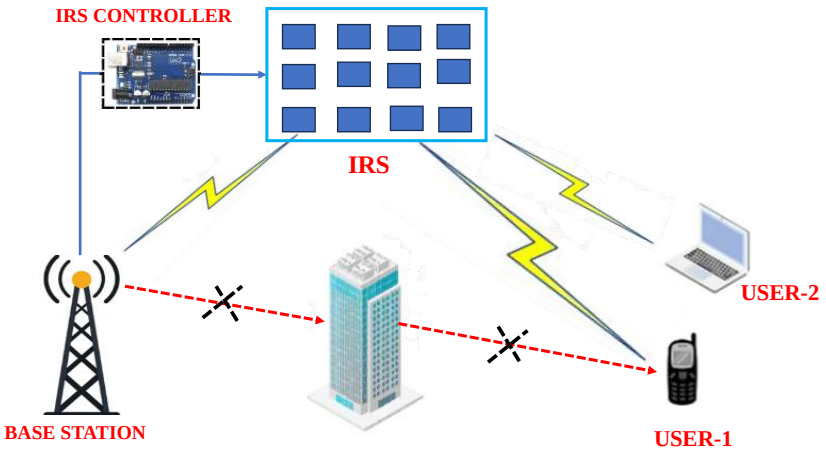

FIGURE 1.9: IRS assisted secondary network

wireless signals' propagation by altering how they bounce off a certain surface. The direction and strength of the signals can be controlled by the numerous tiny, passive components that make up this surface. The best aspect is that IRS can accomplish all of this without generating signals on its own. There are numerous advantages when IRS and CRNs are integrated to form IRS-assisted cognitive radio networks (IRS-CRNs). IRS reconfigures the radio environment by reflecting signals in desired directions rather than creating or amplifying signals. This leads to improved coverage, particularly in places that are blocked, improved quality of the signal, reduced power use, environmentally conscious beamforming [14]. In an IRS-assisted communication system within a cognitive radio network, the overall signal received at the destination is the combination of the direct path and the reflected path via the intelligent reflecting surface (IRS).

Let us define:

h_{sd}: Source to destination direct link channel gain,

h_{sr}: Source to IRS channel gain,

h_{rd}: IRS to destination channel gain,

Θ: IRS phase shifts are represented by a diagonal matrix.
Defining IRS phase shift matrix as:

$$\Theta = \text{diag}\left(e^{j\theta_1}, e^{j\theta_2}, \ldots, e^{j\theta_N}\right)$$

where the IRS's i^{th} reflecting element introduces an adjustable phase shift, denoted by θ_i, and N counts total number of elements.

From source to destination, the effective end-to-end channel is as follows:

$$h_{\text{eff}} = h_{sd} + h_{rd}^T \cdot \Theta \cdot h_{sr} \tag{1.6}$$

The superposition of the reflected path and the direct transmission path is captured by the above expression.

1.8 Motivation of the research work

The best way to address this issue of under-utilization of the spectrum is through wireless communication using cognitive radio (CR) technology. When necessary, CR technology allows for extremely reliable communication between users within the network. The introduction of a relay between the source and destination in a CRN is also a promising technique that helps to extend the range for communication as well as helps to reduce the transmission power. The CRN is supported by the relay-aided communication system, but the IRS network's introduction in the CRN doubles the support for the communication system.
CR systems operates primarily in two modes: underlay, where secondary users (SUs) share the spectrum with active primary users (PUs) under strict interference constraints, and overlay, where SUs opportunistically access the spectrum when it is idle. These modes rely heavily on effective spectrum sensing, typically performed

using techniques like energy detection, to determine PU activity. While significant research has been conducted on both underlay and overlay CR networks, and even on systems that combine both modes, previous works [15, 16, 17, 18], have not addressed the integration of multi-antenna-based proactive decode-and-forward (DF) relaying with adaptive switching between underlay and overlay modes based on real-time PU detection. Moreover, the ability of the secondary transmitter to autonomously decide its operating mode by employing an energy detector circuit has not been explored depending on channel occupancy. Motivated by this gap, the first section of chapter 3 proposes a novel CR framework where the SU dynamically switches between underlay and overlay modes based on PU activity. This adaptive mechanism, supported by multi-relay DF cooperation and adjustable antenna configurations, aims to minimize outage and maximize throughput at the secondary destination, particularly during periods of high PU activity based on channel occupancy.

Energy harvesting from radio frequency signal is a promising solution for powering wireless systems. In [19], the authors proposed and analyzed a dual-hop model based on RF energy harvesting. Wireless energy harvesting and information processing approach using AF relay mode have been illustrated here. In [20], the authors evaluated the effectiveness of the decode-forward (DF) and amplification-forward (AF) protocols for multi-hop EH-based relay networks. The outage and throughput evaluation of the RF energy harvesting assisted DF relay-based CR network has been shown in [21]. In [22], the authors have analyzed the effect of co-channel interference (CCI) along with feedback delay in multi-antenna-based AF relay networks. Antenna selection schemes are being studied in energy harvesting-based decode forward relays system. The authors in [23], have examined the effectiveness of the amplify-and-forward relaying strategy for small cell uplinks using multi-antenna-based relays. Whereas in [24], the authors considered co-channel interference (CCI) from primary users that is non-identical across different hops in a cluster-based multi-hop cognitive network. In other words, the interference experienced at each node varies depending

on its location and surrounding transmitters. CCI is the interference a user experiences from a user in an adjacent cell that uses same frequency. CCI can be used as an alternative energy source for low energy powered communication devices in wireless networks.

However, a significant gap remains in the existing literature—most prior works have not considered an integrated approach where adaptive relay selection coexists with energy harvesting at both the secondary source and relays in the presence of CCI. The work done in second section of chapter 3 is motivated by the need to enhance spectrum efficiency and energy utilization by proposing an adaptive hybrid relay (AHR)-based cognitive radio (CR) network operating in underlay mode.

Instead of half-duplex relaying, full-duplex (FD) relaying significantly improves spectral efficiency by allowing simultaneous transmission and reception over the same channel. In [25], the authors have analyzed the error rate performance of an FD DF relaying scheme. Multi-hop full duplex cognitive relay networks (MH-FDCRNs) operating in the spectrum sharing mode has been introduced in [26], which can enhance the spectral efficiency. Authors in [27], had proposed special cases of diversity gain considering the strength of SI in an environment of distributed FD strategy. A novel hybrid relaying protocol was introduced in [28], that opportunistically switches between FD and HD relaying techniques based on pre-assigned condition. In [29], authors have described the BER performance of a linear and non linear energy harvesting based CR network where a single primary user band is used along with single secondary destination. However, authors did not consider the effect of interference at all receiver nodes from multiple primary user transmitter. Motivated by the need to enhance data transmission in energy-constrained cognitive radio networks, chapter 4 investigates full duplex relay networks in multi-user CRNs. It proposes three system models based on FD relay based CRNs. Of these, the first two section deals with linear energy harvesting and the last section reflects the practical approach on non linear energy harvesting, to evaluate performance under diverse spectrum-sharing and relay communication scenarios.

NOMA has become a cutting-edge solution to meet these goals as to boost spectrum efficiency by making maximum use of the scarce spectrum resources, better user fairness, reduced transmission latency, and high cell edge throughput [30]. Authors in [31] claimed that NOMA can offer a considerable performance improvement over traditional orthogonal multiple access (OMA). The fundamental idea of NOMA is to let several users share the same time period, frequency band and code resource elements using different power levels [32]. The concept of cooperative NOMA (CNOMA) was first put forth in [9], where a nearby user itself takes part as a relay for a distant user experiencing weak channel conditions. The scheme of CNOMA can be mainly categorised into two modes namely half-duplex (HD) [33] and full-duplex (FD) [34, 35, 36], according to their mode of transmission. Driven by this gap, with leaving behind the traditional OMA technology in wireless communication motivates us to build a new approach towards NOMA technique which is adapted in an FD relay network-based CRN with system model and analysis being carried out in the chapter 5.

Intelligent reflecting surfaces (IRSs) have recently emerged as a promising solution to enhance coverage in wireless communication systems [37, 38, 39, 40, 41]. Authors in [42], explored an FD secure communication system enhanced by an IRS, which improves spectrum efficiency and physical layer security by overlapping signals at the eavesdropper, while addressing the practical challenge of imperfect channel state information (CSI) in IRS-assisted cascaded channels. In [43], the authors detail a method of bilateral communication between FD nodes that is supported by an IRS network and that maximizes the sum rate through joint transmit beamforming optimization. To facilitate wireless communication between a terrestrial source and destination, the authors of [44], suggested a hybrid network that combines an IRS network and an FD decode and forward relay. The authors in [45], illustrate an IRS-assisted full-duplex secure communication system, demonstrating improved spectrum efficiency and enhanced physical layer security over traditional FD systems, while addressing challenges posed by imperfect channel state information in cascaded channels. In order to communicate between base station and end user

without a direct link via mm wave MIMO network protocol, the authors in [46], investigated an amplify forward (AF) as well as a decode forward (DF) FD relay containing IRS network. The aforementioned articles motivate us to develop a cognitive radio network in which secondary users connect via both an IRS network and an FD relay network as discussed in chapter 6.

1.9 Objectives and contributions of the research work

The **objectives** of this research are summarized as follows:
1) To analyze the performance of multi-antenna integrated multi-relay based cognitive radio network in presence of energy harvesting and co-channel interference.
2) To evaluate the performance of full-duplex multi-relay based multi-user cognitive radio network under linear and non-linear energy harvesting environment.
3) To analyze the performance of NOMA based hybrid cognitive radio network assist by full-duplex relay.
4) To investigate the performance of full duplex relay based cognitive radio assisted by IRS network.
To meet the above objectives, the contributions of this thesis are summarized as follows:

(i) Mathematical analysis and simulation of closed form expression of hybrid underlay/overlay protocol has been evaluated in terms of outage performance at secondary receiver. The adaptive power allocation policies at secondary transmitter nodes are strategically maintained keeping quality of service of PU outage constraint. The outage performance of joint underlay/overlay technique at SU receiver is compared with the existing overlay and underlay scheme. The attainment of diversity due to impact of variation of number of relays and numbers of antennas incorporated in each relay is analyzed in this system.

The first section of chapter 3 deals with the system model and mathematical derivation.

(ii) The outage performance of secondary user in underlay cognitive radio network using AHR relay scheme has been investigated in presence of CCI environment. AHR is the combination of AF and DF relay protocol which can switch in between depending on the channel condition. The closed-form analytical expression of SU outage has been evaluated in underlay CR network using EH circuit at secondary transmitters (i.e., SU-Tx, SR) while maintaining maximum allowable transmit power policy at secondary transmitters. The impact of number of relays, energy harvesting efficiency factor, and decoding threshold SINR on SU outage performance has been indicated. Second section of chapter 3 contains the general system model with mathematical implementation.

(iii) The first section of chapter 4, explores the operation of a cognitive radio network under different transmission paradigms, including underlay, overlay, and a joint underlay/overlay mode, within the context of a full-duplex (FD) relay network. An adaptive transmission strategy is considered, taking into account multiple primary users and allowing dynamic selection between underlay and overlay modes to enhance spectral efficiency. The analysis thoroughly examines the impact of self-interference inherent in FD relays, along with the cumulative transmitting interference at each receiving node, both of which are critical in determining system performance. A comparative evaluation between FD and traditional HD relaying protocols reveals the advantages of FD relays in terms of spectral efficiency and reduced latency, despite the challenges posed by self-interference. The study further evaluates secondary user outage performance under varying channel occupancy factors, highlighting how FD operation can sustain reliable communication even under high primary user activity. Additionally, the influence of energy harvesting circuit efficiency on the secondary outage probability is analyzed, demonstrating that optimizing the

energy harvesting process is vital for maintaining robust system performance in FD relay-assisted CRNs.

(iv) The second section of chapter 4 investigates the performance of energy harvesting based FD relay network aided CRN in a multi user diversity scenario operating in underlay mode. In this study, we examine the outage performance of a secondary user in a multi-user spectrum sharing scenario using an energy harvesting cognitive radio network with multiple full-duplex (FD) relays. The analysis focuses on the overall transmitting interference at all receiving nodes and the important impact of self-interference at each FD relay's receive antenna. A thorough comparison between FD relaying and a traditional HD relaying scheme is carried out. The precise outage probability expressions for the secondary user in the presence of numerous primary users are obtained analytically, together with adaptive transmit power management strategies for the secondary user (SU) source and secondary relays inside this energy harvesting-assisted FD relaying system.

(v) In the context of FD relaying operations, joint underlay and overlay spectrum sharing approach to evaluate the CR network's outage performance in a multi-PUs scenario under nonlinear EH environment has been addressed. Under this non-linear energy harvesting aided FD relaying network scenario, adaptive transmit power policies for the SU source, secondary relays and exact outage probability of the secondary user are derived analytically in presence of multiple primary users. The system model along with mathematical expression under more practical scenario of non-linear energy harvesting equipped FD relay network in CRN is shown in the last section of chapter 4.

(vi) Chapter 5, considers an adaptive joint underlay/overlay transmission protocol in a NOMA-enabled, multi-user spectrum-sharing environment facilitated by an FD relay network within an energy-harvesting cognitive radio network. The analysis addresses the significant impact of self-interference at each FD relay,

as well as the effects of imperfect successive interference cancellation (SIC) at secondary receivers.The proposed NOMA-enabled CR network is analyzed across underlay, overlay, and joint underlay/overlay transmission modes under FD relay operation. At each transmitting node, different power control algorithms are used to maintain the primary users' quality-of-service (QoS) needs. To illustrate the above study a system model has been designed and mathematical analysis is carried out.

(vii) Chapter 6 explains a full duplex relay assistance using an IRS network based smart spectrum efficient cognitive radio network. The entire closed-form mathematical study has been executed while considering the combined effects of the IRS network and FD relay on transmission throughput and outage performance at the secondary destination. The study examines the effects of secondary transmission rates on outage performance at secondary destinations, taking into account the combined effect of the IRS network and FD relay. An analysis is conducted to evaluate the effects of a combined IRS network and FD relay to a traditional FD relay network operating alone. Throughput analysis has been adequately addressed and compared with the traditional FD relaying approach in order to figure out the impact of the combined IRS-based FD relaying system.

1.10 Thesis organization

Rest of this thesis has been organized as follows.

The literature on cooperative communication based on HD relay and FD relay networks in CRN has been thoroughly reviewed in Chapter 2. There has been a comprehensive assessment of the literature on both linear and non-linear energy harvesting CRN. Furthermore, a study of the literature has been done on the integration of NOMA technology into cognitive radio networks in the context of EH settings.

Lastly, a thorough literature assessment has been carried out based on the IRS network's integration with CRN.

In Chapter 3, two system models based on a multi-antenna embedded multi-HD relay network based CRN in the presence of an EH and CCI environment have been established, and performance study has been completed.

In Chapter 4, three sections describing three diffrent system models based on multi-FD relay network CRN on linear and non-linear EH scenario have been presented. Performance analysis of each sections are described thoroughly.

In Chapter 5, the system model of a NOMA based hybrid CRN assist by FD relay network is described and the performance analysis is illustrated.

In Chapter 6, the system model of an FD relay based cognitive radio network assist by IRS network is described and the performance analysis have been conducted.

In Chapter 7, summary of the contents and related future expansion work are presented.

Chapter 2

Literature review

Radio spectrum which is the backbone of wireless communication system is naturally limited as majority of this spectrum is being licensed by the service providers. Spectrum shortage is one of the challenging issues in the area of wireless communication due to massive increase in data traffic and this has to be suitably addressed. Essentially cognitive radio networks (CRNs) incorporate intelligent wireless communication system protocols in which the secondary users are provided to use the licensed channels of primary users in an efficient manner, ensuring a better model in its approach [1]. Here lies the indispensable role of cognitive radio networks in efficient resource sharing and allocation [3]. Relay-based cognitive radio networks function noticeably better than traditional CRN systems because of their increased spectrum efficiency, longer coverage, and higher signal reliability. The communication performance of secondary users in classic CRNs is limited by low link quality, particularly when deep fading or shadowing is present. Relay aided cooperative CR networks, by efficiently grabbing the task of spectrum sensing, sharing and allocation, make a remarkable achievement for boosting transmission diversity gain in this field. Relays—whether AF, DF, or AHR relays—help strengthen data transfer by bridging weak direct connections between SU transmitters and receivers in the

CRN architecture [20]. It deserves mentioning that different types of enabling technologies have been successfully developed for 5G wireless networks that includes device-to-device (D2D) communication, non-orthogonal multiple access (NOMA) enabled cognitive radio network, in-band full-duplex (IBFD) communication and so forth [47]. Recently, intelligent reflecting surfaces (IRSs) have shown promise as a way to improve wireless communication systems' coverage. FD relay based cognitive radio with the addition of IRS network creates a noteworthy accomplishment for increasing transmission, which improves spectrum efficiency and coverage area [40].
The rest of this chapter is arranged as follows. In section 2.1, an overview on cooperative diversity and relay aided CRN has been discussed. A brief discussion on energy harvesting HD-FD relay based CRN is made in section 2.2. In section 2.3, FD relay based CRN in using of NOMA technology has been provided in details. A brief overview has been given on IRS and FD relay based CRN in section 2.4. Finally, conclusion is drawn in section 2.5.

2.1 Cooperative diversity and relay aided cognitive radio network

In order to produce spatial diversity, cooperative diversity involves a number of nodes (such as relays or users) cooperating to create a virtual antenna array. It enhances signal quality and fights fading. By combining cooperative communication methods with cognitive radio capabilities, the secondary network in a CRN uses cooperative diversity to enhance the wireless network system performance in terms of spectrum utility and energy efficiency. CRNs are immensely benefited from relay-aided cooperative diversity, which makes it possible to implement cooperative communication techniques to ensure a more reliable, successful, and flexible use of spectrum. The source signal is sent through one or more relay nodes in addition to being transmitted directly. As a result, numerous transmission pathways are produced, resulting

in cooperative variety, a type of spatial diversity. Every system model discussed in this thesis includes an explanation of the cooperative diversity concept.

2.1.1 Cooperative diversity in cognitive radio network

Fading is a phenomenon caused by factors such as multipath propagation, signal attenuation over distance, and obstruction by physical objects, leading to time-varying behavior in wireless channels. Even with high transmit power, fading can significantly impact system performance by increasing the likelihood of the channel experiencing deep fades. When this occurs, communication errors are more likely due to the severely weakened signal. Fading can be categorized into two types: small-scale fading and large-scale fading. Small-scale fading occurs when a mobile device moves over distances, causing multiple signal reflections from nearby objects. This results in rapid and significant fluctuations in signal amplitude. In contrast, large-scale fading is caused by broader changes in the environment, such as terrain variations and the overall nature of the surroundings, leading to more gradual changes in signal [48]. Rayleigh fading distribution characterizes the variation in signal strength over short distances and is a typical outcome of small-scale fading in narrowband signals. This type of fading also leads to random power fluctuations. To counteract short-term fading at the receiver, microdiversity techniques involving multiple antennas at a single base station are used. For mitigating shadowing effects, which are more long-term and large-scale, micro-diversity approaches involving multiple base stations are necessary. In contrast, large-scale fading typically follows a log-normal distribution, with long-term fading causing randomness in the average signal power [49]. A common and effective way to combat fading is through diversity techniques, which involve transmitting multiple copies of the signal along different paths. Since these paths undergo statistically independent variations, the likelihood of all paths simultaneously experiencing deep fades is reduced. As a result, reliable communication remains possible as long as at least one path maintains a sufficiently

strong signal. In radio communication, diversity is a technique that takes advantage of the unpredictable nature of radio wave propagation by utilizing multiple independent signal paths. This allows communication to continue even if one path is affected by a deep fade. Importantly, the transmitter does not have knowledge of the diversity decisions made by the receiver and diversity can be classified as follows [50]:

Micro-diversity, is a method that employs multiple antennas placed close together to minimize the effects of small-scale fading. In this approach, the spacing between antennas is shorter than the wavelength of the signal [50].

Macro-diversity, on the other hand, involves transmitters that are spaced much farther apart—typically much greater than the signal's wavelength. It is designed to address large-scale fading caused by major obstacles such as buildings or trees, thereby enhancing signal reliability and coverage [50].

2.1.2 Combining diversity schemes

Distributed diversity takes place in cooperative relay network as the transmitter transmits several independent copies of the same signal. This process is very effective as it reduces the probability that all the transmitted signals are facing fading and co-channel interference at the same time. At the receiver portion, the receiver needs to combine all the received signals to upgrade the signal quality. Three types of combining technique are [50] there, namely:

(i) Maximal Ratio Combining (MRC) : In this combining technique, based on the signal-to-noise (SNR) ratio, every received signal is assigned a weightage. During combining, the higher weightage signal is given more priority compared to the less weightage signal. It is the optimal combining solution. The signal can be returned to its original form using MRC even if no individual signal is permitted in terms of SNR.

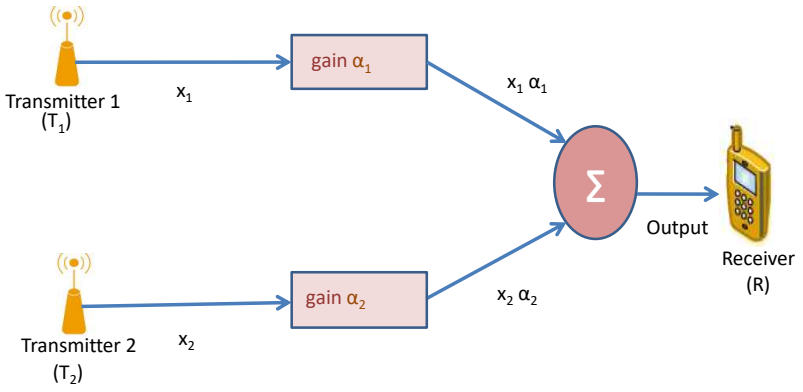

FIGURE 2.1: Maximal ratio combining technique

(ii) Selection Combining (SC) : The receiver chooses the signal with the highest SNR value among several copies of the same signal in order to determine the optimal processing channel. The branch or antenna with the best channel quality is chosen out of all those that are available. The decoding process uses only that signal.

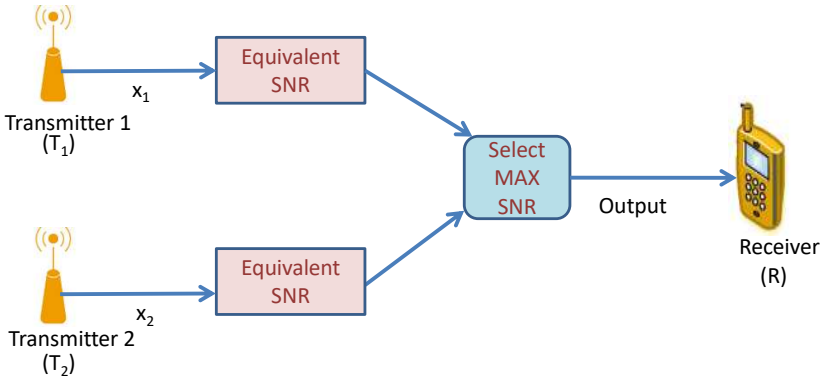

FIGURE 2.2: Selection combining technique

(iii) Equal Gain Combining (EGC) : In this combining process, at first all the received signals are given the same weightage and they are orderly combined. EGC increases the overall signal strength and enhances the signal quality.

Selection combining is widely used over MRC and EGC due to its low complexity, reduced hardware requirements, and energy efficiency. Unlike MRC and EGC, which require multiple active RF chains and precise channel state information, SC only selects the branch with the highest signal strength, making it suitable for low-power and cost-sensitive systems like cognitive radio networks. While MRC offers optimal performance, SC provides a favorable trade-off between performance and implementation simplicity, especially in environments with limited resources. Our suggested models in this thesis primarily employ the selection combining scheme out of all three of these combining technique kinds.

2.1.3 Multi relay selection schemes in cooperative network

A multiple relay network utilizes several relay nodes to deliver the signal from the source to the destination, especially when a direct link is obstructed due to distance or physical barriers. In a parallel relay network, all relay nodes simultaneously forward the signal to the destination, offering enhanced network performance in terms of signal gain and diversity compared to a serial relay network. In a multi-relay system with a parallel topology, the signal can still be successfully sent by other relays even in the event of a relay failure or poor channel conditions. Serial relays rely on each step functioning properly; if one hop fails, the chain may break. Compared to serial architecture, this increases the robustness and dependability of employing a multi-relay parallel network. It is more difficult to control synchronization and power levels between stages in serial relays. This is made simpler by parallel relays, which share a source-destination link. There are typically three types of relaying protocol available, namely Decode-and-Forward, Amplify-and-Forward and Adaptive Hybrid Relay.

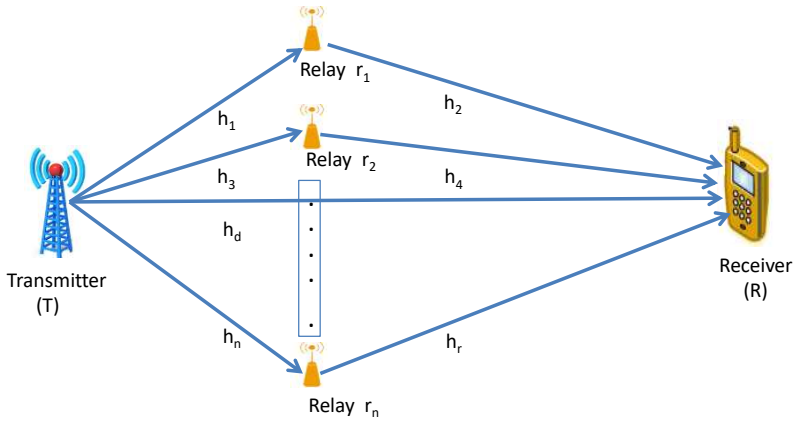

FIGURE 2.3: Multi-relay diversity technique

In Decode-and-Forward (DF) selection cooperation, the relay first decodes the received data, then re-encodes and forwards it to the destination. This process helps reduce both noise and interference, thereby enhancing communication reliability. In DF opportunistic relaying, the relay with the best channel conditions—determined by factors like signal-to-noise ratio (SNR)—is selected from the available set to transmit the signal. The destination can combine signals received from both the source and the relay using an appropriate combining method. However, the amount of information a relay can contribute is ultimately constrained by the weaker link between the source-relay and relay-destination channels. For effective operation, the relay must be able to successfully decode the signal from the source, with its performance limited by the lower capacity of these two links. Signals from many relays may collide or overlap with one another in a multiple relay network, causing interference between the relays and a distorted or corrupted signal at the destination, which may degrade the system performance at large. The bandwidth expense rises with the number of relays in a system, and it could surpass the benefits of a multiple relay network. Relay selection is utilized to get around this problem. It increases the system's spectrum efficiency and dependability by choosing the optimal relay to send the signal to its destination.

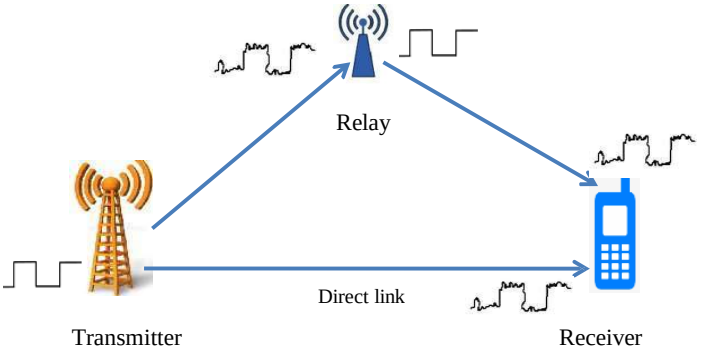

FIGURE 2.4: DF relaying scheme

In Amplify-and-Forward (AF) selection cooperation,the relay forwards the signal

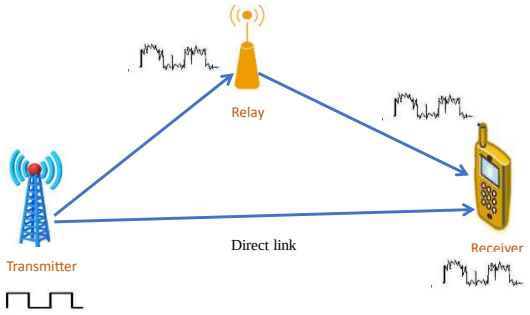

FIGURE 2.5: AF relaying scheme

received from the source without decoding or altering it. Instead, it simply amplifies the entire signal and transmits it to the destination. This amplification helps counteract the effects of fading. However, since the relay does not perform any decoding, any noise present in the received signal is also amplified, which can degrade the signal quality by the time it reaches the destination.

In Adaptive Hybrid Relay (AHR) selection cooperation technique combines both Amplify-and-Forward (AF) and Decode-and-Forward (DF) protocols, with the choice between them depending on the current channel conditions. The primary objective

of AHR is to improve signal quality, throughput, and overall communication reliability by dynamically selecting the most suitable relaying method. Initially, the relay attempts to decode the incoming signal—if successful, it forwards the decoded signal using the DF protocol. If decoding fails, the relay switches to AF mode, amplifying and transmitting the received signal directly to the destination.

2.1.4 Relay-assisted cognitive radio network operating in underlay, overlay, and joint paradigms

While using the underlay mode of transmission, secondary users (SUs) are permitted to transmit concurrently with PUs, but they must respect strict interference constraints to maintain the PUs' quality of service. The basic concept is that the transmission power of SU must be low enough to prevent interference from harming the PU receivers. Relay-assisted communication is crucial in underlay CRNs because it expands the coverage area and compensates for the low power limitation of the SUs. The relay can decode the SU signal and transmit it to its destination as long as the interference levels at the PU receivers remain below a specific threshold [51, 52]. In the overlay mode, SUs exploit unused spectrum, or spectrum holes, by detecting the radio environment. To detect the presence of PU signals in a relay-assisted CRN, the relay node actively performs spectrum sensing. If the relay notices the lack of the PU signal, which denotes a spectrum hole, it permits SU transmission by using the unoccupied channel to send data from the SU transmitter to the SU receiver.
In order to maximize spectrum utilization, the joint underlay/overlay paradigm incorporates the advantages of both underlay and overlay techniques. The CRN initially uses sensing to find out spectrum gaps in this hybrid model. The relay enables SU communication in overlay mode, enabling full-power transmission, if the spectrum is found to be idle (PU absent). The CRN makes transition to underlay mode, where SUs broadcast at lesser power under interference limits, if the PU is active rather than staying silent. In this paradigm, relay nodes are essential for both

adaptive mode switching and sensing. By continuously monitoring PU activity and evaluating interference levels, the relay can help decide whether to operate in overlay or underlay mode at any given time. This dynamic flexibility enhances spectral efficiency and ensures more consistent SU performance across various PU activity patterns [53, 54].

2.1.5 Related works based on relay aided cognitive radio network

In [20], the authors evaluated the effectiveness of the decode-forward (DF) and amplification-forward (AF) protocols for multi-hop EH-based relay networks. Authors in [55], have investigated various relay allocating techniques and assessed the outage performance. The authors gave the idea of a dual-hop spectrum sharing scheme on the basis of the DF relaying method. In the presence of multiple primary users and multi-antenna-based relays network, the outage probability analysis formulas for proactive and reactive relay selective arrangements have been derived in [56]. Outage and throughput evaluation of the RF energy harvesting assisted DF relay-based CR network has been shown in [21]. In [57, 58, 59], the authors analyzed outage performance for multi-hop relay assisted cognitive radio networks with all secondary nodes turned on dedicated power beacon following the Time Switching Relay (TSR) protocol. In [60], the performance of cognitive wireless networks is evaluated in a MIMO environment while maintaining the interference threshold between the primary destination and the CSI. In [22], the authors have analyzed the effect of co-channel interference (CCI) along with feedback delay in multi-antenna-based AF relay networks. Antenna selection schemes are being studied in energy harvesting-based decode forward relays system. The authors in [23] have examined the effectiveness of the amplify-and-forward relaying strategy for small cell uplinks using multi-antenna-based relays.Whereas in [24], the authors considered the impact of non-identical co-channel interference from multiple primary users—modeled

as varying interference levels across different hops—in a cluster-based multi-hop cognitive network.

There are different spectrum sensing methods, but in this thesis, we applied the energy detector process to find out the spectrum holes [61, 62]. There have been many studies on the combination of underlay and overlay mode in CR networks [15, 16, 17, 18, 63, 64]. Spectrally modulated spectrally encoded (SMSE) framework has been proposed using OFDM based soft decision protocol in [15], which supports multi-carrier-based signals undergoing hybrid overlay/underlay waveform for CR network. In [16], authors proposed a hybrid CR system which deals with the arrival rate and departure rate at various nodes under the switching performance of underlay and overlay waveform. Maximum throughput was also calculated taking interference constraint at different nodes. In [17], authors had dealt with the maximum transmission capacity of the SUs under the primary and secondary outage constraints for a hybrid underlay, overlay and interweave mode. The energy-efficient transmission for hybrid spectrum sharing CR networks was investigated in [18], and an optimization model was established to maximize the energy-efficiency capacity. Authors in [65] have compared the system throughput using a learning phase in a secondary network for both underlay and overlay models. A classical idea of using cluster based spectrum sensing and access techniques under hybrid overlay/underlay CR network through optimal relay selection scheme has been proposed in [66]. Authors in [67, 68] demonstrated a fantastic explanation on proactive and reactive DF relaying schemes [69, 70]. A brief DF relaying schemes was also described in [71]. Optimal power allocation algorithm has been developed for a hybrid underlay/overlay Orthogonal Frequency-Division Multiplexing ($OFDM$) based CR network in [63, 72].

2.2 Energy harvesting HD-FD relay based cognitive radio network

Energy harvesting in cognitive radio networks helps make wireless communication systems more sustainable and efficient. By collecting energy from the environment—whether through sunlight, wind, or radio signals—cognitive radios can operate without needing constant battery replacements.

Efficient energy management is crucial in CRNs, especially for non-linear energy harvesting. Smart algorithms decide when to use the energy, whether it's used immediately for communication or stored for later. If the energy is low, the cognitive radio might go into a low-power mode or delay transmission to conserve power.

Linear energy harvesting offers a simple, predictable relationship between the energy source and the energy harvested, while non-linear energy harvesting offers more flexibility and efficiency, especially in unpredictable environments. As technology improves, energy harvesting in CRNs will become more advanced, helping cognitive radios work smarter and more efficiently.

Green communication networks have gained a lot of attention as a viable way to deal with the worldwide energy shortfall and environmental problem [19]. In [73], authors illustrated the energy harvesting (EH) approach at the secondary transmitter from radio frequency (RF) signal of active PU transmitters. Calculation for transmission probability and maximum throughput under outage constraints for secondary receiver is explored apparently. The performance of cooperative spectrum sharing networks is considerably enhanced when employing alternative relay selection schemes, such as amplify-and-forward (AF), decode-and-forward (DF) and adaptive hybrid relays (AHR) relaying protocols [74, 75, 76]. Cognitive radio, in conjunction with Full-Duplex (FD) transmission technology, improves spectrum use and network efficiency [77]. The transmission in a half-duplex relaying network involves two hops, from the source to the relay and then from the relay to the destination. For such relay networks, the FD transmission method has been crucial in

overcoming the problems of spectral inefficiency. The use of FD methods has enabled the relay node to transmit and receive signals simultaneously at the expense of self-interference (SI), which is undesirable. The active and passive cancellation of SI factor with several FD relays in a multi-user spectrum sharing environment has been proposed in [78].

Specifically, the half-duplex (HD) mode, by using different relay selection scheme such as amplify-and-forward (AF) and decode-and-froward (DF) relaying protocol, significantly attains improved performance in cooperative spectrum sharing networks [75, 74, 79, 80]. Cognitive radio in association with full-duplex (FD) communication technology facilitates better spectrum utilization as well as network throughput efficiency. In this respect, CR along with full-duplex certainly provides promising solution for further improvement in communication performance as compared to half-duplex mode [81, 82]. In case of conventional HD relay, two time slots are used for the two distinct operating phases. One phase deals with message listening from the particular information source node while the other phase is specifically involved with message conveyed to the destination node. To overcome the issues of spectral inefficiency, FD techniques have played a vital role for such relay networks [83, 77]. With the implementation of FD techniques, simultaneous transmission and reception of signals by the relay node has been successful at the cost of self interference (SI) which is not desirable. With further progress of antenna technologies and signal processing techniques, FD communication has proved to be very much promising in the domain of wireless communication [84, 85]. In recent times, relay nodes operating in full-duplex mode have received huge interest amongst the researchers [86, 87, 88]. In [89, 90] authors have proposed the self interference variance as a function of transmitted power in an FD protocol characterised by dual hop AF system. Authors in [91] had compared an incremental selective DF relay performance with conventional selective DF performance in an FD m-Nakagami fading environment. The requirement of excess bandwidth in half-duplex relay activity is the major drawback of this kind of relaying architecture, due to hurdle of simultaneous transmission and reception on the same frequency. In order to overcome this,

a NOMA based FD cognitive radio network is proposed in [92]. Authors in [93] discussed the ergodic sum capacity and outage probability of an FD relay CR network. Generally, the protocols rely on HD relay nodes and practical considerations rule out the possibility that FD mode is viable. Moreover, recent works dealing with the favourable outcomes regarding the feasibility of FD transmission have been reported in [94, 95].

2.3 Application of NOMA in cognitive radio network

A crucial technology for 5G and beyond is non-orthogonal multiple Access (NOMA), which superimposes signals at varying power levels to enable several devices to share the same time and frequency resources. The NOMA approach decodes signals using the Successive Interference Cancellation (SIC) concept, which is mostly used at the receiver side. SIC is a technique that allows the received composite signal to extract its own intended message by successively decoding and eliminating stronger interfering signals [9]. By utilizing power-domain multiplexing to enable several secondary users to share the same spectrum resources concurrently, Non-Orthogonal Multiple Access (NOMA) improves the performance of CRNs. NOMA enhances spectral efficiency and facilitates enormous connectivity in CRNs, where spectrum availability is opportunistic and constrained by primary user interference limits. Therefore, in dynamic spectrum contexts, NOMA enables CRNs to attain increased throughput, decreased latency, and enhanced user fairness. This thesis's Chapter 5 discusses the use of the NOMA approach in a CRN based on an FD relay network.

The explosive growth of mobile data traffic, which ultimately leads to the proliferation of the Internet of things (IoT) and related devices, has increased the demand for wireless communication system applications and services that support increased spectral efficiency (SE), high data rates, and wide user access. A new generation

of mobile networks, called the fifth generation (5G), is emerging because a simple upgrade or augmentation of the fourth-generation networks won't be able to meet user needs in the near future. With high system throughput and improvement in SE requirements, 5G wireless networks are primarily anticipated to meet the demands of three different thrust areas: massive machine type communications (mMTC), ultra-reliable low-latency communications (URLLC), and enhanced mobile broadband (eMBB) [96, 97].

NOMA has become a cutting-edge solution to meet these goals as to boost SE by making maximum use of the scarce spectrum resources, better user fairness, reduced transmission latency, and high cell edge throughput [30]. Authors in [31] claimed that NOMA can offer a considerable performance improvement over traditional orthogonal multiple access (OMA). The fundamental idea of NOMA is to let several users share the same time period, frequency band and code resource elements using different power levels [32]. The concept of cooperative NOMA (CNOMA) was first put forth in [9], where a nearby user itself takes part as a relay for a distant user experiencing weak channel conditions. The scheme of CNOMA can be mainly categorised into two modes namely half-duplex (HD) [33] and full-duplex (FD) [34, 35, 36], according to their mode of transmission. However, due to the additional time resources needed for HD cooperation, the higher capacity and reliability come at the expense of reduced resource utilization efficiency, which could negate the capacity increase offered by cooperative communication. On the other hand, as FD wireless devices transmit and receive at the same time, they can overcome the capacity loss in HD CNOMA systems [98]. In [99], the authors explained a throughput analysis of CNOMA mechanism incorporated with an FD relay network in presence of a PU.

The outage probability performance of CR-NOMA networks with randomly placed SUs has been assessed by the authors in [100]. At underlay mode, the outage probabilities of the SUs in the CR-NOMA network have been independently examined by the authors in [101, 102]. In [103], a CR-NOMA network is addressed, where the authors examined the outages and system throughput performance for both

the primary and secondary networks. While [104] examined the end-to-end outage probability of the secondary network in an underlay CR-NOMA system with amplify-and-forward (AF) relaying, [105] took decode-and-forward (DF) relaying into account for the outage analysis. In [106], the authors discussed the CR-NOMA system with energy harvesting circuit and overall secondary outage probability was evaluated. Analytical form of system model with both outage probability as well as ergodic rates of the corresponding SUs in an underlaying CR-NOMA network have been evaluated by the authors of [107]. In [108], the authors have assessed how well the SUs operate during outages when there is imperfect channel state information (i-CSI). In [109] and [110], the authors independently examined the SUs' outage performance and its analysis pertaining to CR-NOMA networks with SWIPT over nakagami-m fading channels and with underlay cognitive radio networks under imperfect SIC. Recent studies by many authors, have examined the effectiveness of traditional cooperative multi-relay NOMA systems that have been merged with effective relay selection algorithm [111, 112, 113, 114, 115, 116]. Partial relay selection (PRS) strategy was taken into consideration as the authors investigated the outage probability and sum rate performance of multiple AF relay-aided NOMA system in [111]. To increase the users' QoS, an optimal user-relay pair selection technique was illustrated in [112]. The performance of the multi-relay assisted cooperative NOMA system has been independently examined by the authors in [113] and [114]. Two optimal relay selection strategies for a cooperative NOMA system with DF relaying are given by the authors in [115]. The authors of [116] evaluated the outage performance of cooperative NOMA networks based on energy harvesting under the PRS scheme. The authors in [26] provide a wonderful notion for implementing multi-hop full-duplex (FD) cognitive relay networks in order to increase spectral efficiency. A full-duplex relay based CRN employing NOMA scheme has been detailed by the authors in [92]. An FD relay CR network's ergodic sum capacity and outage likelihood were studied by the authors in [93]. One primary user band and one secondary destination are employed in the authors' descriptions of the BER performance of linear and non-linear energy harvesting-based CR networks in [29].

In [117], the authors have described a simultaneous wireless information and power transfer (SWIPT) technology which seems as an efficient solution employing cooperative NOMA. In [118], the authors investigated the performance of SWIPT enabled cooperative-NOMA in heterogeneous networks. However, the power management including absolute utilization of spectrum in an EH cooperative sharing network with the assistance of multiple FD relays is not particularly noteworthy in any of the aforementioned cases. This situation motivates us to concentrate on NOMA-based multiple FD-relays assisted CR network with multiple PUs in an energy harvesting scenario. Because of the inclusion of FD relay network, the self interference [78] component has also been taken care of. In [119], considering single primary user, authors have described a NOMA based underlay CR network with partial HD relay selection scheme. In the presence of a single primary user, the authors describe a CR-NOMA network integrated with an HD-FD relay network operating in a partial relay selection scheme in [120]. In [121], the authors put forward the idea of virtual full-duplex (VFD) relaying scheme employing NOMA framework. In [122], considering single primary user, authors have described a NOMA based CR network with FD relay selection scheme.

2.4 Intelligent reflecting surface and FD relay based cognitive radio network

Intelligent reflecting surface (IRS) can assist CRNs by increasing signal strength, decreasing interference, increasing coverage area, and boosting spectrum sensing accuracy. In essence, IRS develops intelligent, controllable wireless signal environments. This is particularly helpful in areas where wireless signals frequently get blocked and don't travel properly, such as in cities or within buildings. The fundamental concept behind IRS-CRNs is their ability to passively and intelligently alter the wireless environment. IRS makes use of inexpensive, basic components that don't require

a lot of energy or complex machinery. To improve signal transmission between the transmitter and the recipient, these components can be readily changed. IRS can improve the communication and sensing operations in CRNs. It can increase the signal strength during sensing to aid secondary users in more precisely detecting available spectrum. It can steer signals to the appropriate secondary users during communication without interfering with the major users. For secondary users, this improves data speed and reduces the likelihood of signal loss. By strategically altering the way signals move through the atmosphere, IRS can assist in resolving these problems. As a result, the system's ability to identify the free spectrum becomes simpler and more accurate. This lessens interference with other users and promotes safer and better communication. Compared to conventional CRNs, this degree of control over the wireless environment is a significant improvement which can notably improve system performance.

However, the inclusion of IRS into Cognitive Radio Networks (CRNs) introduces several challenges too. One of the primary issues lies in developing intelligent algorithms capable of accurately directing signals and adjusting the phase shifts of IRS elements—an inherently complex and computationally demanding task. Effective IRS deployment also requires precise and up-to-date knowledge of the communication channel, which is difficult to maintain in dynamic real-world environments. Additionally, security and privacy become critical concerns, as the ability of IRS to alter signal paths could be exploited by malicious entities if not adequately secured. Therefore, robust protection mechanisms and secure control systems are essential to ensure network integrity. Despite these challenges, the integration of IRS with CRNs is seen as a key enabler for future wireless technologies like 6G, offering the potential for faster, more reliable, and energy-efficient communication capable of supporting vast numbers of connected devices. IRS-enhanced CRNs represent a significant step forward in wireless communication, addressing persistent issues such as inefficient spectrum sensing, interference, and excessive energy consumption. By enabling intelligent manipulation of the wireless environment, IRS can substantially boost the performance and reliability of CRNs.

An IRS is a planar metasurface made up of inexpensive, compact, passive components called phase shifters. Each component can be individually adjusted to reflect incident signals with different phase shifts, improving the efficiency of resource allocation for the wireless channel [37, 38]. The deployment of IRS-assisted multiple user multiple-input single-output (MISO) systems has enhanced resource allocation and physical layer security, as discussed by the authors in [39]. Authors in [40] explained how an IRS is used to improve the energy harvesting capability of a system that supports Simultaneous Wireless Information and Power Transfer (SWIPT). The authors in [41] aim to determine the maximum data transmission capacity of a communication system that uses an IRS to assist point-to-point multiple-input multiple-output (MIMO) communication. Authors in [123] underlined how RIS technology, which consists of surfaces that can dynamically control how signals reflect or propagate, opens up new opportunities for enhancing wireless communication. Authors in [42] explored an FD secure communication system enhanced by an IRS, which improves spectrum efficiency and physical layer security by overlapping signals at the eavesdropper, while addressing the practical challenge of imperfect channel state information (CSI) in IRS-assisted cascaded channels. In [43], the authors detail a method of bilateral communication between FD nodes that is supported by an IRS network and that maximizes the sum rate through joint transmit beamforming optimization. For user-to-user communication, the authors of [42] suggested a reconfigurable intelligent surface (RIS)-assisted full-duplex unmanned aerial vehicle (UAV) that performs better than the HD-RIS mode. To facilitate wireless communication between a terrestrial source and destination, the authors of [44] suggested a hybrid network that combines an IRS network and an FD decode and forward relay. Authors in [124] explored RIS-aided C-NOMA downlink transmission with HD and FD relaying, aiming to minimize all transmitted power through joint optimization of power allocation and passive beamforming under various constraints. In [125], authors underpin physical layer security and data transmission in underlay D2D networks, employing RIS and FD jamming receivers to enhance robustness and security through spectrum sharing and artificial noise emission. The authors in [45]

illustrate an IRS-assisted full-duplex secure communication system, demonstrating improved spectrum efficiency and enhanced physical layer security over traditional FD systems, while addressing challenges posed by imperfect channel state information in cascaded channels. In order to communicate between base station and end user without a direct link via mm wave MIMO network protocol, the authors in [46] investigated an amplify-and-forward (AF) as well as a decode-and-forward (DF) FD relay containing IRS network. The authors of [126] took into consideration an IRS-based NOMA system in which nearby users serve as FD relays for communication with distant users in order to transmit messages from the source. In these systems, an IRS-assisted FD base station provides service to several half-duplex users, allowing IRS to improve performance and lessen interference with primary users.

2.5 Chapter summary

From the review of existing literature, it is evident that the spectrum scarcity problem, exacerbated by exponential growth in wireless data traffic, necessitates innovative solutions. CRN have emerged as a robust paradigm, enabling intelligent spectrum sharing between primary users (PUs) and secondary users (SUs). The integration of relay-aided cooperative communication in CRNs has further enhanced spectral efficiency and system reliability by improving diversity gains. The comparative analysis between full-duplex (FD) and half-duplex (HD) relaying protocols reveals critical insights into the performance trade-offs in cognitive radio networks (CRNs). Studying the performance of secondary users within cognitive radio networks (CRNs) utilizing full-duplex (FD) relay communication under both linear and nonlinear energy harvesting (EH) models reveals several important insights. Cognitive radio networks (CRNs) leveraging non-orthogonal multiple access (NOMA) technology has highlighted the potential of NOMA to significantly enhance spectral efficiency and support multiple secondary users with varying channel conditions. Studies investigating IRS-assisted full-duplex (FD) relay nodes in cognitive radio

networks (CRNs) have demonstrated the substantial potential of intelligent reflecting surfaces in enhancing wireless communication performance.

Chapter 3

Performance analysis of half-duplex multirelay cognitive radio network in energy harvesting and co-channel interference environment

Cognitive radio networks (CRNs) have drawn a lot of interest because of its capacity to improve communication efficiency and maximize spectrum utilization. Specifically, relay-based CRNs use relay nodes to increase coverage and enhance signal quality. In contrast to relay-aided CRNs, a multi-antenna embedded multi-relay CRN approach has been developed in the first section of this chapter that operates under a joint underlay/overlay mode of transmission. The subsequent section addresses the AF, DF, and AHR multi-relay based CRNs in the presence of co-channel interference and energy harvesting scenario.

3.1 Cognitive radio network system based on a multi-antenna integrated multiple relay network

The primary objective of this section is the proposition of an adaptive spectrum sharing CR network consisting of a primary user (PU), secondary user transmitter ($SU-Tx$) communicating with secondary user receiver ($SU-Rx$) via multiantenna based proactive decode-and-forward (DF) relay selection scheme. Based on this, a model has been developed where, strategically an adaptable joint venture on underlay/overlay protocol is defined on the basis of channel occupancy using spectrum sensing technique. Specifically, a simultaneous switching mechanism of underlay or overlay mode is decided by secondary users (SUs), which senses the activity of primary user (PU) by the technique of energy detection. After sensing, if the PU is found out to be busy, SU activates its power restriction mode (i.e., underlay); otherwise SU operates with its maximum power (i.e., overlay) with the assist of multiple relays operating in proactive DF mode. A closed form expression of hybrid underlay/overlay protocol has been evaluated in terms of outage performance at secondary receiver. The adaptive power allocation policies at secondary transmitter nodes are strategically maintained keeping PU outage constraint. The outage performance of joint underlay/overlay technique at SU receiver is compared with the existing overlay and underlay scheme. This system model analyzes the effects of variations in the number of relays and the number of antennas integrated into each relay.

3.1.1 System model for multi-antenna integrated multiple relay cognitive radio network

The system architecture shown in **Fig. 3.1**, is a cognitive radio network consisting of one primary user (PU), secondary user transmitter ($SU-Tx$) communicating with single secondary user receiver($SU-Rx$) via selecting a single DF relay using proactive relay selection scheme [58]. In proactive opportunistic relaying scheme, the best relay is chosen based on a mechanism to maximize the minimum of the weighted channel strength between the links source to relays and relays to destination. The secondary relay node $SR_{kl}; k \in 1,2,...,K, l \in 1,2,...,L$ indicates the l^{th} antenna of k^{th} secondary relay. The secondary relay node consists of K number of relays and each relay possesses L receiving antennas and a transmitting antenna. The $SU-Tx$ is equipped with an energy detector sensing technique that continuously senses the PU activity and can simultaneously transmit it when required. This is a half-duplex mode of operation where relays act as a regenerative repeater between $SU-Tx$ and secondary user receiver ($SU-Rx$), also termed as secondary destination (D). A primary user transmitter ($PU-Tx$) communicates with a primary user receiver ($PU-Rx$) as and when required. This licensed spectrum of the PU is accessed by the secondary user simultaneously whenever needed without hampering the PU. The secondary user can only access the PU spectrum only after being sensed. A smart switching mechanism is decided by ($SU-Tx$) itself depending upon the state of PU (busy or idle) and approach towards underlay or overlay technique is followed respectively. It is also assumed that there is no direct link between source secondary transmitter and secondary destination due to severe shadowing and multipath propagation loss. The channel coefficients are assumed to be independent and follow non-identical Rayleigh distribution. Channel coefficients are defined as follows: h_s is the channel coefficient for $PU-Tx$ to $SU-Tx$; $h_{PR_k}(k=1,2,..,K)$ is for $PU-Tx$ to Secondary relay (SR_k) ; h_{PD} is for $PU-Tx$ to D; $h_{SR_k,l}(k=1,2,..,K; l=1,2,..,L)$ is for $SU-Tx$ to SR_k; h_{Rk_D} is for SR_k to D; $h_{S,I}$ is for $SU-Tx$ to $PU-Rx$; h_p is for $PU-Tx$ to $PU-Rx$. h_{Rk_I} for SR_k

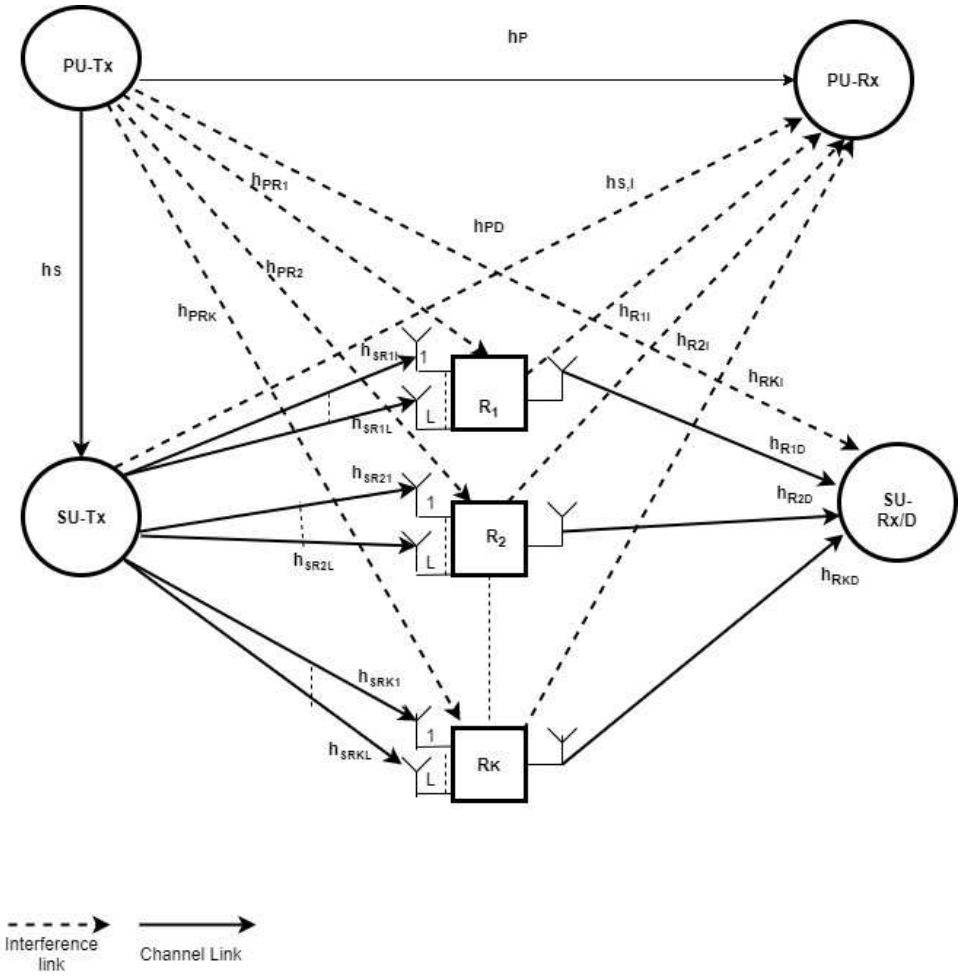

FIGURE 3.1: System model for multi-antenna multi-relay cognitive radio network

to $PU - Rx$. Accordingly, the channel variance of h_s, h_{PR_k}, h_{PD}, $h_{SR_{k,l}}$, h_{Rk_D}, $h_{S,I}$, h_p and h_{Rk_I} are σ_S^2, $\sigma_{PR_k}^2$, σ_{PD}^2, $\sigma_{SR_{k,l}}^2$, $\sigma_{Rk_D}^2$, σ_S^2,$_I$, σ_P^2 and σ_{Rk}^2 respectively. The unlicensed SUs can only access the licensed PU spectrum only after being detected. Here the source $SU - Tx$ is equipped with an energy detector circuit which is based on hypothesis testing.

Therefore, signal received at $SU - Tx$ by $PU - Tx$ is given by

$$r(t) = \sqrt{E_s} h_s s(t) + n(t) \tag{3.1}$$

where, $\sqrt{E_s}s(t)$ is the transmitted signal from PU, $n(t)$ symbolizes Additive White Gaussian Noise (AWGN) with variance N_0.

Thus, the energy detector present at $SU - Tx$ decides the presence of PU activity on the basis of hypothesis testing as follows:

$$H_1 : E_s|h_s|^2 + N_0 \qquad Presence\ of primary\ signal \tag{3.2}$$

$$H_0 : N_0 \qquad Absence\ of primary\ signal \tag{3.3}$$

The output of the energy detector under the hypothesis H_1 and H_0 can be expressed as:

$$T(H_0) = N_0 \tag{3.4}$$

$$T(H_1) = E_s|h_s|^2 + N_0 \tag{3.5}$$

where, $E_s =$ energy of signal transmitted from PU.
The decision taken by energy detector may be formulated as [127],

$$T(H_0) < \lambda, \qquad hypothesis\ H_0\ True \tag{3.6}$$

$$T(H_1) > \lambda, \qquad hypothesis\ H_1\ True \tag{3.7}$$

where, $\lambda =$ energy threshold at energy detector.
False alarm probability (P_f) is the probability of falsely detecting the primary signal whereas actually no primary signal was present [16]. This has been mathematically outlined as:

$$P_f = P_r\Big(T(H_0) > \lambda\Big) \tag{3.8}$$

$$\lambda = -N_0 log(P_f) \tag{3.9}$$

Probability of detection (P_d) which defines the probability of the existence of primary signal [16]. This may be written like

$$\begin{aligned} P_d &= P_r\Big(T(H_1) > \lambda\Big) \\ &= P_r(E_s|h_s|^2 + N_0) > \lambda \end{aligned} \tag{3.10}$$

$$P_d = \exp\left(-\frac{1}{\sigma_s^2} max[\frac{\lambda - N_0}{E_s}, 0]\right) \tag{3.11}$$

According to FCC [128], data, for the measurement period, typical channel occupancy ranges between 15 percentage and peak usage close to 85 percentage. Let α be the probability of channel occupancy ($0 \leq \alpha \leq 1$) i.e., busy state of PU channel. Therefore the probability for PU to be busy is αP_d and PU in sleep mode $(1-\alpha)P_d$.

3.1.2 Power allocation strategies at different nodes

To investigate the power allocation policy for $SU - Tx$ and SR_k, the following property is used.

Property 1: Consider X, Y and Z are random variables (RVs) where Z is defined as [129]:

$$Z = \frac{aX}{bY + c} \quad with \quad a, b, c > 0 \tag{3.12}$$

The RVs X and Y, are exponentially distributed with variances σ_x^2 and σ_y^2 respectively. The cumulative distribution function (CDF) of random variable $Z \leq z$ is given as [129]:

$$F_z\left(a, b, c, \sigma_x, \sigma_y, z\right) = 1 - \frac{a\sigma_x^2}{a\sigma_x^2 + bz\sigma_y^2} \exp\left(-\frac{zc}{a\sigma_x^2}\right) \tag{3.13}$$

3.1.2.1 Power allocation at secondary source

The $SU - Tx$ transmit power should be maintained so that no PUs are subject to excessive interference from the communication of the SU. Thus, the power of transmission by $SU - Tx$ should satisfy an outage of PU receiver given as,

$$\begin{aligned} P_{Out}^{P,SU-T_x} &= Pr\left(\frac{P_p|h_P|^2}{P_s|h_{S,I}|^2 + N_0} \leq \gamma_{th}^{PU}\right) \leq \varepsilon \\ &= 1 - \frac{P_p\sigma_P^2}{P_p\sigma_P^2 + P_s\sigma_{S,I}^2} \exp(-\frac{\gamma_{th}^{PU}}{P_p\sigma_P^2}) \leq \varepsilon \end{aligned} \tag{3.14}$$

where, $\gamma_{th}^{PU} = 2^{R_p} - 1$ and ε denote the outage threshold and outage constraint of the $PU - Rx$ respectively. The transmission rate of PU is R_p.
Simplifying (3.14) and after some manipulations, the maximal transmit power of the $SU - Tx$ under the outage of the PUs is found as,

$$P_s \leq \frac{P_p \sigma_P^2}{\gamma_{th}^{PU} \sigma_{S,I}^2} \left[\frac{\exp - \frac{\gamma_{th}^{PU}}{P_p \sigma_P^2}}{(1-\varepsilon)} - 1 \right] \tag{3.15}$$

where, P_s is the power that can be transmitted and adapted by $SU - Tx$ maintaining QoS of PU.
Let P_s^{under} be the power transmitted by $SU - Tx$ during the underlay mode of operation and can be written as,

$$P_s^{under} = \min \left(P_s, P_s^{max} \right) \tag{3.16}$$

where, P_s^{max} is the maximum allowable power from $SU - Tx$ that can be transmitted. At overlay mode of operation, power transmitted by $SU - Tx$ is maximum due to absence of primary signals which may be reflected as,

$$P_S^{over} = P_s^{max} \tag{3.17}$$

3.1.2.2 Power allocation at secondary relays

The outage performance at $PU - Rx$ due to interference by $SR - Tx$ is also to be maintained. The $SR - Tx$ transmit power should be maintained so that no PUs are subject to excessive interference from the communication of the SR_k. Thus, the transmit power of the $SR - Tx$ should satisfy an outage constraint of the PUs given as,

$$P_{Out}^{P,SR_k} = Pr \left(\frac{P_p |h_P|^2}{P_{R_k} |h_{R_k,I}|^2 + N_0} \leq \gamma_{th}^{PU} \right) \leq \varepsilon \tag{3.18}$$

Since k number of relays are taken under consideration, where k=1,2,...K, the power transmitted from different relays are different. By symbolizing P_R the minimum power under consideration of all the relays and maintaining the primary receiver outage constraint, we can write

$$P_R = \min_{k=1,2,\ldots,K} (P_{R_k}) \tag{3.19}$$

where, the transmitted power from k^{th} relay maintaining the PU receiver outage constraint from equation (3.18) is given by,

$$P_{R_k} \leq \frac{P_p \sigma_P^2}{\gamma_{th}^{PU} \sigma_{R_k}^2} [\frac{\exp - \frac{\gamma_{th}^{PU}}{P_p \sigma_P^2}}{(1-\varepsilon)} - 1] \tag{3.20}$$

At underlay mode, the power transmitted by each relay of $SR - T_x$ is given as,

$$P_R^{under} = \min (P_R, P_R^{max}) \tag{3.21}$$

where, P_R^{max} is the maximum allowable power from each of the k relays.
Similarly, during overlay mode of operation at each relay, the power transmitted by $SR - T_x$ is also the maximum as,

$$P_R^{over} = P_R^{max} \tag{3.22}$$

3.1.2.3 End to end SINR at underlay and overlay mode

During underlay operation, the signal is transmitted from $SU - Tx$ to the relay in the first phase of communication. At underlay mode, the signal to interference noise ratio (SINR) through $SU - Tx$ to l^{th} antenna of k^{th} relay is expressed as,

$$\gamma_{SR_{k,l}}^{under} = \frac{P_s^{under} |h_{SR_{k,l}}|^2}{P_p |h_{PR_k}|^2 + N_0} \tag{3.23}$$

Now SINR through $SU-Tx$ to k^{th} relay,

$$\gamma_{SR_k}^{under} = \max_{l=1,2,...,L}[\gamma_{SR_{k,l}}^{under}] \tag{3.24}$$

During the second phase of operation, each proactive DF relay at underlay mode facing SINR through SR_k to D is given by,

$$\gamma_{Rk_D}^{under} = \frac{P_R^{under}|h_{Rk_D}|^2}{P_p|h_{PD}|^2 + N_0} \tag{3.25}$$

End to end SINR operating under proactive DF relay scheme at underlay mode is given by,

$$\gamma_k^{under} = \min(\gamma_{SR_k}^{under}, \gamma_{Rk_D}^{under}) \tag{3.26}$$

As there are K ($k \in 1, 2, ..., K$) numbers of proactive DF relays, the best relay is choosen which gives the maximum SINR,

$$\gamma_{under}^{PRO} = \max_{k=1,2,...,K}(\gamma_k^{under}) \tag{3.27}$$

End to end outage probability using proactive DF relay scheme at underlay mode,

$$P_{OUT,under}^{PRO} = Pr\big(\gamma_{under}^{PRO} \leq \gamma_{th}\big) \tag{3.28}$$

where, $\gamma_{th} = 2^{2R} - 1$, denote the outage threshold of secondary user destination and R is the outage transmission rate of SU-transmitters.
At overlay mode, as the power transmitted by $SU-Tx$ and SR_k is the most, the SINR through $SU-Tx$ to l^{th} antenna of k^{th} relay can be written as,

$$\gamma_{SR_{k,l}}^{over} = \frac{P_s^{over}|h_{SR_{k,l}}|^2}{N_0} \tag{3.29}$$

SINR through $SU-Tx$ to k^{th} relay,

$$\gamma_{SR_k}^{over} = \max_{l=1,2,...,L}[\gamma_{SR_{k,l}}^{over}] \tag{3.30}$$

While operating in overlay mode each proactive DF relay facing SINR through SR_k to D is given by,

$$\gamma_{Rk_D}^{over} = \frac{P_R^{over}|h_{Rk_D}|^2}{N_0} \tag{3.31}$$

End to end SINR using proactive DF relay scheme at overlay mode,

$$\gamma_k^{over} = \min(\gamma_{SR_k}^{over}, \gamma_{Rk_D}^{over}) \tag{3.32}$$

Considering K ($k \in 1, 2, ..., K$) numbers of proactive DF relays, the best relay is chosen which gives the maximum SINR.

$$\gamma_{over}^{PRO} = \max_{k=1,2,...,K}(\gamma_k^{over}) \tag{3.33}$$

End to end outage probability using proactive DF relay scheme,

$$P_{OUT,over}^{PRO} = Pr\big(\gamma_{over}^{PRO} \leq \gamma_{th}\big) \tag{3.34}$$

The total outage probability during joint underlay/overlay mode is given as follows,

$$P_{OUT}^{PRO} = [(1 - P_d) + \alpha P_d]P_{OUT,under}^{PRO} + (1 - \alpha)P_{OUT,over}^{PRO} \tag{3.35}$$

3.1.3 Mathematical analysis for cognitive radio network operating under joint underlay/overlay mode

An analytical evaluation of closed form expression for outage performance at secondary destination using joint underlay/overlay mode has been carried out in this section.

The outage probability at k^{th} relay for l^{th} antenna can be expressed as,

$$P_{OUT,under}^{l} = Pr\left(\gamma_{SR_{k,l}}^{under} \leq \gamma_{th}\right) \tag{3.36}$$

Substituting (3.23) into (3.36), we have

$$P^{l}_{OUT,under} = Pr\left(\frac{\overline{P}^{U}_{s}|h_{SR_k,l}|^2}{\overline{P_p}|h_{PR_k}|^2 + 1} < \gamma_{th}\right) \tag{3.37}$$

where,

$$\overline{P}^{U}_{s} = \frac{P^{under}_{s}}{N_0} \tag{3.38}$$

$$\overline{P_p} = \frac{P_p}{N_0} \tag{3.39}$$

Using *Property 1*, the equation (3.37) can be resolved to find the outage probability at relay as follows,

$$P^{l}_{OUT,under} = \underbrace{1 - \left\{\frac{\overline{P}^{U}_{s}\sigma^2_{SR_k,l}\exp -(\frac{\gamma_{th}}{\overline{P}^{U}_{s}\sigma^2_{SR_k,l}})}{\overline{P}^{U}_{s}\sigma^2_{SR_k,l} + \overline{P_p}\sigma^2_{PR_k}\gamma_{th}}\right\}}_{A} \tag{3.40}$$

Considering (3.24) and from the above equation (3.40), we get to know that out of L ($l \in 1, 2, ..., L$) receiving antennas of each relay the best is chosen by selection combining scheme as follows,

$$P^{L}_{OUT,under} = \prod_{l=1}^{L}\left(P^{l}_{OUT,under}\right) = A^L \tag{3.41}$$

For simplicity, we may assume that all the channel mean power are equal i.e., $\sigma^2_{SR_k,l}$ and $\sigma^2_{PR_k}$ are same $\forall\ l, k$.

Similarly taking help from *Property 1* and simplifying the equations, the outage probability at secondary destination has been calculated as follows,

$$P^{k}_{OUT,under} = \underbrace{1 - \left\{\frac{\overline{P}^{U}_{R}\sigma^2_{Rk_D}\exp -(\frac{\gamma_{th}}{\overline{P}^{U}_{R}\sigma^2_{Rk_D}})}{\overline{P}^{U}_{R}\sigma^2_{Rk_D} + \overline{P_p}\sigma^2_{PD}\gamma_{th}}\right\}}_{B} \tag{3.42}$$

where,

$$\overline{P}_R^U = \frac{P_R^{under}}{N_0} \tag{3.43}$$

Finally, during underlay operation, the end to end outage is calculated from (3.26), (3.27), (3.28) and (3.42), where the best relay is chosen out of K number of relays

$$P_{OUT,under}^{PRO} = \left\{A^L + (1 - A^L)B\right\}^K \tag{3.44}$$

Considering no interference from primary source, applying *Property 1*, considering (3.29) and (3.34), outage at k^{th} relay for l^{th} antenna can be written as,

$$P_{OUT,over}^l = Pr\left(\overline{P}_s^O |h_{SR_{k,l}}|^2 \leq \gamma_{th}\right) \tag{3.45}$$

where,

$$\overline{P}_s^O = \frac{P_s^{over}}{N_0} \tag{3.46}$$

Thus, the outage probability calculated from (3.44) is

$$P_{OUT,over}^l = \underbrace{1 - \exp(-\frac{\gamma_{th}}{\overline{P}_s^O \sigma_{SR_{k,l}}^2})}_{C} \tag{3.47}$$

Considering (3.30) and from the above equation (3.47), we get to know that out of L ($l \in 1, 2, ..., L$) receiving antennas of each relay, the best is chosen by selection combining scheme as follows,

$$P_{OUT,over}^L = \prod_{l=1}^{L} \left(P_{OUT,over}^l\right) = C^L \tag{3.48}$$

For simplicity, we may consider that all the channel mean power are equal i.e., $\sigma_{SR_{k,l}}^2$ are same $\forall\ l, k$.

Similarly from (3.31) we get,

$$P^{k}_{OUT,over} = \underbrace{1 - \exp(-\frac{\gamma_{th}}{\overline{P}^{O}_{R}\sigma^{2}_{Rk_D}})}_{E} \tag{3.49}$$

where,

$$\overline{P}^{O}_{R} = \frac{P^{over}_{R}}{N_0} \tag{3.50}$$

Finally, the end to end outage in overlay mode is calculated from (3.32), (3.33) and (3.34) in which the best relay is chosen out of K number of relays,

$$P^{PRO}_{OUT,over} = \left\{C^{L} + (1 - C^{L})E\right\}^{K} \tag{3.51}$$

Eventually, based on the activity of sensing, detection of primary user and their state of channel occupancy while maintaining their outage constraint (i.e, QoS) by the secondary user, their total outage probability during adaptive switching of underlay or overlay mode is achieved.

Finally, substituting equations (3.44) and (3.51) into (3.35), the outage probability for the proactive DF scheme in joint underlay/overlay protocol can be written as,

$$P^{PRO}_{OUT} = \left[(1 - P_d) + \alpha P_d\right]\left\{A^{L} + (1 - A^{L})B\right\}^{K} + (1 - \alpha)\left\{C^{L} + (1 - C^{L})E\right\}^{K} \tag{3.52}$$

The above expression on outage probability of SU for proactive DF relay scheme under joint underlay/overlay protocol is one of the novel developments in this thesis.

3.1.4 Results and discussions

This section deals with the result analysis performed using MATLAB simulation testbed and a brief discussion is made on the basis of the analyzed result. The numerical results provided here illustrate the performance improvement obtained

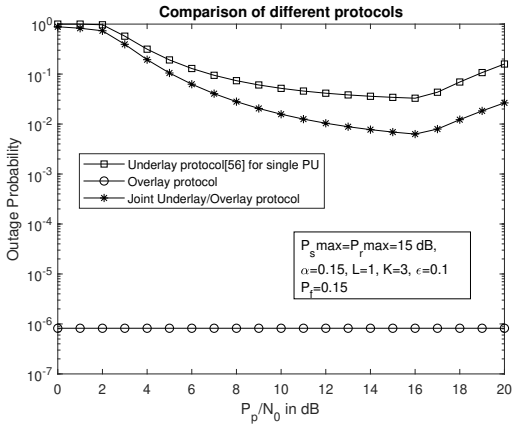

FIGURE 3.2: Comparison of outage performance w.r.t P_p/N_0 under underlay, overlay and joint underlay/overlay mode

when applying the proposed relay assisted adaptive joint underlay/overlay spectrum access scheme. To examine the system performance, let us assume the system parameters as follows: The cut-in transmission rate for both PU and SU is taken equal i.e. R_p=R=0.2 bits/s/Hz. The outage constraint of PU is fixed at $\varepsilon = 0.1$. The noise power is normalized to unit value. Based on the value of false alarm probability $P_f = 0.15$ (assumed), the detection probability (P_d) is calculated depending on which the outage behaviour is analyzed.

Fig. 3.2 shows the outage probability of the $SU - T_x$ to D as a function of P_p/N_0 for different protocols such as underlay, overlay and joint underlay/overlay. The number of relays (K), number of receiving antennas at each relay are (L) are kept constant at K=3, L=1, the probability of channel occupancy ($0 \leq \alpha \leq 1$) is assumed to be kept at $\alpha = 0.15$. It is observed that the outage performance of overlay mode does not depend on the transmitting power of PU (Pp) (i.e., the secondary users do not maintain the QoS of PU). So this overlay scheme solely can not take part in the spectrum sharing model. Also it has been shown that the outage performance of joint underlay/ overlay scheme is better than the existing underlay mode [56] for a single PU. This is because if the primary user (PU) is active, the secondary transmitter must operate in a power-restricted mode; otherwise, it can transmit at full power to maximize its benefit.

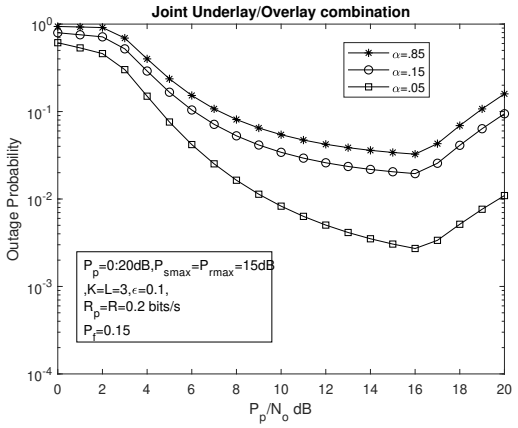

FIGURE 3.3: Comparison of outage performance of joint underlay/overlay mode w.r.t P_p/N_0 under varying α with fixed L=K=3

Fig. 3.3 shows the outage probability at secondary receiver (D) versus P_p/N_0 under joint underlay/overlay protocol with R_p=R=0.2 bits /sec/Hz, and keeping L=K=3. The outage analysis has been studied for three different values of α, i.e. α=0.85, 0.15, 0.05. We consider the maximum primary transmitting power to be 20 dB, whereas the the $SU-Tx$ and $SR-Tx$ transmit at a maximum power of 15 dB. Considering a realistic scenario based on channel occupancy (α), it is investigated that the outage performance gets deteriorated as α value increases. This reflects that outage is worst during busy hours which improves at inactive hours of PUs. This worst case of outage can be strategically improved by carefully adjusting the number of antennas and relays. We have also observed that the outage probability at the secondary receiver reduces gradually as the $PU-Tx$ power increases, up to a value which is decided by maximum transmit power of secondary transmitters. This is in true sense as the behavior observed in [17]. But as the primary transmit power increase beyond that value there is a degradation of outage behaviour at secondary receiver. The explanation of this behaviour can be justified by (3.14) and (3.18) which bounds the peak transmit power of secondary transmitter.

Fig. 3.4 shows the outage probability at secondary receiver versus P_p/N_0 under joint underlay/overlay protocol considering the variation of primary and secondary rates. It is observed that the outage probability at destination is improved with

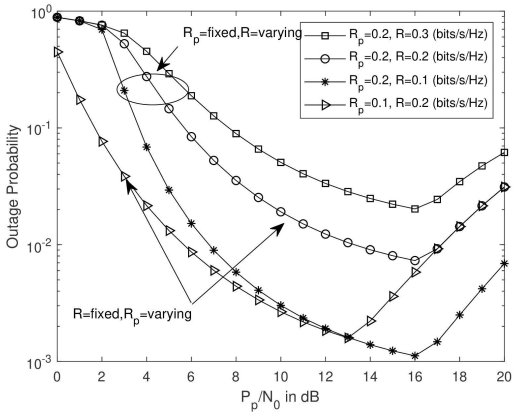

FIGURE 3.4: Comparing the outage at secondary D for different data rates

decreasing values of data rates at both SU and PU. The data rate of SU is compensated by reducing its value to achieve the desired level of outage performance when PU communicates with low power and high data rate.

In **Fig. 3.5**, keeping R_p=R= 0.2 bits /sec/Hz, α= 0.15 and K=5, the outage

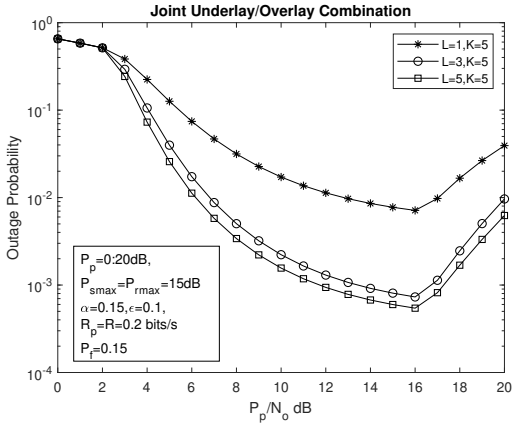

FIGURE 3.5: Comparing outage performance of joint underlay/overlay mode under fixed K, α and varying L

performance of secondary under joint underlay/overlay mode is analyzed by varying L from 1 to 5. The result also concludes that with increasing number of receiving antennas at each relay, the outage gives a good performance.

Similarly **Fig. 3.6** also shows the outage probability of the $SU - Tx$ to D as a function of P_p/N_0 under joint underlay/overlay mode keeping α=0.15, L=5 and with varying number of relays i.e. K=1, 3, 5. It has been observed that the outage

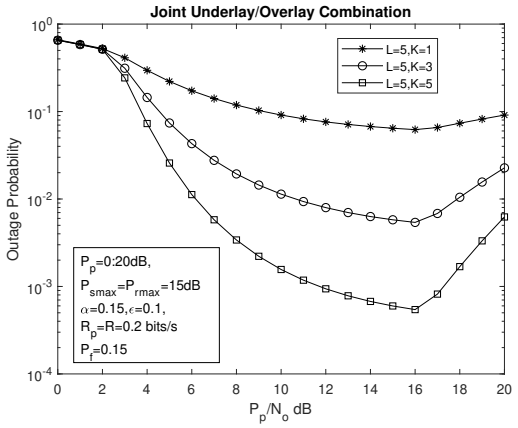

FIGURE 3.6: Comparing outage probability of joint underlay/overlay mode under fixed L, α and varying K

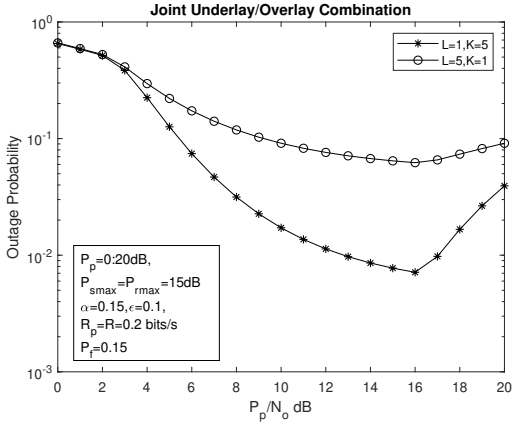

FIGURE 3.7: Comparing outage probability of joint underlay/overlay mode with same diversity order

performance is also better as the number of relays gets increased. So by adjusting the number of relays and number of receiving antennas at each relay, the outage performance can be improved during the busy hour of PU. Hence throughput of the secondary users can be maximized by this model.

It has also been found in **Fig. 3.7** that keeping the diversity order constant, the outage performance with L=1, K=5 is better than K=1, L=5. It is possible to trade-off between the number of antennas and relays to achieve a desired level of performance. Hence it is expected to have a better performance with increasing values of both L and K as required for the system performance leading a cooperative cognitive radio solution.

A comprehensive discussion based on joint underlay/overlay mode of transmission assisted by half duplex relay networks is presented in this section. In the next section, we expand on our discussion of AF, DF, and AHR relay-based cognitive radio networks in an energy harvesting and co-channel interference scenario.

Section 3.1 presented a cognitive radio system where SU transmission relies on underlay/overlay access and cooperative relaying, but the analysis was carried out assuming fixed-power relays without considering energy limitations at the secondary nodes. Although this model is useful for understanding the interaction between SU performance and PU protection, it does not fully capture the practical operating constraints of modern low-power cognitive devices (e.g., IoT-based SUs, sensor-assisted relays). To address this limitation, Section 3.2 extends the system model by incorporating energy harvesting (EH) capability and adaptive hybrid relaying (AHR).

3.2 The cognitive radio network system based on AF, DF and AH relay in presence of energy harvesting and co-channel interference environment

In this section, a performance analysis of multi relay-based CR network has been proposed in presence of co-channel interference (CCI) environment. Here the secondary nodes in the form of corresponding secondary transmitter (SU-Tx) along with secondary relay (SR) modules can harvest energy from the primary transmitter as well as CCI. This section proposes an adaptive hybrid relay (AHR) based underlay CR network, which uses an energy harvesting technique to capture energy from CCI and PU radio frequency (RF) signals in order to increase spectrum utility. AHR is the combination of AF and DF relay protocol which can switch in between depending on the channel condition. The closed form expression of secondary outage performance of AHR relay based CR network has been derived and compared with the conventional AF and DF mode in different conditions. In this scenario, secondary source (SU-Tx) communicates with secondary destination (SU-Rx) via multiple adaptive hybrid relays (SR) in presence of CCI including primary transmitter (PU-Tx) and primary receiver (PU-Rx). The relays as well as secondary source are furnished with energy harvesting circuits and rechargeable battery. Both can obtain energy from the source signal and interference from the primary transmitter, CCI, and use this energy for advancing the received signal to the destination. The proposed technique's analytical model supports the simulation test result which has been developed under MATLAB testbed.

3.2.1 System model AH relay based cognitive radio network in presence of co-channel interference environment

The system configuration as depicted in **Fig. 3.8**, is a proposed cognitive radio network model consisting of one primary user (PU), one secondary transmitter $(SU - Tx)$, single secondary receiver $(SU - Rx/D)$ and multiple relays $(R_k; k = 1, 2 \ldots K)$. Now it is assumed that the $(SU - Tx)$, $(SU - Rx/D)$, $(R_k; k = 1, 2 \ldots K)$ have a single transmitting and receiving antenna. Considering higher shadowing ef-

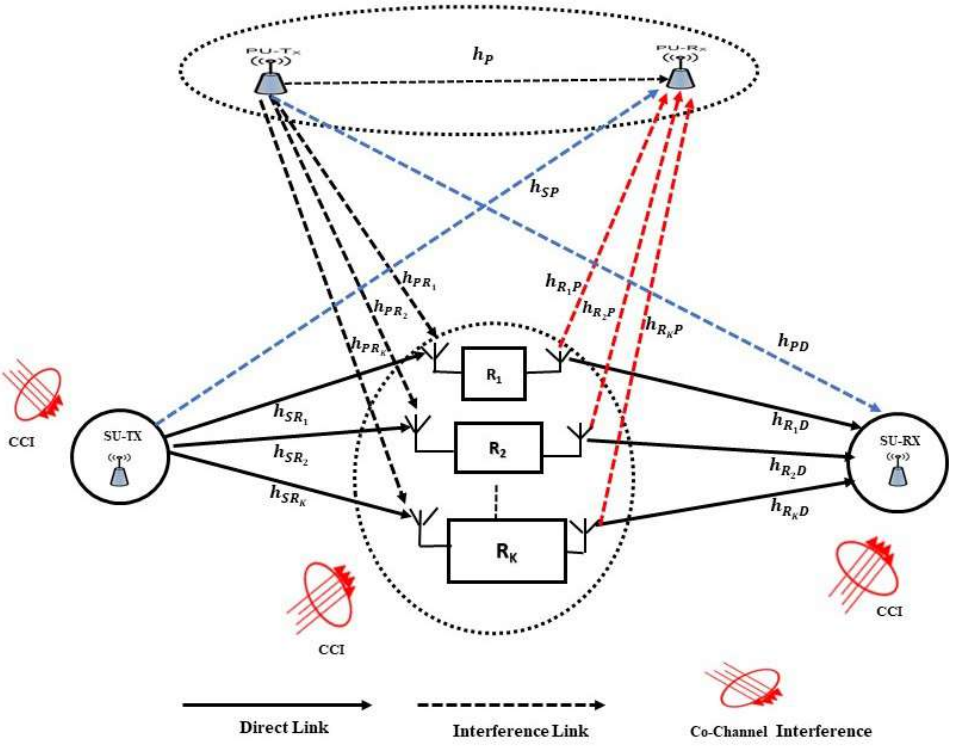

FIGURE 3.8: System model on AF, DF and AHR based cognitive radio network

fects, the direct link between $(SU-Tx)$ and $(SU-Rx)$ has been neglected here. All the relays are in AHR mode, i.e. in adaptive selection mode which can switch as a combination of AF and DF protocol depending on the channel quality. In this system model, we consider the effects of CCI at secondary transmitter, relays and secondary receiver. Additionally, all the secondary nodes get affected by the transmitted signal from PU-Tx, as an interference source. The impact of interference at primary receiver by the transmitted signal from SU-Tx and SRs is also addressed here. This has been assumed that, the secondary source and all relays are partially powered by collecting energy from ambient RF sources through EH circuits present at these nodes. The entire communication process is carried out using Time Switching Protocol (TSP) in dual hop mode. The important steps of the TSP protocol for information processing and energy harvesting at the relay are shown in **Fig.** 3.9. In consideration, T is the total time that is necessary for the information to travel from the secondary source to the secondary destination node through relays, where, $\hat{\tau}\ T$, $(0 < \hat{\tau} \leq 1)$ is the fraction of the total time that secondary source and relays use for energy harvesting. In the first time slot of transmission, $SU-Tx$ sends signal to relay $(R_k; k \in 1, 2, ..., K)$ under the condition of transmit power to ensure the interference to the primary user does not exceed the threshold constrained power (I_P). During the second time slot, the relay uses the AH protocol to transfer received signals to the secondary destination while keeping the interference threshold at I_P. According to the adapted hybrid relay (AHR) protocol, if the relay can de-

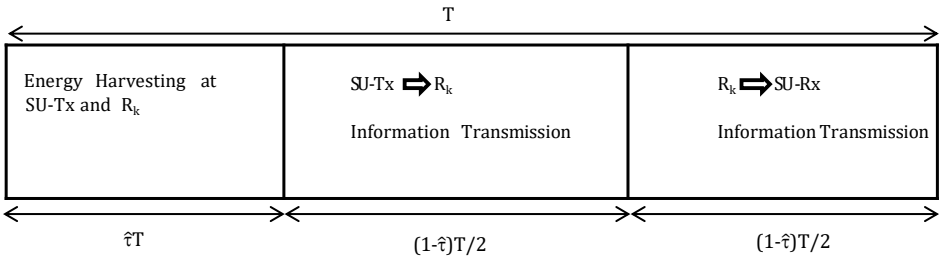

FIGURE 3.9: TSP frame for energy harvesting and information processing

code the received signal effectively, then DF scheme is followed, else the AF scheme

is continued. In this model, the channel path coefficients are presumed to be zero mean, unit variance independent non-identical Rayleigh distribution type as well as all noise factors are considered as additive white gaussian noise (AWGN) with variance N_0. Channel coefficients are denoted as follows: h_p denotes the channel path coefficient for $PU-Tx$ to $PU-Rx$, $h_{SR_k}(k=1,2,..,K)$ represents channel coefficient for $SU-Tx$ to k_{th} relay (R_K), $h_{PR_k}(k=1,2,..,K)$ is for $PU-Tx$ to k^{th} relay (R_k), h_{SP} is used to represent the channel coefficient for $SU-Tx$ to $PU-Rx$, $h_{R_kD}(k=1,2,..,K)$ is the channel coefficient for k_{th} relay (R_k) to $SU-Rx$, h_{PD} signifies the channel coefficient for $PU-Tx$ to $SU-Rx$. $h_{C_nR_k}$, h_{C_nD} are the channel coefficients from n^{th} CCI source to k^{th} relay and SU-Rx, respectively. The relay is chosen in such a way that it will improve the end-to-end SINR of the $SU-Tx$ to $SU-Rx$ channel path. Secondary sources $(SU-Tx)$ and relays have the capability to choose transmitted power amount which is varied between constrained transmitting power and energy harvesting power. All the channel power gains, denoted by g_x, follows an exponential nature distribution with a mean of λ_x, where x signifies appropriate channel link indicator suffix from each nodes. The exact link parameters are shown in TABLE 3.1 below. The power distribution at secondary sources

Table 3.1: Channel gain with parameter list

Path-Channel Gain indicator with parameter List		
Path-link	Channel Gain	Parameter
$PU-Tx$ - $SU-Tx$	g_{PS}	λ_{PS}
$PU-Tx$ - $SU-Rx$	g_{PD}	λ_{PD}
$n^{th}CCI$ - $SU-Tx$	g_{C_nS}	λ_{C_nS}
$PU-Tx$ - R_K	g_{PR_k}	λ_{PR_k}
$SU-Tx$ - R_K	g_{SR_k}	λ_{SR_k}
$n^{th}CCI$ - R_K	$g_{C_nR_k}$	$\lambda_{C_nR_k}$

$(SU-Tx)$ and relays are described in the following section.

3.2.2 Energy harvesting and power allocation strategies

The theory described here is employed to explore the power allocation strategy for $SU-Tx$ and SR_k.

Let us consider, total time taken to transmit the data packets from $SU-Tx$ to the $SU-Rx$ is T. Initially, fraction time $\hat{\tau}$ of T is reserved for harvesting energy at $SU-Tx$ and SR. The remaining time is used for data transmission in this dual hop communication process.

Energy harvested at $SU-Tx$ is expresses as,

$$E_S^H = \eta\hat{\tau}\left(P_p g_{PS} + \sum_{n=1}^{N} P_C g_{C_n S}\right) \tag{3.53}$$

P_p is denoted as the transmitted power by $PU-Tx$ and P_C is the power transmitted by single CCI node. The efficiency factor for the EH circuit at each node is defined by η.

Transmitted power at $SU-Tx$ due to this harvested energy is given by,

$$P_S^H = \left(\frac{E_S^H}{\frac{T(1-\hat{\tau})}{2}}\right) \tag{3.54}$$

Transmitted power of the $SU-Tx$ must be regulated so that the PU does not receive significant interference from the SU's communication. Therefore, the $SU-Tx$ transmit power should meet the PU receiver's interference power restriction, which is stated as,

$$P_S^T = \left(\frac{I_P}{|h_{SP}|^2}\right) \tag{3.55}$$

where, I_P is the threshold value of interference power at primary receiver $PU-Rx$.

Let P_S be the power transmitted by $SU-Tx$ during different mode of operation and can be written as,

$$P_S = \min(P_S^T, P_S^H) \tag{3.56}$$

Energy harvested at secondary relays SR_k is given by

$$E_R^H = \eta\tau \left(P_S g_{SR_k} + P_p g_{PR_k} + \sum_{n=1}^{N} P_C g_{C_n R_k} \right) \tag{3.57}$$

Transmitted power at each relay of SR_k due to EH is given by,

$$P_R^H = \left(\frac{E_R^H}{\frac{T(1-\hat{\tau})}{2}} \right) \tag{3.58}$$

Similarly, in order to prevent the PU from experiencing too much interference from the SU's transmission, the SR_k transmit power must also be controlled. As a result, transmitted power of SR_k must fulfil the interference power limitation of the PU receiver, which is given as,

$$P_{R_k}^T = \min_{k=1,2,\ldots,K} \left(\frac{I_P}{|h_{R_{kP}}|^2} \right) \tag{3.59}$$

Let P_R be the power transmitted by each relay of SR_k during different mode of operation which can be written as,

$$P_R = \min(P_{R_k}^T, P_R^H) \tag{3.60}$$

The secondary source $(SU - Tx)$ and relays SR_k must maintain the interference power threshold (I_P) with regards to the primary network.
The mathematical expression of received signal at k^{th} relay is given as:

$$y_{R_k}(t) = \sqrt{P_S} h_{SR_k} x_s(t) + \sqrt{P_P} h_{PR_k} x_p(t) + \sum_{n=1}^{N} \sqrt{P_C} h_{C_n R_k} x_c(t) + n_o(t) \tag{3.61}$$

The SINR through $SU - Tx$ to k^{th} relay is expressed as:

$$\gamma_{SR_k} = \frac{P_S |h_{SR_k}|^2}{P_p |h_{PR_k}|^2 + \sum_{n=1}^{N} P_C |h_{C_n R_k}|^2 + N_o} \tag{3.62}$$

The received signal at destination $SU-Rx$ coming from k^{th}relay is given as,

$$y_D(t) = \sqrt{P_R} h_{R_k D} x_r(t) + \sqrt{P_P} h_{PD} x_p(t) + \sum_{n=1}^{N} \sqrt{P_C} h_{C_n D} x_c(t) + n_o(t) \tag{3.63}$$

The SINR through SR_k to D is expressed as,

$$\gamma_{R_k D} = \frac{P_R |h_{R_k D}|^2}{P_p |h_{PD}|^2 + \sum_{n=1}^{N} P_C |h_{C_n D}|^2 + N_o} \tag{3.64}$$

where, $x_p(t)$, $x_s(t)$, $x_r(t)$, $x_c(t)$ are the transmitting signals from $PU-Tx$, $SU-Tx$, SR_k and co-channel transmitter respectively. This $n_0(t)$ is considered to be AWGN receiver noise with power spectral density N_0.

3.2.3 Performance analysis of AHR protocol

The AHR scheme adaptively changes between AF and DF mode depending upon channel condition. DF mode is applicable, if and only if relays decode the incoming signal successfully. This scheme utilizes all the relay to work effectively, which in term makes the system performance better than the conventional AF and DF. Therefore, relay allocating scheme is performed to choose the best link via the set of relays from source to destination.
The process of decoding at R_k succeeds only when $\gamma_{SR_k} > \mu_{th}$ i.e., DF protocol is continued otherwise AF protocol is pursued. μ_{th} is the threshold predefined SINR for successful decoding decision at the relay.

The DF relay scheme [56] defines a subset δ of k_1 relays out of K relays that can properly decode the received signal. Thus, the set can be described as $\delta = \{\forall k \in (1, 2..k_1)\,; \gamma_{SR_k} \geq \mu_{th}\}$. The relays k_1 effectively decodes the input signal when $\gamma_{SR_{k_1}} > \mu_{th}$. Now these k_1 relays of subset δ are participated in transmission from relays to destination in DF mode. Remaining $(K - k_1)$ count of relays operate in AF mode to transmit the message from relays to destination.

Therefore, the probability for a relay to operate in the AF scheme can be expressed as,

$$\begin{aligned} P^{AF} &= Pr\big(\gamma_{SR_k} < \mu_{th}\big) \\ &= Pr\Big(\frac{P_S|h_{SR_k}|^2}{P_p|h_{PR_k}|^2 + \sum_{n=1}^{N} P_C|h_{C_nR_k}|^2 + N_o} < \mu_{th}\Big) \end{aligned} \tag{3.65}$$

For determining the cumulative distribution function (CDF) of equation (3.65), we assume that $|h_{SR_k}|^2$ is denoted as independent exponentially distributed random variable X_1 with the PDF $f_{X_1}(x_1) = \frac{1}{\lambda_1} exp(-\frac{x_1}{\lambda_1})$ and $P_p|h_{PR_k}|^2 + \sum_{n=1}^{N} P_C|h_{C_lR_k}|^2 = \sum_{n=1}^{N+1} P_T|h_{nR_k}|^2$, represented as gamma distributed random variable X_2 with the PDF $f_{X_2}(x_2) = \frac{(x_2)^{n-1} exp(-\frac{(x_2)}{\lambda_2})}{\Gamma(n)\lambda_2^n}$. Since all channel power gain are independent identical exponential distribution with equal parameter of distribution, $\lambda_{PR_k} = \lambda_{C_lR_k} = \lambda_2$. λ_1 and λ_2 are considered as parameter of the distribution for respective random variables X_1 and X_2. So equation (3.65) can be rewritten as:

$$\begin{aligned} P^{AF} &= Pr\Big(\frac{P_S X_1}{P_T X_2 + N_0} < \mu_{th}\Big) \\ &= \int_{x_2=0}^{+\infty} \int_{x_1=0}^{\frac{(P_T\mu_{th}x_2 + \mu_{th}N_0)}{P_S}} f_{X_1}(x_1) f_{X_2}(x_2)\, dx_1\, dx_2 \\ &= \int_{x_2=0}^{+\infty} \int_{x_1=0}^{\frac{(P_T\mu_{th}x_2 + \mu_{th}N_0)}{P_S}} \frac{1}{\lambda_1} exp(-\frac{x_1}{\lambda_1}) f_{X_2}(x_2)\, dx_1\, dx_2 \\ &= \int_{x_2=0}^{+\infty} \Big[1 - exp\big(\frac{-(P_T\mu_{th}x_2 + \mu_{th}N_0)}{P_S\lambda_1}\big)\Big] f_{X_2}(x_2)\, dx_2 \\ &= 1 - exp(-\frac{\mu_{th}N_0}{P_S\lambda_1})\Big(\frac{P_S\lambda_1}{P_S\lambda_1 + \mu_{th}P_T\lambda_2}\Big)^n \end{aligned} \tag{3.66}$$

On the other hand, the probability for a relay operated in the DF scheme can be expressed as:

$$\begin{aligned} P^{DF} &= Pr\big(\gamma_{SR_k} \geq \mu_{th}\big) \\ &= 1 - P^{AF} \\ &= \Big[exp(-\frac{\mu_{th}N_0}{P_S\lambda_1})\big(\frac{P_S\lambda_1}{P_S\lambda_1 + \mu_{th}P_T\lambda_2}\Big)^n\Big] \end{aligned} \tag{3.67}$$

As per our proposed model, k_1 number of relays out of K relays are operated in DF mode. The probability distribution of successfully decoded k_1 relays out of total relays follows the binomial distribution, with parameters P^{AF}, P^{DF} and K. The outage probability for AHR scheme is dependent on outage performance of the corresponding relays for AF and DF mode ($i.e., P_O^{AF}, P_O^{DF}$). By the law of probability, the average outage probability for AHR scheme can be described as:

$$P_O^{AHR} = \sum_{k_1=0}^{K} C_{k_1}^{K} (P_{DF})^{k_1} (P_O^{DF})^{k_1} (P_{AF})^{K-k_1} (P_O^{AF})^{K-k_1} \tag{3.68}$$

Where, P_O^{AF} and P_O^{DF} are denoted as outage probabilities for AF, DF scheme at each relay, respectively. In the following section, analysis of outage probabilities for AF, DF scheme at each relay are described.

3.2.3.1 Outage analysis of AF protocol for single relay

The received signal at the relay is amplified and transferred to the secondary destination using the AF relaying method. The AF scheme has the advantages of being easy to implement and having a low computational load on the relay. But due to this amplification process, the additive noise causes serious problem. The instantaneous end to end SINR from secondary source to $SU - Rx$ via k^{th} relay can be written as [130]:

$$\gamma_k^{AF} = \frac{\gamma_{SR_k} \gamma_{R_k D}}{1 + \gamma_{SR_k} + \gamma_{R_k D}} \tag{3.69}$$

The end to end outage probability using AF relay scheme is expressed as:

$$P_O^{AF} = Pr\left(\gamma_k^{AF} \leq \gamma_{th}^{s}\right) \tag{3.70}$$

where, $\gamma_{th}^{s} = 2^{2R_s} - 1$ denotes the outage threshold at the $SU - Rx$. Let us consider the transmission rate of SU is R_s.

For calculating the CDF of equation (3.70) γ_{SR_k}, γ_{R_kD} are considered as random variables M, P respectively. Then γ_k^{AF} can be expressed as:

$$\gamma_k^{AF} = \frac{MP}{1+M+P} \tag{3.71}$$

$$F_{\gamma_k^{AF}}(\gamma_{th}^s) = Pr\Big(\frac{MP}{1+M+P} \leq \gamma_{th}^s\Big) \tag{3.72}$$

The probability in (3.72) is calculated using two integrations as follows [129, 130]:

$$\begin{aligned} F_{\gamma_k^{AF}} &= \int_{m=0}^{\gamma_{th}^s}\int_{p=0}^{+\infty} f_M(m)f_P(p)\,dm\,dp + \int_{m=\gamma_{th}^s}^{\infty}\int_{p=0}^{\frac{(m+1)\gamma_{th}}{m-\gamma_{th}}} f_M(m)f_P(p)\,dm\,dp \\ &= \underbrace{\int_{m=0}^{\gamma_{th}^s}\int_{p=0}^{+\infty} f_M(m)f_P(p)\,dm\,dp}_{S} + \underbrace{\int_{m=\gamma_{th}^s}^{\infty}\int_{p=0}^{\frac{(m+1)\gamma_{th}}{m-\gamma_{th}}} f_M(m)f_P(p)\,dm\,dp}_{T} \end{aligned} \tag{3.73}$$

Where $f_M(m)$, $f_M(m)$ are the PDF of respective random variables M, N. Here M is expressed as:

$$M = \frac{P_S|h_{SR_k}|^2}{P_p|h_{PR_k}|^2 + \sum_{n=1}^{N} P_C|h_{C_nR_k}|^2 + N_o} \tag{3.74}$$

For calculating the value of CDF for random variable M,

$$\begin{aligned} F_M(m) &= Pr(M \leq m) \\ &= Pr\Big(\frac{P_S|h_{SR_k}|^2}{P_p|h_{PR_k}|^2 + \sum_{n=1}^{N} P_C|h_{C_nR_k}|^2 + N_o} \leq m\Big) \end{aligned} \tag{3.75}$$

We assume that $|h_{SR_k}|^2$ is independent exponentially distributed random variable X_1 with the PDF $f_{X_1}(x_1) = \frac{1}{\lambda_1}exp(-\frac{x_1}{\lambda_1})$ and $P_p|h_{PR_k}|^2 + \sum_{n=1}^{N} P_C|h_{C_lR_k}|^2 = \sum_{n=1}^{N+1} P_T|h_{nR_k}|^2$ is represented as gamma distributed random variable X_2 with the PDF $f_{X_2}(x_2) = \frac{(x_2)^{n-1}exp(-\frac{(x_2)}{\lambda_2})}{\Gamma(n)\lambda_2^n}$. Since all channel power gain are independent identical exponential distribution with equal parameter of distribution, $\lambda_{PR_k} = \lambda_{C_lR_k} = \lambda_2$. λ_1 and λ_2 are considered as parameter of the distribution for respective random variables X_1 and

X_2. So equation (3.75) can be rewritten as:

$$\begin{aligned} F_M(m) &= Pr\Big(\frac{P_S X_1}{P_T X_2 + N_0} < m\Big) \\ &= \int_{x_2=0}^{+\infty} \int_{x_1=0}^{\frac{(P_T m x_2 + m N_0)}{P_S}} f_{X_1}(x_1) f_{X_2}(x_2)\, dx_1\, dx_2 \\ &= \int_{x_2=0}^{+\infty} \int_{x_1=0}^{\frac{(P_T m x_2 + m N_0)}{P_S}} \frac{1}{\lambda_1} exp(-\frac{x_1}{\lambda_1}) f_{X_2}(x_2)\, dx_1\, dx_2 \\ &= \int_{x_2=0}^{+\infty} \Big[1 - exp\big(-\frac{(P_T m x_2 + m N_0)}{P_S \lambda_1}\big)\Big] f_{X_2}(x_2)\, dx_2 \\ &= 1 - exp(-\frac{m N_0}{P_S \lambda_1})\Big(\frac{P_S \lambda_1}{P_S \lambda_1 + m P_T \lambda_2}\Big)^n \end{aligned} \tag{3.76}$$

The PDF of random variable M can be expressed as:

$$\begin{aligned} f_M(m) &= \frac{d(F_M(m))}{dm} \\ &= exp\big(-\frac{N_0}{P_S \lambda_1} m\big)\big(1 + \frac{P_T \lambda_2}{P_S \lambda_1} m\big)^{-(n+1)}\big(\frac{N_0}{P_S \lambda_1} + \frac{N_0 P_T \lambda_2}{P_S^2 \lambda_1^2} m + \frac{P_T \lambda_2}{P_S \lambda_1} n\big) \end{aligned} \tag{3.77}$$

Assuming $\frac{P_T \lambda_2}{P_S \lambda_1} = X$, $\frac{N_0 P_T \lambda_2}{P_S^2 \lambda_1^2} = Y$, $\frac{N_0}{P_S \lambda_1} = Z$, the equation (3.77) can be written as,

$$f_M(m) = exp(-Zm)(1 + Xm)^{-(n+1)}(Z + Ym + Xn) \tag{3.78}$$

The random variable P can be expressed as,

$$P = \frac{P_R |h_{R_k D}|^2}{P_p |h_{PD}|^2 + \sum_{n=1}^{N} P_C |h_{C_n D}|^2 + N_o} \tag{3.79}$$

For determining the value of CDF for random variable P,

$$\begin{aligned} F_P(p) &= Pr(P \le p) \\ &= Pr(\frac{P_R |h_{R_k D}|^2}{P_p |h_{PD}|^2 + \sum_{n=1}^{N} P_C |h_{C_n D}|^2 + N_o} \le p) \end{aligned} \tag{3.80}$$

We assume that $|h_{R_kD}|^2$ is denoted as independent exponentially distributed random variable X_3 with the PDF $f_{X_3}(x_3) = \frac{1}{\lambda_3} exp(-\frac{x_3}{\lambda_3})$ and $P_p|h_{PD}|^2 + \sum_{n=1}^{N} P_C|h_{C_nD}|^2 = \sum_{n=1}^{N+1} P_T|h_{xD}|^2$ is represented as gamma distributed random variable X_4 with the PDF $f_{X_4}(x_4) = \frac{(x_4)^{n-1} exp(-\frac{(x_4)}{\lambda_4})}{\Gamma(n)\lambda_4^n}$, since each channel power gain follows identical exponential distribution with equal distribution of parameter, $\lambda_{PD} = \lambda_{C_nD} = \lambda_4$. λ_3, λ_4 are considered as parameter of the distribution for respective random variables X_3 and X_4.

$$P = \frac{P_R X_3}{P_O X_4 + N_0} \tag{3.81}$$

$$Pr\Big(\frac{P_R X_3}{P_O X_4 + N_0} \leq \gamma_{th}^s\Big) \tag{3.82}$$

$$\begin{aligned} F_P(p) = & \int_{x_4=0}^{+\infty} \int_{x_3=0}^{\frac{(P_O p x_4 + p N_0)}{P_R}} f_{X_3}(x_3) f_{X_4}(x_4)\, dx_3\, dx_4 \\ & = \int_{x_4=0}^{+\infty} \int_{x_3=0}^{\frac{(P_O p x_4 + p N_0)}{P_R}} \frac{1}{\lambda_3} exp(-\frac{x_3}{\lambda_3}) f_{X_4}(x_4)\, dx_3\, dx_4 \\ & = \int_{x_4=0}^{+\infty} \Big[1 - exp\big(-\frac{(P_O p x_4 + p N_0)}{P_R \lambda_1}\big)\Big] f_{X_4}(x_4)\, dx_4 \\ & = 1 - exp(-\frac{p N_0}{P_R \lambda_3}) \Big(\frac{P_R \lambda_3}{P_R \lambda_3 + p P_O \lambda_4}\Big)^n \end{aligned} \tag{3.83}$$

The PDF for random variable P being expressed as:

$$\begin{aligned} f_P(p) &= \frac{d(F_P(p))}{dp} \\ &= exp\big(-\frac{p N_0}{P_R \lambda_3}\big)\big(1 + \frac{p \lambda_4 P_O}{P_R \lambda_3}\big)^{-(n+1)} \big(\frac{N_0}{P_R \lambda_3} + \frac{N_0 P_O \lambda_4}{P_R^2 \lambda_3^2} p + \frac{P_O \lambda_4}{P_S \lambda_3} n\big) \end{aligned} \tag{3.84}$$

After considering $\frac{P_O \lambda_4}{P_R \lambda_3} = A$, $\frac{N_0 P_O \lambda_4}{P_R^2 \lambda_3^2} = B, \frac{N_0}{P_R \lambda_3} = C$, the equation (3.84) is written as:

$$f_P(p) = exp(-Cp)(1 + Ap)^{-(n+1)}(C + Bp + An) \tag{3.85}$$

The solution of integration under notation S in equation (3.73) can be expressed as

$$\begin{aligned} S = & \int_{m=0}^{\gamma_{th}^{s}} \int_{p=0}^{+\infty} f_M(m) f_P(p)\, dm\, dp \\ = & \int_{m=0}^{\gamma_{th}^{s}} exp(-Zm)(1+Xm)^{-(n+1)}(Z+Ym+Xn)\, dm \end{aligned} \tag{3.86}$$

Applying the approximation of $n+1 \approx n$, $(1+\alpha x)^{-n} = exp(-n\alpha x)$ and considering $Z + nX = S$

$$\begin{aligned} S = & \int_{m=0}^{\gamma_{th}^{s}} exp(-(Z+nX)m)(Z+Ym+Xn)\, dm \\ = & \int_{m=0}^{\gamma_{th}^{s}} exp(-Sm)(Ym+S)\, dm \\ = & -\frac{exp(-\gamma_{th}^{s}S)(\gamma_{th}^{s}SY + S^2 + Y) + S^2 + Y}{S^2} \end{aligned} \tag{3.87}$$

In equation (3.73), the solution of integration under notation T can be written as [131]:

$$\begin{aligned} T = & \int_{m=\gamma_{th}^{s}}^{\infty} \int_{p=0}^{\frac{(m+1)\gamma_{th}}{m-\gamma_{th}}} f_M(m) f_P(p)\, dm\, dp \\ = & \int_{m=\gamma_{th}^{s}}^{\infty} \int_{p=0}^{\infty} f_M(m) f_P(p)\, dm\, dp \\ = & \int_{m=\gamma_{th}^{s}}^{+\infty} exp(-Sm)(Ym+S)\, dm \\ = & \int_{m=\gamma_{th}^{s}}^{\infty} exp(-Sm)(Ym+S)\, dm \\ = & \frac{Y exp(\frac{S^2}{Y})}{S^2} \cdot \Gamma\left(2, S\gamma_{th}^{s} + \frac{S^2}{Y}\right) \end{aligned} \tag{3.88}$$

After putting the value of S and T in equation (3.73), the CDF of γ_k^{AF} is

$$\begin{aligned} F_{\gamma_k^{AF}} = \Bigg[& \left(-\frac{exp(-\gamma_{th}^{s}S)(\gamma_{th}^{s}SY + S^2 + Y) + S^2 + Y}{S^2} \right) \\ & + \left(\frac{Y exp\frac{S^2}{Y}}{S^2} \cdot \Gamma\left(2, S\gamma_{th}^{s} + \frac{S^2}{Y}\right) \right) \Bigg] \end{aligned} \tag{3.89}$$

So, the expression of equation (3.89) is the outage probability of k^{th} relay using AF relay scheme.

3.2.3.2 Outage analysis of DF protocol for single relay

The DF relay scheme [56] defines that a relay successfully decodes the incoming signal before transmission to secondary destination. The relay effectively decodes the input signal when $\gamma_{SR_k} > \mu_{th}$. The received SINR at destination from k^{th} relay can be expressed as:

$$\gamma_D^{DF} = \gamma_{R_k D} \tag{3.90}$$

As probability for a relay operated in the DF scheme can be expressed as P^{DF}, mathematically outage probability using DF relay scheme is formulated as [67]:

$$\begin{aligned} P_O^{DF} &= Pr(\gamma_D^{DF} \leq \gamma_{th}^s) P^{DF} \\ &= Pr(\frac{P_R |h_{R_k D}|^2}{P_p |h_{PD}|^2 + \sum_{n=1}^{N} P_C |h_{C_n D}|^2 + N_o} \leq \gamma_{th}^s) P^{DF} \end{aligned} \tag{3.91}$$

where, $\gamma_{th}^s = 2^{2R_s} - 1$ denotes the outage threshold at the $SU - Rx$. R_s is the transmission rate of SUs.

For calculating the CDF of equation $Pr(\gamma_D^{DF} \leq \gamma_{th}^s)$, $|h_{R_k D}|^2$ is denoted as independent exponentially distributed random variable X_3 with the PDF $f_{X_3}(x_3) = \frac{1}{\lambda_3} exp(-\frac{x_3}{\lambda_3})$ and $P_p |h_{PD}|^2 + \sum_{n=1}^{N} P_C |h_{C_n D}|^2 = \sum_{n=1}^{N+1} P_T |h_{xD}|^2$ is represented as gamma distributed random variable X_4 with the PDF $f_{X_4}(x_4) = \frac{(x_4)^{n-1} exp(-\frac{(x_4)}{\lambda_4})}{\Gamma(n) \lambda_4^n}$. Since each channel power gain follows identical exponential distribution with equal distribution of parameter, $\lambda_{PD} = \lambda_{C_n D} = \lambda_4$. λ_3, λ_4 are considered as parameter of the distribution for respective random variables X_3 and X_4.

$$P = \frac{P_R X_3}{P_O X_4 + N_0} \tag{3.92}$$

$$Pr\Big(\frac{P_R X_3}{P_O X_4 + N_0} \leq \gamma_{th}^s\Big) \tag{3.93}$$

$$\begin{aligned} F_P(\gamma_{th}^s) = & \int_{x_4=0}^{+\infty} \int_{x_3=0}^{\frac{(P_O \gamma_{th}^s x_4 + \gamma_{th}^s N_0)}{P_R}} f_{X_3}(x_3) f_{X_4}(x_4)\, dx_3\, dx_4 \\ & = \int_{x_4=0}^{+\infty} \int_{x_3=0}^{\frac{(P_O p x_4 + \gamma_{th}^s N_0)}{P_R}} \frac{1}{\lambda_3} exp(-\frac{y}{\lambda_3}) f_{X_4}(x_4)\, dx_3\, dx_4 \\ & = \int_{x_4=0}^{+\infty} \Big[1 - exp\big(-\frac{(P_O p x_4 + \gamma_{th}^s N_0)}{P_R \lambda_1}\big)\Big] f_{X_4}(x_4)\, dx_4 \\ & = 1 - exp(-\frac{\gamma_{th}^s N_0}{P_R \lambda_3}) \Big(\frac{P_R \lambda_3}{P_R \lambda_3 + \gamma_{th}^s P_O \lambda_4}\Big)^n \end{aligned} \tag{3.94}$$

The PDF for random variable P being expressed as:

$$f_P(\gamma_{th}^s) = exp\big(\frac{-\gamma_{th}^s N_0}{P_R \lambda_3}\big) \big(1 + \frac{\gamma_{th}^s \lambda_4 P_O}{P_R \lambda_3}\big)^{-(n+1)} \big(\frac{N_0}{P_R \lambda_3} + \frac{N_0 P_O \lambda_4 \gamma_{th}^s}{P_R^2 \lambda_3^2} + \frac{P_O \lambda_4 n}{P_S \lambda_3}\big) \tag{3.95}$$

After applying the value of $Pr[\gamma_D^{DF} \leq \gamma_{th}^s]$ and P^{DF}, the solution of the outage probability in DF relay scheme in (3.91), is expressed as:

$$\begin{aligned} P_O^{DF} = & \Big[1 - exp(-\frac{\gamma_{th}^s N_0}{P_R \lambda_3}) \Big(\frac{P_R \lambda_3}{P_R \lambda_3 + \gamma_{th}^s P_O \lambda_4}\Big)^n\Big] \\ & \times \Big[exp(-\frac{\mu_{th} N_0}{P_S \lambda_1}) \Big(\frac{P_S \lambda_1}{P_S \lambda_1 + \mu_{th} P_T \lambda_2}\Big)^n\Big] \end{aligned} \tag{3.96}$$

The solutions of P_O^{AF} and P_O^{DF} for single relay based system are applied in equation (3.68) to find out the close form of outage probability for AHR scheme; so the

expression is written as:

$$
\begin{aligned}
P_O^{AHR} &= \sum_{k_1=0}^{K} C_{k_1}^{K} (P_{DF})^{k_1} (P_O^{DF})^{k_1} (P_{AF})^{K-k_1} (P_O^{AF})^{K-k_1} \\
&= \sum_{k_1=0}^{K} C_{k_1}^{K} \Big\{ exp(-\frac{\mu_{th} N_0}{P_S \lambda_1}) \big(\frac{P_S \lambda_1}{P_S \lambda_1 + \mu_{th} P_T \lambda_2} \big)^n \Big\}^{k_1} \\
&\quad \times \Bigg[\Big\{ 1 - exp(-\frac{\gamma_{th}^s N_0}{P_R \lambda_3}) \big(\frac{P_R \lambda_3}{P_R \lambda_3 + \gamma_{th}^s P_O \lambda_4} \Big)^n \Big\} \\
&\quad \times \Big\{ exp(-\frac{\mu_{th} N_0}{P_S \lambda_1}) \big(\frac{P_S \lambda_1}{P_S \lambda_1 + \mu_{th} P_T \lambda_2} \Big)^n \Big\} \Bigg]^{k_1} \\
&\quad \times \Big\{ exp(-\frac{\mu_{th} N_0}{P_S \lambda_1}) \big(\frac{P_S \lambda_1}{P_S \lambda_1 + \mu_{th} P_T \lambda_2} \Big)^n \Big\}^{K-k_1} \\
&\times \Bigg[\Big\{ - \frac{exp(-\gamma_{th}^s S)(\gamma_{th}^s SY + S^2 + Y) + S^2 + Y}{S^2} \Big\} \\
&\quad + \Big\{ \frac{Y exp\frac{S^2}{Y}}{S^2} \cdot \Gamma \left(2, S\gamma_{th}^s + \frac{S^2}{Y} \right) \Big\} \Bigg]^{K-k_1}
\end{aligned}
\tag{3.97}
$$

Depending on the working mode of relays, AHR scheme exhibits two extreme conditions which are as follows:

Condition 1:

In the AHR scheme, it is assumed that decoding SINR for all the relays (K) is below the threshold decoding SINR (μ_{th}), so all relays operate in AF mode. In this case, number of DF operated relays (k_1) is zero.With the help of equation (3.68) and (3.89), the outage performance at secondary receiver for this case is expressed as:

$$
\begin{aligned}
P_O^{AHR} &= (P_{AF})^K (P_O^{AF})^K \\
&= \Bigg[\Big\{ exp(-\frac{\mu_{th} N_0}{P_S \lambda_1}) \big(\frac{P_S \lambda_1}{P_S \lambda_1 + \mu_{th} P_T \lambda_2} \Big)^n \Big\}^K \\
&\times \Bigg[\Big\{ - \frac{exp(-\gamma_{th}^s S)(\gamma_{th}^s SY + S^2 + Y) + S^2 + Y}{S^2} \Big\} \\
&\quad + \Big\{ \frac{Y exp\frac{S^2}{Y}}{S^2} \cdot \Gamma \left(2, S\gamma_{th}^s + \frac{S^2}{Y} \right) \Big\} \Bigg]^K \Bigg]
\end{aligned}
\tag{3.98}
$$

Condition 2:

In this case, all relays (K) are considered in DF mode because the decoding SINR for the relays is above the threshold decoding SINR (μ_{th}). The number of DF operated relays (k_1) is now K. With the help of equation (3.68) and (3.96), the outage performance at the secondary receiver in this scenario is as follows:

$$\begin{aligned} P_O^{AHR} &= (P_{DF})^K (P_O^{DF})^K \\ &= \left[\left\{ exp(-\frac{\mu_{th} N_0}{P_S \lambda_1}) \left(\frac{P_S \lambda_1}{P_S \lambda_1 + \mu_{th} P_T \lambda_2} \right)^n \right\}^K \right. \\ &\times \left[\left\{ 1 - exp(-\frac{\gamma_{th}^s N_0}{P_R \lambda_3}) \left(\frac{P_R \lambda_3}{P_R \lambda_3 + \gamma_{th}^s P_O \lambda_4} \right)^n \right\} \right. \\ &\left. \left. \times \left\{ exp(-\frac{\mu_{th} N_0}{P_S \lambda_1}) \left(\frac{P_S \lambda_1}{P_S \lambda_1 + \mu_{th} P_T \lambda_2} \right)^n \right\} \right]^K \right] \end{aligned} \tag{3.99}$$

3.2.4 Results and discussion

This section summarizes the outcomes of the experiments conducted using the MATLAB simulation testbed, as well as a brief comments based on the results. The numerical results presented here exhibit how the suggested relay-assisted AHR protocol yields improved performance during spectrum access.

Fig. 3.10 shows the comparison of outage performance at destination between AF, DF and AHR scheme. In this figure, it has been shown that with the same number of relays (K=4), AHR scheme achieves better outage performance than individual outage performance of AF and DF scheme respectively. This implies that the AHR scheme is highly efficient than individual DF and AF schemes wroking at a time. The working principle of AHR protocol is dynamic depending upon the decoding procedure of the received signal at relays. The successfully decoded signal follows DF protocol; else AF protocol is maintained. Every relay takes part in this process, which improves the diversity numbers of the relay to select the best one. Finally this scheme of adaptive control increases the system performance with respect to other two individual schemes.

Fig. 3.11 shows the probability of outage in the secondary receiver (D) versus

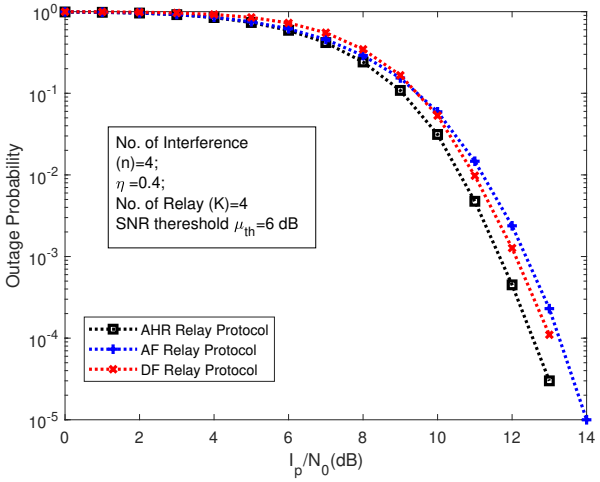

FIGURE 3.10: Comparison of outage performance w.r.t I_p/N_0 under AF, DF and AHR mode

I_p/N_0 under the AHR protocol. The outage analysis at the secondary receiver (D) has been investigated for various numbers of relays ($i.e., K = 2,\ 3,\ 4$). It is observed that outage performance at destination is improved with increasing number of relays. This indicates that the increase in diversity is causing the outages to improve. In **Fig. 3.12** depicts the probability of outage at the secondary receiver (D) versus

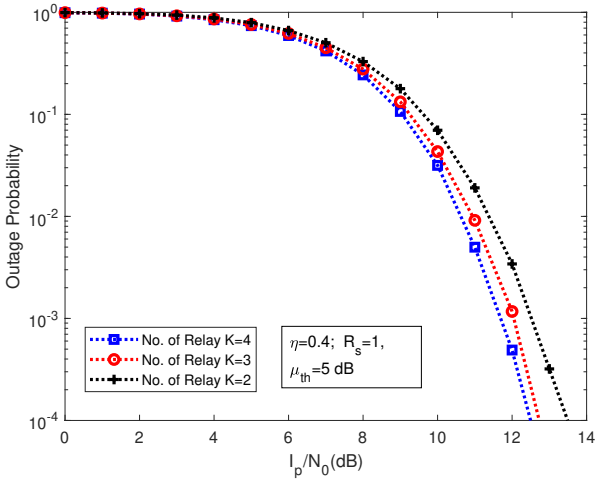

FIGURE 3.11: Comparison of outage performance w.r.t I_p/N_0 under AHR mode with varying K= 2,3,4

I_p/N_0 under the AHR protocol, with constant $R_s = 1$ bit / sec / Hz and fixed number of relays (K=4) with varying energy harvesting efficiency ($i.e, \eta = 0.2,\ 0.4,\ 0.6$).

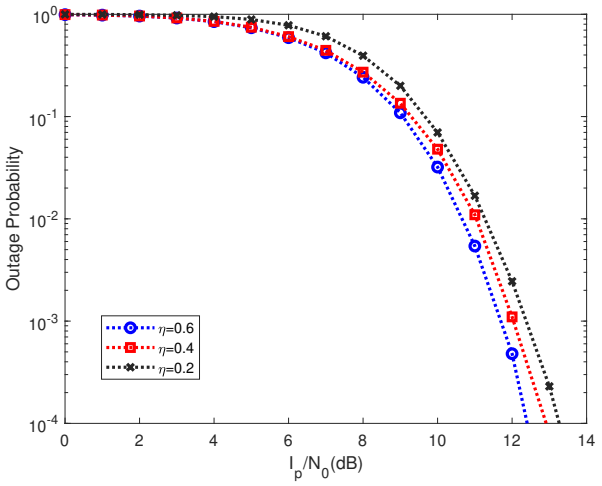

FIGURE 3.12: Comparison of outage performance w.r.t I_p/N_0 under AHR mode with fixed K = 4 varying η= 0.2, 0.4 and 0.6

The result also concludes that the increasing energy harvesting efficiency factor provides good outage performance. Due to the higher value of η, the amount of energy harvested at the SU transmitter and SU relays is higher eventually leading to highly powered signals to be transmitted from these nodes to their desired destinations. The effect of noise and interference is reduced at the secondary destination due to the highly powered received signal.

The probability of outage at the secondary receiver (D) versus I_p/N_0 under the

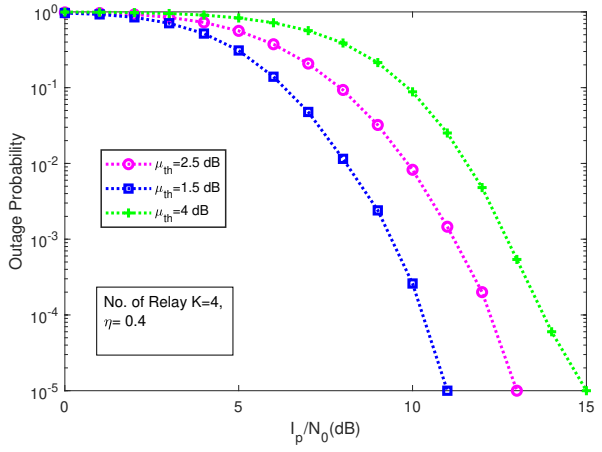

FIGURE 3.13: Comparison of outage performance w.r.t I_p/N_0 under AHR mode varying μ_{th}= 2.5 dB, 1.5 dB, 4 dB with fixed K=4

AHR protocol with fixed relays (K=4) is represented in **Fig. 3.13**. Using various SINR decoding thresholds ($\mu_{th} = 2.5\ dB,\ 1.5\ dB,\ 4\ dB$), the performance of secondary receiver outage is explored in the AHR scheme with a fixed number of relays. The outcome of the figure shows that the decrease in the SINR decoding threshold (μ_{th}) provides good outage performance.

3.3 Chapter summary

In this chapter, we have covered the analysis of adaptive transmission and relaying strategies to enhance spectrum efficiency and reliability in cognitive radio networks. The adaptive joint underlay/overlay transmission scheme dynamically switches between modes based on primary user (PU) activity, offering improved outage performance and throughput, especially when the number of secondary user (SU) relays exceeds the number of receiving antennas at each relay. An increase in the number of antennas incorporated in each relay has the added benefit of increasing diversity order, which improves system performance. Therefore, changing the number of relays and receiving antennas at each relay can improve the outage performance during PU's peak hours. Consequently, this model optimizes the throughput of the SUs. Additionally, we introduced and evaluated Amplify-and-Forward (AF), Decode-and-Forward (DF), and Adaptive Hybrid Relaying (AHR) protocols under co-channel interference (CCI) and energy harvesting scenarios. A comparison between all the modes of transmission has been discussed with a better outage being reflected in the AHR protocol. Overall, the integration of adaptive mode switching, cooperative diversity through multi-antenna and multi-relay configurations, and energy harvesting from CCI and PU signals results in a highly efficient and robust spectrum access strategy for CR networks, particularly under high interference and busy traffic conditions.

Chapter 4

Performance analysis of full-duplex multirelay based multi user cognitive radio network under linear and non-linear energy harvesting environment

This chapter is divided into three sections, each of which focuses on a cognitive radio network with a full-duplex (FD) relay network. However, the principles of operation of each section vary depending on the system design. An energy harvesting-based cognitive radio network (CRN) that uses a joint underlay/overlay protocol to assess the end-to-end outage performance of secondary user communications under a full-duplex relay network opens the first section.

In the second section, an investigation is performed on the outage performance of secondary receiver with an energy harvesting cognitive radio network employing multiple full-duplex relaying protocol in the presence of a multi-user spectrum sharing environment. Under this energy harvesting aided FD relaying network scenario,

adaptive transmit power policies for the secondary user (SU) source, secondary FD relays and exact outage probability of the secondary user are derived analytically in presence of multiple primary users and multiple secondary destinations. Impact of self interference at the receive antenna of each FD relay in addition to all the transmitting interference at all receive nodes is being addressed. A comparative study considering all the interference together in an FD relaying protocol with that of conventional half-duplex (HD) relaying protocol is carried out. With the same diversity order, a trade-off between FD multi-relay and multi-destination is shown. Finally, in the last section of this chapter, the outage performance of secondary users under a practical nonlinear energy harvesting scenario in a cognitive radio network communicating via full-duplex relay network, using a joint underlay/overlay protocol has been presented.

4.1 Performance analysis on multiple full-duplex relay based multi primary cognitive radio network

A dynamically adaptable amalgamation of the underlay/overlay protocol is created based on channel occupancy to improve the efficiency of the spectrum. A radio frequency energy detector circuit is present in each secondary transmitter node, allowing it to detect energy from the transmitters of several primary users. The FD relays together with the hybrid functioning of joint mode of transmission allows for an improvement in system throughput. We devised a mathematical study to jointly assign power at each transmitting node in such a way that improves the throughput of the system. Lastly, all analytical mathematical statements in closed form have been verified using MATLAB simulations.

4.1.1 System model on multiple full-duplex relay based cognitive radio network

Fig. 4.1 depicts the system architecture of a cognitive radio network where a secondary user transmitter (SU_{TR}) makes a communication with secondary user receiver (SU_R) via multi- FD relays ($R_l; l = 1, 2 \dots L$) in presence of multi-primary users ($PU_m; m = 1, 2 \dots M$). Each of the FD relays are incorporated with one

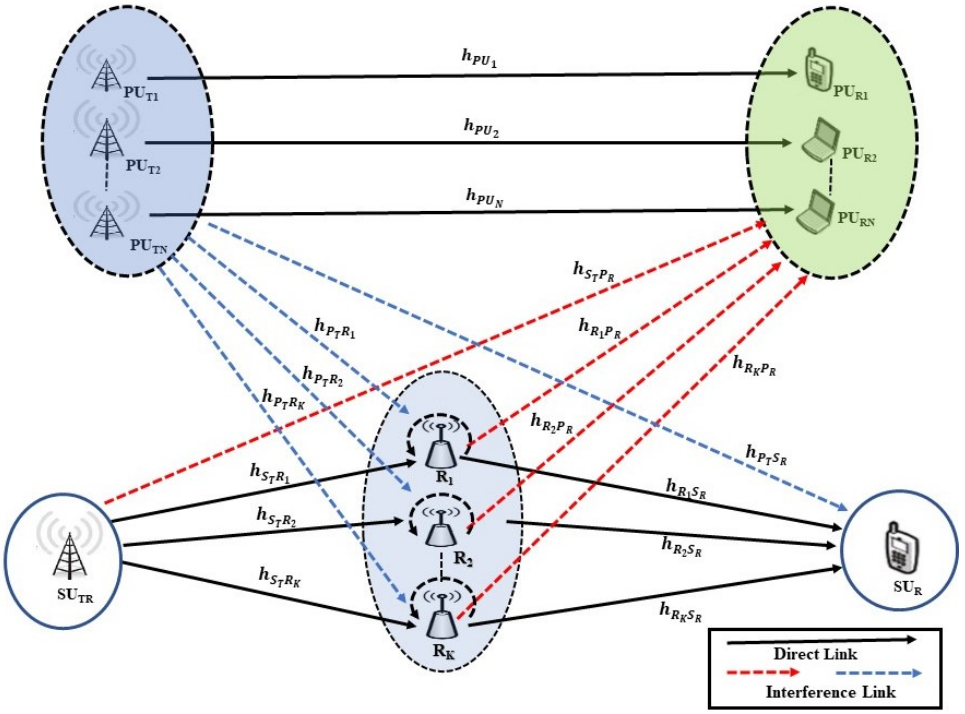

FIGURE 4.1: System model on multi-FD relay based CRN

transmitting and one receiving antenna while all other nodes carry single antenna. It is also assumed that in the suggested system model, there is no direct connectivity between SU_{TR} and SU_R due to excessive shadowing and multipath propagation loss. The EH-enabled circuits are attached on both FD relays and (SU_{TR}), allowing them to draw power from RF signals in the surrounding area. The interference source of the M active PUs can be used by the secondary transmitting nodes (i.e. SU_{TR}, FD relays) to generate some amount of their energy. The SU_{TR} connects with the SU_R over the FD relay network in a concurrent transmitting-receiving procedure. All of

the channel coefficients are considered by $h_{x,y}$, which obeys the Rayleigh distribution and the equivalent power gains are expressed as $g_{x,y}$. This follows an exponential distribution with mean λ_m, where'x,y' represents the relevant channel pathway with suffix $m = a, .., h$ from each node. The distinct path specifications are displayed in the following Table 4.1. In the proposed system, the transmission procedure is considered to be of a dual-hop nature.The first hop is concerned with transmitting data from SU_{TR} to R_L, where the best relay R_L is selected in accordance with the relay section scheme and channel quality, respectively. The principal operation

TABLE 4.1: Path-with channel gain parameter chart

Path-with channel gain parameter chart		
Path-(i,j),channel coefficient($h_{i,j}$)	gain $g_{i,j}$	Parameter chart λ_m
PU_{TM}-PU_{RM}, h_{p_m}	g_{p_n}	λ_a
SU_{TR}-PU_{RM}, $h_{S_TP_R}$	$g_{S_TP_R}$	λ_b
R_L-PU_{RM}, $h_{R_LP_R}$	$g_{R_LP_R}$	λ_c
PU_{TM}-R_L, $h_{P_TR_L}$	$g_{P_TR_L}$	λ_d
PU_{TM}-SU_R, $h_{P_TS_R}$	$g_{P_TS_R}$	λ_e
SU_{TR}-R_L, $h_{S_TR_L}$	$g_{S_TR_L}$	λ_f
R_L-SU_R, $h_{R_LS_R}$	$g_{R_LS_R}$	λ_g
R_L-R_L, h_{R_L}	g_{R_L}	λ_h

is based on two phases of time slots as in phase one, the secondary transmitters take part in sensing as well as energy harvesting activity by energy detector and EH circuit respectively. Additionally, in phase two, all the secondary transmitters actively take part in data transmission. The optimal relay is selected using this relaying selection combination (SC) strategy based on a process to optimise the minimum of the weighted channel strength between the links from the source to the relays and from the relays to the destination. As the relay R_L has been assumed to operate in full-duplex mode, it is receiving and transmitting data at the same time, which is what mostly causes self-interference (SI) at the receive antenna of R_L. This SI is being modelled as an independent Rayleigh distributed channel.The implementation of the successive interference cancellation (SIC) process is unable to

fully eliminate SI at the relay.

In order to increase the spectrum efficiency of the CR network, this study provides an adaptive hybrid underlay/overlay transmission system. SU_{TR} and all relays can detect PU activity using an energy detector circuit built into them. Relays and SU_{TR} made wise decisions by switching between underlay and overlay mode depending on the outcome of the PU activity to communicate with secondary receiver. Upon detection, if PU is found out to be engaged, SU_{TR} shifts to underlay mode; else, SU_{TR} functions at its maximum power in overlay mode, assisted by a number of active FD relays. According to data from the FCC [128], average channel occupancy for the measuring period is close to 15%,while peak utilisation is close to 85%. It is assumed that α represents probability of channel occupancy ($0 \leq \alpha \leq 1$), which depicts the busyness of PUs. As a result, the probability of PU being busy is αP_d, while the probability of PU being inactive is $(1-\alpha)P_d$, where, this probability of detection P_d identifies the probability of the presence of primary signal.

4.1.2 Compact power allocation at every nodes

Time Switching Relaying (TSR) protocol is used by the secondary source SU_{TR} and the relays R_L for manual energy harvesting and signal transfer. It is presumed that T is the entire amount of time needed for a message packet from SU_{TR} to the secondary destination. Additionally, the assumption has been made that secondary transmitting nodes requires τ amount of time to sense as well as gather energy from the M number of PU transmitter. The remaining time $(T-\tau)$ is utilised to transmit data.

Over a given time τ, the total harvested energy from M active primary transmitters at secondary sources are calculated as described below.

The amount of harvested energy at SU_{TR} is given by:

$$E_{S_{TR}}^{H} = \eta\tau \left(\sum_{m=1}^{M} P_m g_{m_s} \right) \tag{4.1}$$

where, P_m represents the transmitted power from a single PU_{TR} and g_{m_s} is the associated channel gain. η specifies the energy harvesting circuit's efficiency factor at each secondary transmitter node. The amount of transmit power at SU_{TR} during the time $(T-\tau)$ is expressed as,

$$P_{S_{TR}}^{H} = \left(\frac{E_{S_{TR}}^{H}}{T-\tau}\right) \tag{4.2}$$

The amount of harvested energy at R_L relay during time τ from M active primary transmitters and secondary source SU_{TR} is given by

$$E_{R_L}^{H} = \eta\tau \left(P_{st} g_{S_T R_L} + \sum_{m=1}^{M} P_m g_{P_T R_L}\right) \tag{4.3}$$

where, P_{st} represents the underlay mode transmit power by SU_{TR}, that maintains the outage constraint of primary. In a similar way, accompanied by EH circuit, R_L operates with its transmit power at time $(T-\tau)$ which is expressed as:

$$P_{R_L}^{H} = \left(\frac{E_{R_L}^{H}}{T-\tau}\right) \tag{4.4}$$

The peak interference parameter I_p of the primary network limits the simultaneous transmit power from SU_{TR} and R_L. This has been reflected in the following equation as we depend on the idea of sharing spectrum with R_L operating in full-duplex communication process [132].

$$I_p \geq (P_{st} g_{S_T P_R} + P_{R_L} g_{R_L P_R}) \tag{4.5}$$

From above expression, assuming non optimal condition for P_{st} and P_{R_L} for simplicity, the necessary condition reflects that the transmit power of SU_{TR} and R_L are maintained such that the communication of SUs does not cause any PUs to be overly interfered.

The received signal at n^{th} PU face the signal-to-interference-noise-ratio (SINR) as:

$$\gamma_n = \frac{P_m g_{P_m}}{P_{st} g_{S_T P_R} + P_{R_L} g_{R_L P_R} + N_0} \tag{4.6}$$

The SU_{TR} and R_L transmit powers should be maintained in order to prevent any PUs from experiencing severe interference from the SU's transmission.
Therefore, the outage value at the PU receiver can be expressed as:

$$P_O^p = Pr\left[\min_{m=1,\ldots,M}\left(\frac{P_m g_{P_m}}{P_{st} g_{S_T P_R} + P_{R_L} g_{R_L P_R} + N_0} \leq \gamma_{th}^{Pr}\right)\right] \leq \varepsilon \tag{4.7}$$

here, $\gamma_{th}^{Pr} = 2^{R_{Pr}} - 1$ and ε signify the outage threshold and constraint of a primary receiver (PU_{Re}), respectively where PU transmits data at the rate of R_{Pr}.
After considering non optimal power condition, equation (4.7) can be modified as

$$\begin{aligned} P_O^p &= Pr\left[\min_{m=1,2,\ldots,M}\left(\frac{P_m g_{P_m}}{2P_{st} g_{S_T P_R} + N_0} \leq \gamma_{th}^{Pr}\right)\right] \leq \varepsilon \\ &= 1 - \sum_{m=1}^{M}\left[1 - \underbrace{Pr\left(\frac{P_m g_{P_m}}{2P_{st} g_{S_T P_R} + N_0} \leq \gamma_{th}^{Pr}\right)}_{P^w}\right] \leq \varepsilon \end{aligned} \tag{4.8}$$

The aforementioned expression can be used to demonstrate the outage probability of P^w as [67],

$$P^w = 1 - \exp\left(-\frac{\gamma_{th}^{Pr} N_0}{P_p \lambda_a}\right)\left(\frac{P_p \lambda_a}{P_p \lambda_a + 2\gamma_{th}^{Pr} P_{st} \lambda_b}\right) \tag{4.9}$$

Consequently, after solving equation (4.8), the primary receiver's final outage behaviour is as follows:

$$P_O^p = 1 - \left[\exp\left(-\frac{\gamma_{th}^{Pr} N_0}{P_p \lambda_a}\right)\left(\frac{P_p \lambda_a}{P_p \lambda_a + 2\gamma_{th}^{Pr} P_{st} \lambda_b}\right)\right]^N \leq \varepsilon \tag{4.10}$$

Given the aforementioned expression, the transmitted power by SU_{TR} should be sufficient to prevent a PU receiver outage, which is expressed as,

$$P_{st} = \frac{P_p \lambda_a}{2\gamma_{th}^{Pr} \lambda_b} \left[\frac{\exp\left(-\frac{\gamma_{th}^{Pr} N_0}{P_p \lambda_a}\right)}{(1-\varepsilon)^{\frac{1}{N}}} - 1 \right] \tag{4.11}$$

In similar manner, R_L would transmit power satisfying outage performance criteria of PU which can be expressed as,

$$P_{R_L} = \frac{P_p \lambda_a}{2\gamma_{th}^{Pr} \lambda_c} \left[\frac{\exp\left(-\frac{\gamma_{th}^{Pr} N_0}{P_p \lambda_a}\right)}{(1-\varepsilon)^{\frac{1}{N}}} - 1 \right] \tag{4.12}$$

The output power of the secondary-source transmitter in underlay mode is determined by,

$$P_s^u = \min\left(P_{S_{TR}}^H, P_{st}\right) \tag{4.13}$$

The transmitting power from the secondary FD relay R_L in underlay mode is given by,

$$P_r^u = \min\left(P_{R_L}^H, P_{R_L}\right) \tag{4.14}$$

The transmitting power from SU_{TR} and FD relay R_L in overlay mode is expressed as,

$$P_s^o = P_{S_{TR}}^H \tag{4.15}$$

$$P_r^o = P_{R_L}^H \tag{4.16}$$

According to the mode of transmission, which opportunistically switches between underlay or overlay on the basis of sensing result, the transmission power policies are monitored.

4.1.3 Performance and mathematical analysis

The received signal at the L^{th} relay during the underlay mode of operation is provided by:

$$y^u_{R_L}(t) = \sqrt{P^u_s} h_{S_T R_L} x_s(t) + \sqrt{P^u_r} h_{R_L} x_r(t) + \sum_{m=1}^{M} \sqrt{P_m} h_{P_T R_L} x_p(t) + n_o(t) \quad (4.17)$$

Thus, SINR at L^{th} FD relay under underlay transmission mode is derived from the above expression as:

$$\gamma^u_F = \frac{P^u_s g_{S_T R_L}}{P^u_r h_L + \sum_{m=1}^{M} P_m g_{P_T R_L} + N_o} \quad (4.18)$$

The received signal at SU_R from the L^{th} FD relay in underlay mode is expressed by:

$$y^u_{Re}(t) = \sqrt{P^u_r} h_{R_L} x_r(t) + \sum_{m=1}^{M} \sqrt{P_m} h_{P_T S_R} x_p(t) + n_o(t) \quad (4.19)$$

Thus at underlay transmission mode, the SINR at secondary receiver is given from the above expression as:

$$\gamma^u_{Re} = \frac{P^u_r g_{R_L}}{\sum_{m=1}^{M} P_m g_{P_T S_R} + N_o} \quad (4.20)$$

The end-to-end outage at receiver of secondary network under the performance of underlay protocol is calculated using selection combination technique and can be expressed as:

$$P^{un}_O = Pr\left[\left\{ \max_L \left(\min\left(\gamma^u_F, \gamma^u_{Re}\right)\right)\right\} < \gamma^{Re}_{th}\right] \quad (4.21)$$

here, $\gamma^{Re}_{th} = 2^{R_{Tr}} - 1$, SU_{TR} transmits data at the rate of R_{Tr}.
By using order statistics [133],

$$Pr\left[\min\left(\gamma^u_F, \gamma^u_{Re}\right) < \gamma^{Re}_{th}\right] = Pr\left[\gamma^u_F < \gamma^{Re}_{th}\right] + Pr\left[\gamma^u_F > \gamma^{Re}_{th}\right] Pr\left[\gamma^u_{Re} < \gamma^{Re}_{th}\right] \quad (4.22)$$

$$
\begin{aligned}
P_O^{un} = \; & \left[1 - \exp\left(-\frac{\gamma_{th}^{Re} N_0}{P_s^u \lambda_f}\right)\left(\frac{P_S^u \lambda_f}{P_s^u \lambda_f + \gamma_{th}^{Re} P_n \lambda_d}\right)\right. \\
& \left(\frac{P_r^u \lambda_h}{P_r^u \lambda_h - P_n \lambda_d}\right)^N + \left\{\exp\left(-\frac{\gamma_{th}^{Re} N_0}{P_s^u \lambda_f}\right)\right. \\
& \left.\left(\frac{P_S^u \lambda_f}{P_s^u \lambda_f + \gamma_{th}^{Re} P_n \lambda_d}\right)\left(\frac{P_r^u \lambda_h}{P_r^u \lambda_h - P_n \lambda_d}\right)^N\right\} \times \\
& \left.\left\{1 - \exp\left(-\frac{\gamma_{th}^{Re} N_0}{P_r^u \lambda_g}\right)\left(\frac{P_r^u \lambda_g}{P_r^u \lambda_g + \gamma_{th}^{Re} P_n \lambda_e}\right)^N\right\}\right]^K
\end{aligned}
\tag{4.23}
$$

Now during overlay mode of operation, the received signal at k^{th} relay being transmitted from SU_{TR} is given by:

$$
y_{R_L}^o(t) = \sqrt{P_s^o} h_{S_T R_L} x_s(t) + \sqrt{P_r^o} h_{R_L} x_r(t) + n_o(t) \tag{4.24}
$$

Thus at overlay transmission mode, the SINR at k^{th} FD relay is given from the above expression as:

$$
\gamma_F^o = \frac{P_s^o g_{S_T R_L}}{P_r^o g_{R_L} + N_o} \tag{4.25}
$$

During overlay mode of operation, the received signal at SU-Rx from k^{th} FD relay is given by:

$$
y_{Re}^o(t) = \sqrt{P_r^o} h_{R_L} x_r(t) + n_o(t) \tag{4.26}
$$

Thus at overlay transmission mode, the SINR at secondary receiver is given from the above expression as:

$$
\gamma_{Re}^o = \frac{P_r^o g_{R_L}}{N_o} \tag{4.27}
$$

In a similar manner, SC technique is used at the destination. Thus the end to end outage probability at the secondary receiver during overlay mode is found out to be:

$$
P_O^{ov} = \; Pr\left[\left\{\max_k \left(\min\left(\gamma_F^o, \gamma_{Re}^o\right)\right)\right\} < \gamma_{th}^S\right] \tag{4.28}
$$

So, the end to end outage at SU_R for overlay transmission mode can be expressed as:

$$P_O^{ov} = \left[1 - \exp\left(-\frac{\gamma_{th}^{Re} N_0}{P_s^o \lambda_f}\right)\left(\frac{P_s^o \lambda_f}{P_s^o \lambda_f + \gamma_{th}^{Re} P_r^o \lambda_h}\right) + \left\{\exp\left(-\frac{\gamma_{th}^{Re} N_0}{P_s^o \lambda_f}\right)\left(\frac{P_s^o \lambda_f}{P_s^o \lambda_f + \gamma_{th}^{Re} P_r^o \lambda_h}\right)\right\} \times \left\{1 - \exp\left(-\frac{\gamma_{th}^{Re} N_0}{P_r^o \lambda_g}\right)\right\}\right]^K \tag{4.29}$$

Finally, based on the activity of sensing, the detection of the primary user, and their state of channel occupancy with their outage constraint (i.e., QoS) maintained by the secondary user, their overall outage probability during adaptive switching of underlay or overlay mode is achieved. Therefore, the outage probability under the joint underlay/overlay protocol at the secondary receiver can be expressed as:

$$P_O^{joint} = [(1 - P_d) + \alpha P_d] P_O^{un} + (1 - \alpha) P_O^{ov} \tag{4.30}$$

4.1.4 Result analysis and discussion

In this section, we examine the system performance using a MATLAB simulation testbed, followed by an extensive discussion based on these results. The numerical outcomes shown here demonstrate the performance enhancement attained while using the suggested relay-assisted adaptive joint underlay /overlay spectrum access approach. Additionally, it has been demonstrated that FD relay-based CR networks outperform HD relay-based CR networks. Following system parameters have been considered to verify the performance of the system: R_p and R_s are the target rates for both PU and SU, with values of 0.15 bits/s/Hz and 0.1 bits/s/Hz, respectively. The power limitation for PU is set to $\varepsilon = 0.1$. The noise power is standardized to a unit value. In this study, the EH circuit's efficiency factor (η) value is taken as 0.3. It is also assumed that the initial energy harvesting time τ is allocated as 20 ms out of total estimated time $T = 100$ ms.

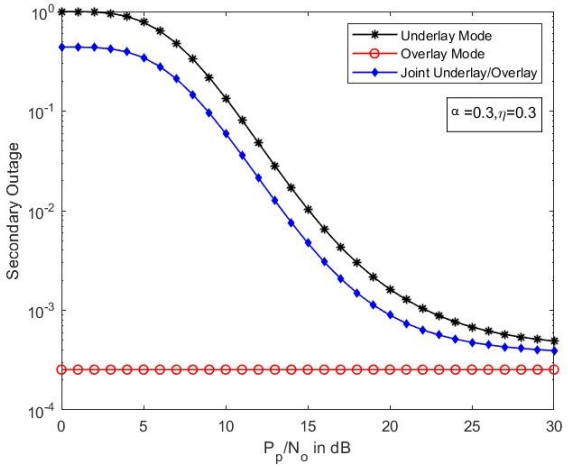

FIGURE 4.2: Comparison of outage performance under underlay, overlay, and joint underlay/overlay mode

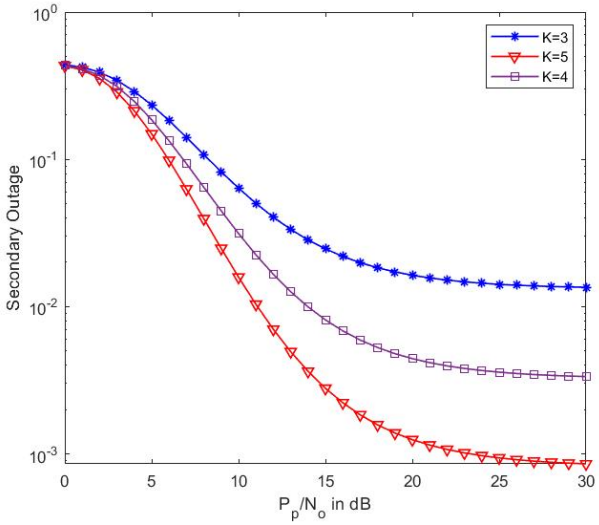

FIGURE 4.3: Comparison of outage performance of joint underlay/overlay mode under varying K with respect to P_p/N_0

Fig. 4.2 depicts the SU_R outage performance as a function of P_p/N_0 for various protocols, including underlay, overlay, and joint underlay and overlay. The probability of channel occupancy (α), no of PUs (N), probability of detection (P_d) and no of relays (K) are kept constant at 0.3, 4, 0.8 and 5 respectively. It has been found

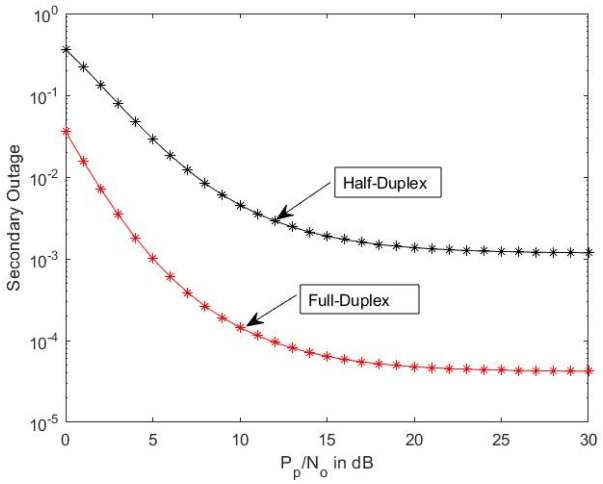

FIGURE 4.4: Comparison of SU outage performance with respect to P_p/N_0 under full-duplex vs half-duplex relaying mode

that the overlay mode's outage performance is independent of the PU's transmitting power. Therefore, this overlay method alone cannot participate in the model of spectrum sharing. Furthermore, it has been demonstrated that the joint underlay/overlay scheme outperforms the current underlay scheme for this proposed model during outages.

The outage probability of SU_R is also shown in **Fig. 4.3** as a function of P_p/N_0 in the joint underlay/overlay mode for varied numbers of relays i.e. K = 3, 4 and 5. It has been noticed that as the number of relays increases, the outage performance improves accordingly.

Fig. 4.4 shows that the secondary network's outage performance is affected by the joint underlay/overlay mode under the FD relay network in comparison to the HD relay network.The results precisely depict that the outage performance of secondary receivers under the FD relay network is improved compared to the HD relay network under multiple PUs.

The outage probability of SU_R is also depicted in **Fig. 4.5** as a function of P_p/N_0 in the joint underlay/overlay mode under varying probability of channel occupancy (α). It has been observed that as the values of α increases, the outage performance

deteriorate accordingly. The outcome we achieved reflects that more and more channel occupancy factor signifies more traffic involved which results in drop of outage performance at secondary network. The secondary receiver outage performance of

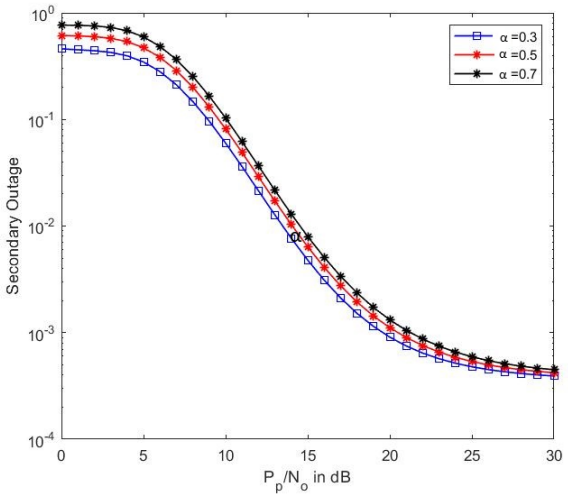

FIGURE 4.5: Comparison of outage under adaptive underlay/overlay mode under varying probability of channel occupancy (α) with reference to P_p/N_0

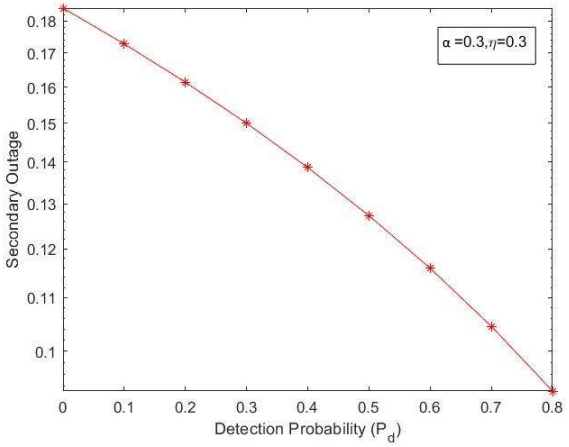

FIGURE 4.6: Comparison of outage performance of joint underlay/overlay mode under varying probability of detection (P_d)

the combined underlay/overlay mode is shown in **Fig. 4.6** as a function of variations in probability of detection values (P_d). It is precisely illustrated that increasing the value of P_d reflects on the results of secondary receiver outage performance. A higher P_d value provides the most accurate information on the activity of the PUs. As a result, there is a lower probability of error at the secondary receiver, which improves outage performance.

As a final illustration, **Fig. 4.7** depicts outage probability at SU_R as a function of

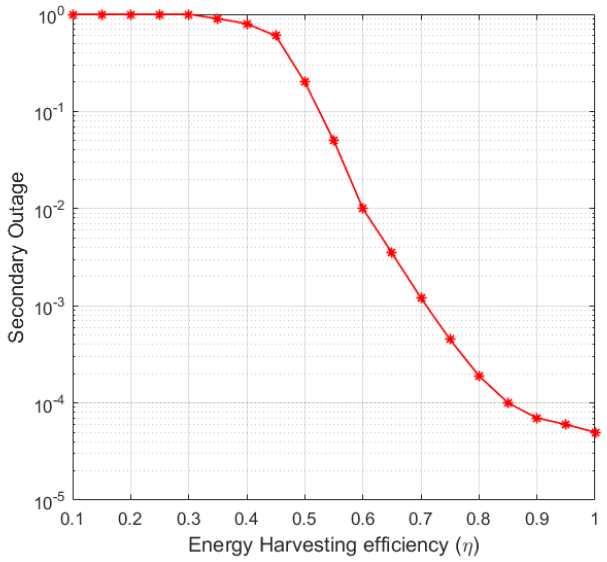

FIGURE 4.7: Outage probability at secondary network with respect to efficiency factor η of the EH circuit

the EH circuit's efficiency factor(η) in an FD relay mode. It can be inferred that as the efficiency factor (η) grows, the system's outage performance gets better. This indicates that the outage improves when the EH efficiency is higher because the SU transmitter can capture more energy from the RF environment. However, it subsequently stabilizes as a result of the transmit power limitation to preserve the QoS of the PUs.

The outage floor appearing in Figs. 4.2 onward primarily results from residual self-interference (RSI) and energy-harvesting constraints in the FD multirelay system. Even at high SNR, the RSI term does not vanish, and therefore the achievable SINR saturates, producing a non-zero error floor, which is a well-known characteristic of

FD systems with imperfect SI cancellation. In contrast, the Chapter 3 system does not involve RSI or simultaneous EH–information processing at the relay, and therefore no such floor arises in those figures. The floor observed for the HD case in Fig. 4.4 is due to EH saturation: at high SNR, the EH model limits the relay transmit power, causing the system to reach a performance ceiling. This behavior is consistent with established results for linear energy-harvesting relaying.

After discussing the FD relay operation for a single secondary transmitter and single secondary destination in a cognitive radio network, we move on to a study based on a multi-destination goal to broaden the user base.

4.2 Performance analysis on multi-user multiple full-duplex relay based cognitive radio network in linear energy harvesting environment

This section has covered the use of multiple FD relay in a cognitive radio network to create a multiuser spectrum sharing environment. Furthermore, when discussing adaptive transmit power policies, each secondary transmitting node's linear energy harvesting techniques are taken into consideration.In order to maintain quality of service (QoS) of multiple primary users (PUs), power allocation strategies at each secondary transmitting node is taken care of. Finally, all the analytical closed form expressions have been validated through Monte-Carlo simulations.

4.2.1 System model based on multi-user multi-FD relay based cognitive radio network

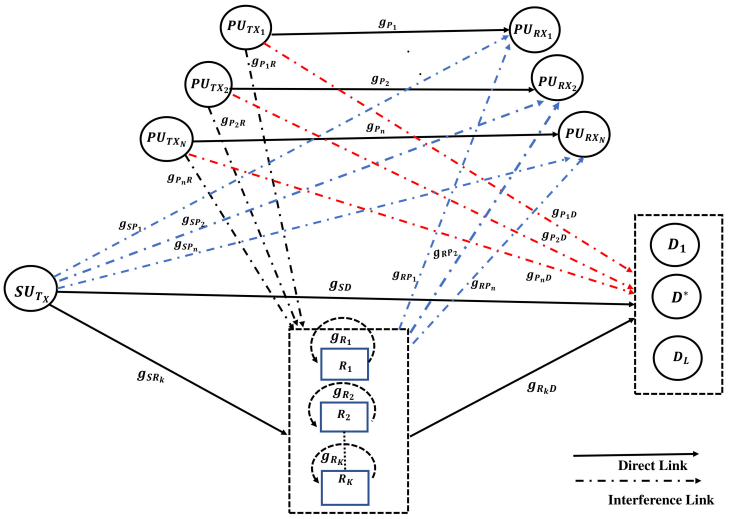

FIGURE 4.8: System model based on multi-user multi-FD relay based CRN

The system architecture, proposed here in **Fig. 4.8**, is a cognitive radio network built up with multiple primary users (PU_n ; $n = 1, 2, \ldots, N$), a secondary user transmitter ($SU - Tx$), multiple secondary user receivers (D_l ; $l = 1, 2, \ldots, L$) and multiple FD relays (R_k ; $k = 1, 2, \ldots, K$). This has been presumed that the secondary source, primary users, and secondary destinations all have a single antenna except multiple FD relays which are accompanied by single transmitting and single receiving antenna each. Both FD relays and ($SU - Tx$) are equipped with EH circuit which can harvest energy from the ambient radio-frequency (RF) signals. All the secondary transmitting nodes are capable of building a part of energy from the interference source of N number of active PU_s. The ($SU - Tx$) communicates with the secondary destinations D_l via these FD relay network, which is a simultaneous trans-receive process. It is also assumed that ($SU - Tx$) is having direct links with all the SU destinations. All the channel coefficients are denoted by $h_{i,j}$ following Rayleigh distribution and corresponding channel power gains are denoted by $g_{i,j}$ which follow an exponential distribution with mean λ_m, where (i, j) denotes respective channel paths with parameter suffix $m = 1, 2, \ldots, 9$. TABLE 4.2 below makes a clear listing of the aforementioned parameters.

However, before the beginning of communication process, an efficient destination

TABLE 4.2: Channel gain with parameter list

Path-link (i, j)	Channel $g_{i,j}$	Parameter λ_m
PU_{TX_N}-PU_{RX_N}	g_{P_n}	λ_1
SU_{TX}-D^*	g_{SD}	λ_2
SU_{TX}-R_K	g_{SR_k}	λ_3
R_K-D^*	g_{R_kD}	λ_4
SU_{TX}-PU_{RX_N}	g_{SP_n}	λ_5
PU_{TX_N}-R_K	g_{P_nR}	λ_6
PU_{TX_N}-D^*	g_{P_nD}	λ_7
R_K-PU_{RX_N}	g_{RP_n}	λ_8
R_K-R_K	g_{R_k}	λ_9

selection scheme is carried out at SU-Tx by employing pilot bits symbols [134, 119]. This is how the process begins where it is expected that pilot signals are initially

sent to the accessible destinations by the secondary source. Subsequently, each destination will provide acknowledgement to the estimated channel state information (CSI) of their individual links after receiving the corresponding pilot signals. More specifically, the best destination D^* chosen on the basis of channel quality of the direct links. Transmission process is carried out in dual hop manner. First hop deals with the transmission of information from SU-Tx to both (R_k ; $k = 1, 2, \ldots, K$) and D^*. Whereas in the second hop of transmission, the information is being forwarded from relays to the best destination D^*. After the SU destination is selected, the relay selection process is performed in such a way that the chosen relay will maximize the end-to-end SINR from SU-Tx to the selected SU destination D^*. This has been detailed in section 5.3. Instead of HD relays, full-duplex (FD) approaches for relay networks have been considered here to address the spectrum inefficiency by the former one. These techniques allow relay nodes to simultaneously transmit and receive signals at the cost of self-interference. This SI can not be fully mitigated even if with the application of self-interference supression and modeled as an independent Rayleigh distributed channel [135] in this work. Additionally, we consider the impact of interference from different transmitting nodes on every receiving points.

4.2.2 Energy harvesting and compact power allocation

The secondary source $SU-Tx$ and the relays R_k use Time Switching Relaying (TSR) protocol for the manual task of energy harvesting and signal transmission [136]. Let us consider that T be the total time for transmission of a data packet from $SU - Tx$ to secondary destination. Let us also assume τ to be the time taken by each secondary transmitting node for harvesting energy from N number of PU_s network. The remaining $(T - \tau)$ is used for data transmission.

The total energy harvested by secondary sources during the time τ from N number

of active primary transmitter is given by:

$$E_{ST}^{H} = \eta\tau \left(\sum_{n=1}^{N} P_n g_{n_s} \right) \tag{4.31}$$

where, P_n is the transmitted power by single $PU - Tx$ with corresponding channel gain g_{n_s}. η defines the efficiency factor for energy harvesting circuit at each secondary transmitter node. The transmit power of $SU - Tx$ during the time $(T - \tau)$, accompanied by EH circuit, can be written as:

$$P_S^H = \left(\frac{E_{ST}^H}{T - \tau} \right) \tag{4.32}$$

The total energy harvested by each of the secondary FD relays during the time τ from N number of active primary transmitters as well as from secondary source $SU - Tx$ is given by:

$$E_{SR}^{H} = \eta\tau \left(P_S g_{S_{R_k}} + \sum_{n=1}^{N} P_n g_{P_n R} \right) \tag{4.33}$$

where, P_S is the actual transmitted power by $SU - Tx$, selected in such a way so that it can maintain primary outage constraint. Similarly, the transmit power of R_k during the time $(T - \tau)$, accompanied by EH circuit is given by:

$$P_R^H = \left(\frac{E_{SR}^H}{T - \tau} \right) \tag{4.34}$$

Since, we lean on the concept of spectrum sharing and R_k are in full-duplex mode, the simultaneous transmit power from $SU - Tx$ and R_k is constrained by the primary network's peak interference parameter I_p as follows [132]:

$$I_p \geq \left(P_s^0 g_{SPn} + P_{R_k}^0 g_{RP_n} \right) \tag{4.35}$$

where, P_s^0 and $P_{R_k}^0$ are the transmitted power by $SU - Tx$ and R_k respectively, while maintaining primary outage constraint.

Thus the signal-to-interference-plus-noise ratio ($SINR$) at n^{th} PU receiver is given by:

$$\gamma_n = \frac{P_n g_{P_n}}{P_s^0 g_{SPn} + P_{R_k}^0 g_{RP_n} + BN_0} \tag{4.36}$$

, where B defines the total bandwidth of PUs. From (4.35), with the assumption of non optimal condition for P_s^0 and $P_{R_k}^0$, the $SU - Tx$ and R_k transmit power should be maintained so that no PU_s are subject to excessive interference from the communication of the SU [29, 132].

Thus, the power of transmission by $SU - Tx$ should satisfy an outage of PU receiver given as,

$$P_O^1 = Pr\left[\min_{n=1,\ldots,N}\left(\frac{P_n g_{P_n}}{P_s^0 g_{SP_n} + P_{R_k}^0 g_{RP_n} + BN_0} \leq \gamma_{th}^P\right)\right] \leq \varepsilon \tag{4.37}$$

where, $\gamma_{th}^P = 2^{R_p} - 1$ and ε denote the outage threshold and outage constraint of the $PU - Rx$ respectively and the transmission rate of PU is R_p.

Equation (4.37) can be rewritten by considering non optimal power condition as:

$$\begin{aligned} P_O^1 &= Pr\left[\min_{n=1,2,\ldots,N}\left(\frac{P_n g_{P_n}}{2P_s^0 g_{SP_n} + BN_0} \leq \gamma_{th}^P\right)\right] \leq \varepsilon \\ &= 1 - \sum_{n=1}^{N}\left[1 - \underbrace{Pr\left(\frac{P_n g_{P_n}}{2P_s^0 g_{SP_n} + BN_0} \leq \gamma_{th}^P\right)}_{P^o}\right] \leq \varepsilon \end{aligned} \tag{4.38}$$

From the above expression, the outage probability of P^o can be calculated as:

$$P^o = 1 - \exp\left(-\frac{\gamma_{th}^P BN_0}{P_p\lambda_1}\right)\left(\frac{P_p\lambda_1}{P_p\lambda_1 + 2\gamma_{th}^P P_s^0\lambda_5}\right) \tag{4.39}$$

The final outage behaviour P_O^1 at the primary can be obtained as:

$$P_O^1 = 1 - \left[\exp\left(-\frac{\gamma_{th}^P BN_0}{P_p\lambda_1}\right)\left(\frac{P_p\lambda_1}{P_p\lambda_1 + 2\gamma_{th}^P P_s^0\lambda_5}\right)\right]^N \leq \varepsilon \tag{4.40}$$

Considering the above expression, the transmitted power by $SU-Tx$ should satisfy an outage of PU receiver as:

$$P_s^0 = \frac{P_p \lambda_1}{2\gamma_{th}^P \lambda_5} \left[\frac{\exp\left(-\frac{\gamma_{th}^P BN_0}{P_p \lambda_1}\right)}{(1-\varepsilon)^{\frac{1}{N}}} - 1 \right] \tag{4.41}$$

Similarly, the transmitted power by R_k should satisfy an outage of PU receiver as:

$$P_{R_k}^0 = \frac{P_p \lambda_1}{2\gamma_{th}^P \lambda_8} \left[\frac{\exp\left(-\frac{\gamma_{th}^P BN_0}{P_p \lambda_1}\right)}{(1-\varepsilon)^{\frac{1}{N}}} - 1 \right] \tag{4.42}$$

The actual power to be taken from the secondary source transmitter is given by:

$$P_S = \min\left(P_S^H, P_s^0\right) \tag{4.43}$$

The actual power, to be taken from the best secondary FD relay out of this FD relay network R_k transmitter is given by:

$$P_R = \min\left(P_R^H, P_{R_k}^0\right) \tag{4.44}$$

4.2.3 Performance and mathematical analysis

In our proposed model, a sub-optimal node selection strategy is used, i.e., the best SU destination D^* is first selected based on the channel quality of the direct links instead of optimal joint relay-destination selection scheme, where relays also participate in destination selection process. We, therefore, need to compare (L+K) potential links in each transmission process whereas a joint relay-destination selection scheme requires L(K+1) potential links. In this context, we can observe that in case of large-scale multi-relay multi-destination cooperative spectrum sharing systems, the proposed methodology has the adequate potential to reduce the overhead amount to an appreciable extent in contrast to the optimal strategy, for the purpose of attaining

same diversity order [134]. Therefore, choice of direct path for D^* can be expressed as,

$$D^* = \arg \max_{l=1,2,...,L} (\gamma_{SD_l}) \tag{4.45}$$

where, γ_{SD_l} is the signal-to-interference-plus-noise ratio ($SINR$) at D^* for direct link [134].

$$\gamma_{SD_l} = \frac{P_S g_{s_D}}{\sum_{n=1}^{N} P_n g_{P_n D} + N_o} \tag{4.46}$$

, where transmitted power from each primary is considered to be P_n.

It is generally known that the received signal at any node in a wireless fading channel can be written as:

$$r(t) = \sqrt{P} h x(t) + n(t) \tag{4.47}$$

where, $x(t)$ is the transmitted signal with power P and $\mathbb{E}|x(t)|^2 = 1$, h defines fading channel coefficient, $n(t)$ is receiver noise.

The signal-to-noise-ratio at receiver can be obtained as:

$$\gamma = \frac{P|h|^2}{N_o} \tag{4.48}$$

Upon the selection of SU destination, the FD relay selection is performed in such a way that the chosen relay will maximize the end-to-end SINR from the SU source to the selected SU destination i.e., D^*.

Now, taking into account the SI of each FD relay node along with interference from N active PUs, the information which has been transmitted by the secondary source and received at R_k is given by:

$$y_{Rk^*} = \sqrt{P_S} h_1 x_s(t) + \sqrt{P_R} h_2 x_r(t) + \sum_{n=1}^{N} \sqrt{P_n} h_n x_n(t) + n_o(t) \tag{4.49}$$

where, $x_s(t)$, $x_r(t)$ and $x_n(t)$ represent the transmitted signals from $SU - Tx$, R_k^* and n^{th} $PU - Tx$ respectively. It is also considered that $\mathbb{E}|x_s(t)|^2 = 1$, $\mathbb{E}|x_r(t)|^2 = 1$,

$\mathbb{E}|x_n(t)|^2 = 1$ with $n_o(t) \sim \mathcal{N}(0, N_0)$ is the zero mean Additive White Gaussian Noise at each receiver node. h_1 and h_2 are the channel coefficient from $SU - Tx$ to R_k and R_k's transmitter antenna to receiver antenna respectively.

The signal-to-interference-plus-noise ratio ($SINR$) at k^{th} relay of R_k can be written as:

$$\gamma_1 = \frac{P_S g_{SR_k}}{P_R g_{R_k} + \sum_{n=1}^{N} P_n g_{P_n R} + N_o} \tag{4.50}$$

Considering the interference from N number of active PUs, the received signal at D^* from k^{th} relay of R_k is given by:

$$y_{D^*} = \sqrt{P_R} h_3 x_r(t) + \sum_{n=1}^{N} \sqrt{P_n} h_n x_n(t) + n_o(t) \tag{4.51}$$

The signal-to-interference-plus-noise ratio ($SINR$) at D^* can be outlined as:

$$\gamma_2 = \frac{P_R g_{R_k D}}{\sum_{n=1}^{N} P_n g_{P_n R} + N_o} \tag{4.52}$$

The end to end outage probability at the secondary receiver is found out to be:

$$\begin{aligned} P_{out}^{total} &= Pr\left[\max\left\{ \max_{l} \left(\gamma_{SD_l}\right), \max_{k} \left(\min\left(\gamma_1, \gamma_2\right)\right) \right\} < \gamma_{th}^{S}\right] \\ &= \underbrace{Pr\left[\max_{l} \left(\gamma_{SD_l}\right) < \gamma_{th}^{S}\right]}_{A_1} \underbrace{Pr\left[\max_{k} \left(\min\left(\gamma_1, \gamma_2\right)\right) < \gamma_{th}^{S}\right]}_{A_2} \end{aligned} \tag{4.53}$$

where, $\gamma_{th}^{S} = 2^{R_s} - 1$ denotes the outage threshold of the selected destination D^* and transmission rate of $SU - Tx$ is R_s.

The outage behavior of A_1 and A_2 can be expressed as given below. The solution of the expression A_1 and A_2 are discussed in APPENDIX section.

$$A_1 = \left[1 - \exp\left(-\frac{\gamma_{th}^{S} N_0}{P_S \lambda_2}\right)\left(\frac{P_S \lambda_2}{P_S \lambda_2 + \gamma_{th}^{S} P_n \lambda_7}\right)^{N}\right]^{L} \tag{4.54}$$

$$
\begin{aligned}
A_2 = & \left[1-\exp\left(-\frac{\gamma_{th}^S N_0}{P_S\lambda_3}\right)\left(\frac{P_S\lambda_3}{P_S\lambda_3+\gamma_{th}^S P_R\lambda_9}\right)\right. \\
& \left(\frac{P_R\lambda_9}{P_R\lambda_9-P_n\lambda_6}\right)^N + \left\{\exp\left(-\frac{\gamma_{th}^S N_0}{P_S\lambda_3}\right)\right. \\
& \left.\left(\frac{P_S\lambda_3}{P_S\lambda_3+\gamma_{th}^S P_R\lambda_9}\right)\left(\frac{P_R\lambda_9}{P_R\lambda_9-P_n\lambda_6}\right)^N\right\}\times \\
& \left.\left\{1-\exp\left(-\frac{\gamma_{th}^S N_0}{P_R\lambda_4}\right)\left(\frac{P_R\lambda_4}{P_R\lambda_4+\gamma_{th}^S P_n\lambda_8}\right)^N\right\}\right]^K
\end{aligned} \tag{4.55}
$$

The total outage probability from secondary source to secondary destination can therefore be expressed as:

$$
\begin{aligned}
P_{out}^{total} = & \left[1-\exp\left(-\frac{\gamma_{th}^S N_0}{P_S\lambda_2}\right)\left(\frac{P_S\lambda_2}{P_S\lambda_2+\gamma_{th}^S P_n\lambda_7}\right)^N\right]^L\times \\
& \left[1-\exp\left(-\frac{\gamma_{th}^S N_0}{P_S\lambda_3}\right)\left(\frac{P_S\lambda_3}{P_S\lambda_3+\gamma_{th}^S P_R\lambda_9}\right)\right. \\
& \left(\frac{P_R\lambda_9}{P_R\lambda_9-P_n\lambda_6}\right)^N + \left\{\exp\left(-\frac{\gamma_{th}^S N_0}{P_S\lambda_3}\right)\right. \\
& \left.\left(\frac{P_S\lambda_3}{P_S\lambda_3+\gamma_{th}^S P_R\lambda_9}\right)\left(\frac{P_R\lambda_9}{P_R\lambda_9-P_n\lambda_6}\right)^N\right\}\times \\
& \left.\left\{1-\exp\left(-\frac{\gamma_{th}^S N_0}{P_R\lambda_4}\right)\left(\frac{P_R\lambda_4}{P_R\lambda_4+\gamma_{th}^S P_n\lambda_8}\right)^N\right\}\right]^K
\end{aligned} \tag{4.56}
$$

Proof of A_2 for $F(\gamma_1)$ is shown in APPENDIX A and for $F(\gamma_2)$ is in APPENDIX B. By using order statistics [133],

$$
Pr\left[\min\left(\gamma_1,\gamma_2\right) < \gamma_{th}^S\right] = F(\gamma_1)+F(\gamma_2)-F(\gamma_1)F(\gamma_2) \tag{4.57}
$$

where $F(\gamma)$ is the CDF function.

Rewriting above equation, we can express in terms of the outage probability as follows:

$$
P_{out} = Pr\left[\gamma_1 < \gamma_{th}^S\right] + Pr\left[\gamma_1 > \gamma_{th}^S\right] Pr\left[\gamma_2 < \gamma_{th}^S\right] \tag{4.58}
$$

4.2.4 Results and discussion

This section covers up with the result analysis based on system performance through Monte-Carlo simulations testbed and we discussed the behaviour of the system performance from these analyzed results. Numerical results provided for FD relay based CRN shows the performance improvement obtained with respect to conventional HD relaying protocol. The factor of SI is introduced at each FD relay and other interference factors from each transmitters are also considered as well. Including all these above mentioned factors, a comparison of FD relaying protocol with conventional HD relaying protocol is carried out. To verify the system performance, the following system parameters are assumed: the transmission rate for both PU and SU is taken as $R_p = 0.15\ bits/s/Hz$ and $R_s = 0.1\ bits/s/Hz$ respectively. The outage constraint of PU is fixed at $\varepsilon = 0.1$. The noise power is normalized to unit value. An efficiency factor $\eta = 0.3$ of the EH circuit has been considered in this study. The total time taken is considered as $T = 100ms$ with initial harvesting time of $\tau = 20ms$.

Fig. 4.9 shows a comparison in terms of outage probability of the $SU - T_x$ to

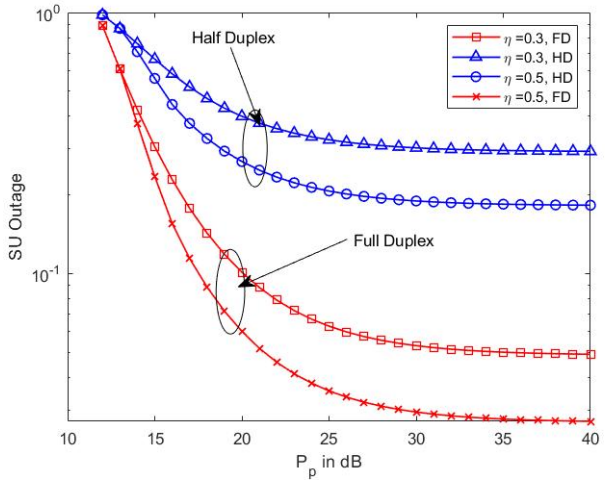

FIGURE 4.9: Comparison of SU outage performance with respect to P_p under FD and HD relaying mode

D^* as a function of P_p in dB at different values of efficiency parameter η for FD relaying protocol versus conventional HD relaying protocol. This has been clearly

observed that irrespective of the value of P_p and η, our proposed model for FD relaying scheme gives better result than that of HD relaying scheme [56] in terms of outage performance. Additionally, we have also considered the self interference for FD relaying scheme, which was not present in the previously proposed HD scheme. This is because of the fact that the throughput gets increased due to simultaneous trans-receive in FD operation as compared to HD operation.

Fig. 4.10 shows the effect of outage performance of the secondary network for HD

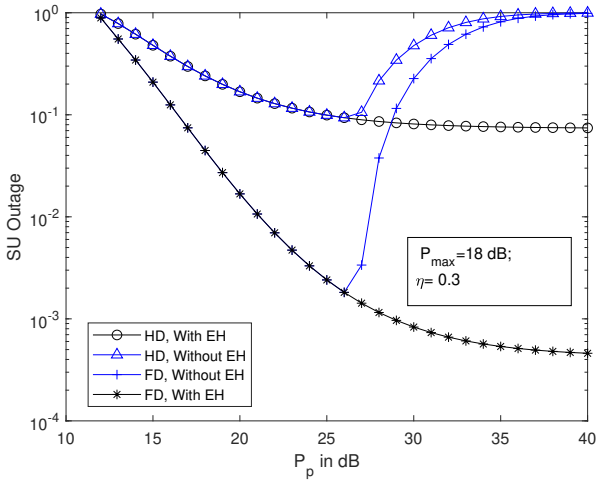

FIGURE 4.10: Comparison of SU outage performance with respect to P_p under FD and HD relaying mode considering EH circuit

and FD communication systems in presence of EH circuit at secondary transmitter nodes. The selected EH relay transmits with the maximum power allowed by PU's outage constraint. We notice that an increase in the PU transmit power P_p, significantly increases the maximum transmit power of the secondary transmitter P_s and secondary relay P_r respectively. However, it is observed that in the non-energy harvesting scenario outage again increases as the PU transmit $P_p \geq 25$ dB due to the power limitation of transmitter itself. In case of non-energy harvesting scenario, the maximum secondary transmit power from each node is assumed to be $P_{max} = 18\ dB$. In energy harvesting scenario, however, this is avoided because even if the PU transmit power P_p increases the energy harvesting at secondary source and relay also increases, and thus we see a noteworthy outage performance enhancement.

Fig. 4.11 shows the outage probability at secondary receiver D^* with respect to P_p

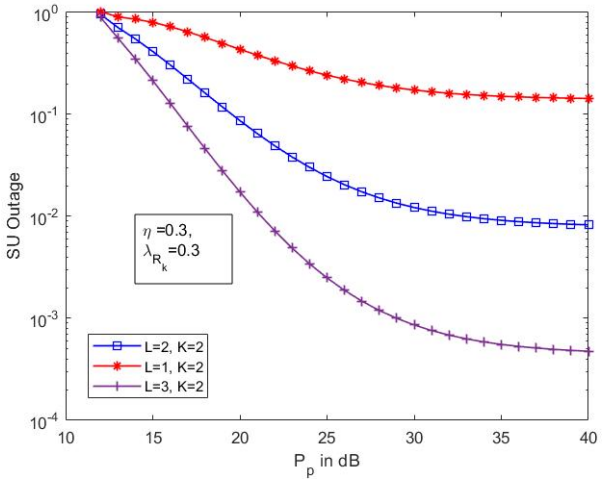

FIGURE 4.11: Comparison of outage performance in FD relaying mode with respect to Pp in dB for fixed K and varying L

in dB for FD relaying protocol. For the simulation, we assume the mean of channel power gain of self interference $\lambda_9 = 0.3$ and EH efficiency factor $\eta = 0.3$. Considering $R_p = R_s = 0.2bits/sec/Hz$, count of FD relay $K = 2$ and the variation of count in destination $L = 1, 2, 3$, the outage analysis has been studied. We consider the maximum primary transmitting power to be 40dB, whereas the $SU - Tx$ and R_k transmit a maximum power depending on outage constraint of PU which is fixed at $\varepsilon = 0.1$. This investigation shows that the outage behaviour gets better for the increase in count in number of destinations. This reflects that taking multiple destinations in our discussion enhances the system performance. Similar study has been carried out by keeping $L = 2$ and making a variation in count of FD relays such as $K = 1, 2, 3$. Simulation result has been depicted in **Fig. 4.12** which shows that the outage performance becomes better with the increase in number of FD relays.

It has also been found in **Fig. 4.13** that with constant diversity order defined as $(L + K)$ i.e., with $L = 1, K = 3$ and $L = 2, K = 2$ and again taking $L = 3, K = 1$; the outage performance is significantly better in the last case as compared to the previous two. It is possible to trade-off between the number of multiple destinations and FD relays to achieve a desired level of performance. Hence, it is expected to

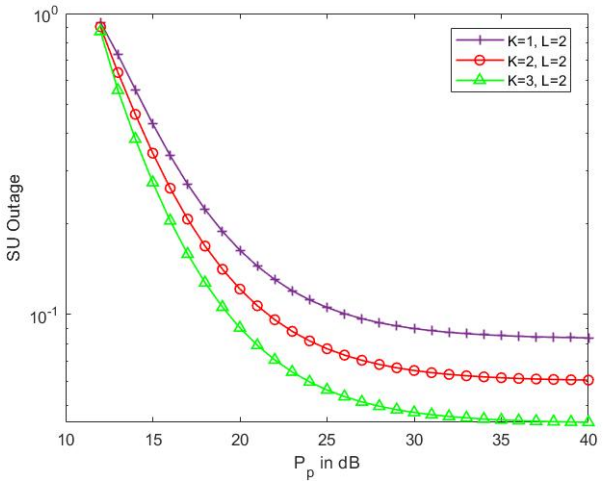

FIGURE 4.12: Comparison of outage performance in FD relaying mode for fixed L and varying K w.r.t P_p in dB

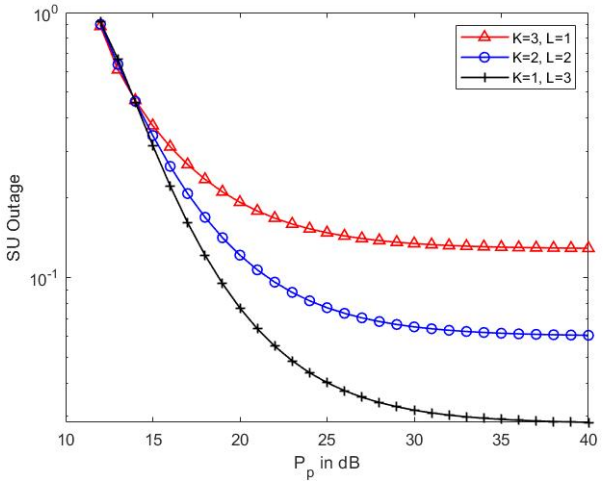

FIGURE 4.13: Outage performance at secondary in FD relaying mode with diversity combining

have a better performance with increasing values of destination L as required for an improved cooperative cognitive radio solution.

Finally, in **Fig. 4.14**, we have shown the outage probability of the $SU - Tx$ to D^* as a function of efficiency factor η of the EH circuit under FD relaying mode. It can be seen that the outage performance is also getting better as the efficiency factor gets increased and reached to a steady value ultimately. This is because of the fact that when the EH efficiency is more, SU transmitter can harvest more energy from

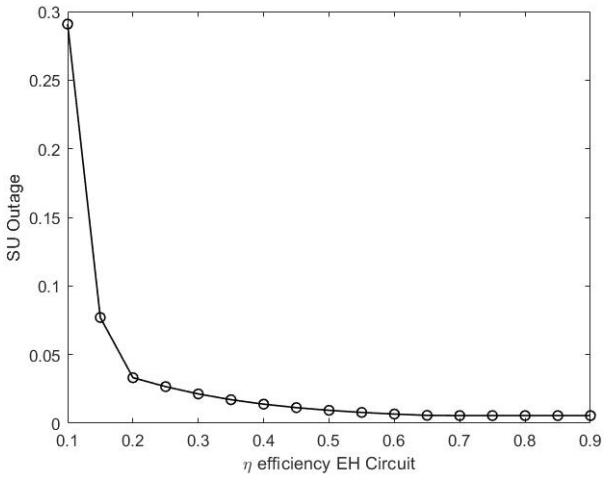

FIGURE 4.14: Outage probability of FD relaying protocol versus efficiency factor η of the EH circuit

ambient which in turn increases the transmit power and as a result the outage gets better. It has also been observed that 20% efficiency of EH circuit is good enough to reach the desired outcomes in our proposed model. Thus it can be concluded that at low efficiency factor η, our model can perform quite efficiently.

In contrast to the first two sections, which already illustrated a linear energy harvesting scenario, the following section follows a multi user FD relay based CRN under a nonlinear energy harvesting scenario.

4.3 Performance analysis on non linear energy harvesting multiple full-duplex relay based cognitive radio network

Secondary user transmitters equipped with sensing mechanism are able to switch between overlay mode, with peak power of transmission as primary user (PU) remains inactive, or underlay mode with limited transmit power as PU remains active. The system performance gets enhanced by incorporating multiple full-duplex (FD) relays which use energy detection circuits to sense RF energy from PUs. A mathematical study has been conducted to optimize power allocation and closed form expressions have been developed considering all interferences in the network. MATLAB simulations have validated the analytical results on outage probability.

4.3.1 System model on non linear energy harvesting based cognitive radio network

The system design shown in **Fig. 4.15** depicts a CR network composed of multi primary user transmitters including receivers ($P_{TXn}, P_{RXn};\ n = 1, 2, 3, \ldots, N$), a secondary transmitter (S_{Tx}) able to communicate with a secondary receiver (S_{Rx}) through these multiple FD relays ($R_k\ ;\ k = 1, 2, 3 \ldots, K$). Except for nodes with a single antenna, each FD relay is assumed to have a pair of trans-receive antennas. Secondary transmitting nodes have energy detectors to sense primary users' activity (i.e; busy or idle). Furthermore, it has been assumed that direct communication between the secondary transmitter and destination is hindered by shadowing and multi path propagation losses. Each proper channel coefficient, represented by $h_{p,q}$ is Rayleigh-distributed. The channel power gains $g_{p,q}$ should be an exponentially distributed variables with a mean (λ_m), where (p, q) specifies the channel indexing

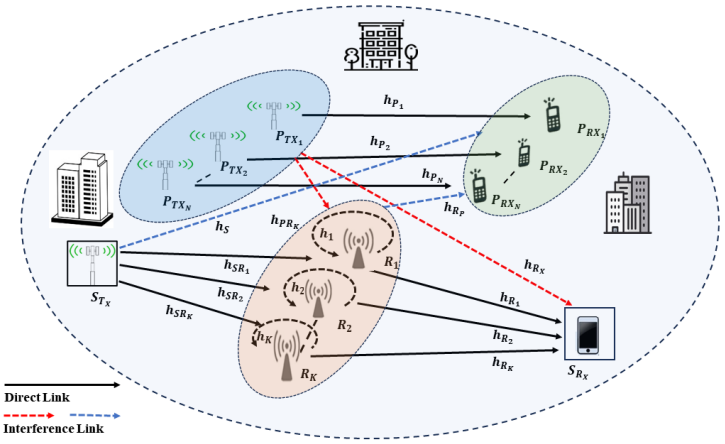

FIGURE 4.15: System model on non linear EH multi-FD relay based cognitive radio network

by suffixes $m = 1, 2, 3, \ldots, 8$. TABLE 4.3 lists these details. However, before start-

TABLE 4.3: Different pathlink associated gain parameter chart

Pathlink-(p,q), wireless channel coefficients$(h_{p,q})$	**channel-gain $(g_{p,q})$**	**Parameter chart (λ_m)**
P_{TXn}-P_{RXn}, h_{p_n}	g_{p_n}	λ_1
S_{Tx}-P_{RXn}, h_S	g_S	λ_2
R_K-P_{RXn}, h_{R_p}	g_{R_p}	λ_3
P_{TXn}-R_K, h_{PR_k}	g_{PR_k}	λ_4
P_{TXn}-S_{Rx}, h_{R_x}	g_{R_x}	λ_5
S_{Tx}-R_K, h_{SR_k}	g_{SR_k}	λ_6
R_K-S_{Rx}, h_{R_k}	g_{R_k}	λ_7
R_K-R_K, h_k	g_k	λ_8

ing communication, secondary transmitters detect primary users' activity using an energy detector during the first time slot. In the second time slot, FD relays simultaneously transmit information from (S_{Tx}) to (S_{Rx}). The best relay is chosen using selection combination, optimizing the weakest source-relay and relay-destination channels. This section discusses a hybrid underlay/overlay transmission technique to enhance the spectrum efficiency of cognitive radio networks. The role of energy detector in S_{Tx} is to detect PU activity and hence allows secondary transmitters to

switch between underlay or overlay modes for communication as required. Following detection, if the PUs are busy, both S_{Tx} and R_k take part in power limitation protocol (underlay); if not, both transmit at its full power (overlay).
As per FCC [128], channel occupancy typically ranges from 15% to 85% during peak times. The busy status of a primary user channel (i.e; probability of channel occupancy) is represented by α $(0 \leq \alpha \leq 1)$. The notation for the probability of a busy and ideal primary user is αP_d and $(1-\alpha)P_d$, respectively, where P_d represents the detection probability. In our study, we model the impact of self-interference (SI) caused by full-duplex (FD) relays, despite the application of self-interference suppression (SIS) techniques. The SI is assumed to follow an independent Rayleigh distribution, as suggested in [135], indicating that the interference is not entirely mitigated.

4.3.2 Power allocation at secondary transmitter

The secondary user and secondary relays utilize the Time Switching Relaying (TSR) protocol for sensing as well as signal transmission purposes [136]. Assuming total time T for whole data packets, τ is used for sensing at transmitting nodes from PU signals, and remaining $(T-\tau)$ time for data transmission from S_{Tx} to S_{Rx}.
The overall signal received at the n^{th} primary receiver is expressed as follows:

$$y_{P_{rn}}(t) = \sqrt{P_n} h_{P_n} x_p(t) + \sqrt{P_S^u} h_S x_S(t) + \sqrt{P_{R_k}^u} h_{R_P} x_r(t) + n_o(t) \tag{4.59}$$

where $x_p(t)$, $x_r(t)$, and $x_s(t)$ are used for the signals sent by the n^{th} primary transmitter P_{TXn}, relay R_k, and secondary transmitter S_{Tx}, respectively. We assume that the signals $x_p(t)$, $x_r(t)$, and $x_s(t)$ have unit energy, n(t) is zero-mean additive white gaussian noise (AWGN) distributed at every recipient of secondary network. Additionally, P_n symbolizes power from primary transmitter, while P_S^u and $P_{R_k}^u$ denote powers from S_{Tx} and R_k, respectively in underlay mode.

Time τ be the harvesting time during which SU_T gets its energy from all the active PU's as:

$$E_s^h = \eta\tau \sum_{n=1}^{N} P_n |h_{p,s}|^2 \tag{4.60}$$

The transmitted power of SU_T resulting from the nonlinear EH circuit during the time $(T-\tau)$ is expressed as:

$$P_s^h = \begin{cases} \frac{E_s^h}{T-\tau}, & \sum_{n=1}^{N} P_n |h_{p,s}|^2 \leq \Gamma_{th} \\ \frac{\eta\tau\Gamma_{th}}{T-\tau}, & \sum_{n=1}^{N} P_n |h_{p,s}|^2 > \Gamma_{th} \end{cases} \tag{4.61}$$

where, Γ_{th} defines EH circuit's maximum power of harvesting. The total energy gathered at R_K relay by active PU during the time τ is provided by:

$$E_{R_K}^h = \eta\tau \left(P_S |h_{S,R}|^2 + \sum_{n=1}^{N} P_n |h_{P,R}|^2 \right) \tag{4.62}$$

The power that each relay R_k transmits accompanied by non-linear EH circuit during $(T-\tau)$ transmission time is expressed as:

$$P_{R_k}^h = \begin{cases} \frac{E_{R_K}^h}{T-\tau}, & \left(P_S |h_{S,R}|^2 + \sum_{n=1}^{N} P_n |h_{P,R}|^2 \right) \leq \Gamma_{th} \\ \frac{\eta\tau\Gamma_{th}}{T-\tau}, & \left(P_S |h_{S,R}|^2 + \sum_{n=1}^{N} P_n |h_{P,R}|^2 \right) > \Gamma_{th} \end{cases} \tag{4.63}$$

Consequently, the expression for the signal-to-interference-noise ratio ($SINR$) at any of the n^{th} primary receiving node can be expressed as:

$$\gamma_n^{th} = \frac{P_n g_P}{P_S^u g_s + P_{R_k}^u g_{RP} + N_0} \tag{4.64}$$

The power required for transmission from S_{Tx} and R_k is limited by the peak interference power factor I_p of the primary user, which is determined using the formula

provided in [132],

$$I_p \geq \left(P_S^u g_S + P_{R_k}^u g_{R_P}\right) \tag{4.65}$$

Based on the above expression and assuming suboptimal conditions, it is vital to keep P_S^u and $P_{R_k}^u$ low to prevent excessive interference from PUs.
Therefore, the transmitted power of S_{Tx} must adhere to an outage constraint for the PU receiver, as expressed:

$$\begin{aligned} P_{out}^{primary} = Pr\left[\min_{n=1,\ldots,N}\left(\frac{P_n g_P}{P_S^u g_s + P_{R_k}^u g_{R_P} + N_0} \leq \gamma_{th}^{Pr}\right)\right] \\ \leq \varepsilon \end{aligned} \tag{4.66}$$

, where $\gamma_{th}^{Pr} = 2^{R_p} - 1$, and ε represents the outage threshold for P_{Rx}. R_p denotes the transmission rate of the PU network. Considering sub optimal power conditions, expression (4.66) is rephrased accordingly:

$$\begin{aligned} P_{out}^{primary} &= Pr\left[\min_{n=1,2,\ldots,N}\left(\frac{P_n g_P}{2P_S^u g_s + N_0} \leq \gamma_{th}^{Pr}\right)\right] \leq \varepsilon \\ &= 1 - \sum_{n=1}^{N}\left[1 - \underbrace{Pr\left(\frac{P_n g_P}{2P_S^u g_s + N_0} \leq \gamma_{th}^{Pr}\right)}_{P_{out}}\right] \leq \varepsilon \end{aligned} \tag{4.67}$$

Using the expression above, the outage probability P_{out} can be represented as shown in,

$$P_{out} = 1 - \exp\left(-\frac{\gamma_{th}^{Pr} N_0}{P_n \lambda_1}\right)\left(\frac{P_n \lambda_1}{P_n \lambda_1 + 2\gamma_{th}^{Pr} P_s^u \lambda_2}\right) \tag{4.68}$$

So, finally outage calculated for $P_{out}^{primary}$ at the primary receiver node from equation (4.64) is evaluated as:

$$\begin{aligned} P_{out}^{primary} = 1 - \left[\exp\left(-\frac{\gamma_{th}^{Pr} N_0}{P_n \lambda_1}\right)\left(\frac{P_n \lambda_1}{P_n \lambda_1 + 2\gamma_{th}^{Pr} P_S^u \lambda_2}\right)\right]^N \\ \leq \varepsilon \end{aligned} \tag{4.69}$$

Based on the expression above, secondary transmitters must adjust their transmit power to ensure PU receiver outage requirements are met. Corresponding power expressions are as follows:

$$P_S^u = \frac{P_n \lambda_1}{2\gamma_{th}^{Pr} \lambda_2} \left[\frac{\exp\left(-\frac{\gamma_{th}^{Pr} N_0}{P_n \lambda_1}\right)}{(1-\varepsilon)^{\frac{1}{N}}} - 1 \right] \tag{4.70}$$

$$P_{R_k}^u = \frac{P_n \lambda_1}{2\gamma_{th}^{Pr} \lambda_3} \left[\frac{\exp\left(-\frac{\gamma_{th}^{Pr} N_0}{P_n \lambda_1}\right)}{(1-\varepsilon)^{\frac{1}{N}}} - 1 \right] \tag{4.71}$$

In underlay mode, P_s^{un} and $P_{R_k}^{un}$ denote the transmitted powers of SU_T and the K^{th} relay, respectively, and are expressed as:

$$P_s^{un} = \min\left(P_s^h, P_S^u\right) \tag{4.72}$$

$$P_{R_k}^{un} = \min\left(P_{R_k}^h, P_S^u\right) \tag{4.73}$$

During overlay mode, secondary transmitters transmit at maximum power $P_{s,max}$ and $P_{R_k,max}$ for source and relay, respectively which are given as:

$$P_S^o = P_{s,max} \tag{4.74}$$

$$P_{R_k}^o = P_{R_k,max} \tag{4.75}$$

Where, P_S^o and $P_{R_k}^o$ are transmitted power from S_{Tx} and R_k, respectively at overlay mode.

4.3.3 Analysis of outage performance

During underlay mode of transmission, the received signal at the k^{th} relay from S_{Tx} is expressed as:

$$y^u_{Rk}(t) = \sqrt{P^u_S} h_{SR_k} x_s(t) + \sqrt{P^u_{R_k}} h_k x_r(t) + \sum_{n=1}^{N} \sqrt{P_n} h_{PR_k} x_p(t) + n_o(t) \tag{4.76}$$

Therefore, using the aforementioned expression, the SINR at the k^{th} FD relay node for the underlay method of transmission is defined as follows:

$$\gamma^u_1 = \frac{P^u_S g_{SR_k}}{P^u_{R_k} g_k + \sum_{n=1}^{N} P_n g_{P_{R_k}} + N_o} \tag{4.77}$$

In the underlay mode of operation, the signal received at S_{R_x} from the k^{th} FD relay is described as:

$$y^u_{Rx}(t) = \sqrt{P^u_{R_k}} h_{R_k} x_r(t) + \sum_{n=1}^{N} \sqrt{P_n} h_{Rx} x_p(t) + n_o(t) \tag{4.78}$$

Consequently, using the aforementioned expression, the SINR at the secondary receiver for the underlay spectrum sharing approach of transmission is obtained as:

$$\gamma^u_2 = \frac{P^u_{R_k} g_{R_k}}{\sum_{n=1}^{N} P_n g_{R_x} + N_o} \tag{4.79}$$

Since the secondary destination employs a selection combination (SC) technique, the end-to-end outage probability for the corresponding S_{R_x} under the underlay method is defined as:

$$P^{under}_{out} = Pr\left[\left\{ \max_k \left(\min\left(\gamma^u_1, \gamma^u_2\right)\right) \right\} < \gamma^S_{th}\right] \tag{4.80}$$

where, $\gamma^S_{th} = 2^{R_s} - 1$ denote the outage threshold at S_{R_x} with R_s the transmission rate of secondary user.

By using order statistics [133],

$$Pr\left[\min\left(\gamma_1^u,\gamma_2^u\right)<\gamma_{th}^S\right]=Pr\left[\gamma_1^u<\gamma_{th}^S\right]+Pr\left[\gamma_1^u>\gamma_{th}^S\right]Pr\left[\gamma_2^u<\gamma_{th}^S\right] \tag{4.81}$$

Finally, during the underlay mode of transmission, the outage probability P_{out}^{under} can be calculated combining both the above expression as:

$$\begin{aligned}P_{out}^{under}=&\left[\left\{1-\exp\left(-\frac{\gamma_{th}^S N_0}{P_S^u\lambda_6}\right)\left(\frac{P_S^u\lambda_6}{P_S^u\lambda_6+\gamma_{th}^S P_n\lambda_4}\right)\right.\right.\\&\left.\left(\frac{P_{R_k}^u\lambda_8}{P_{R_k}^u\lambda_8-P_n\lambda_4}\right)^N\right\}+\left\{\exp\left(-\frac{\gamma_{th}^S N_0}{P_S^u\lambda_6}\right)\right.\\&\left.\left(\frac{P_S^u\lambda_6}{P_S^u\lambda_6+\gamma_{th}^S P_n\lambda_4}\right)\left(\frac{P_{R_k}^u\lambda_8}{P_{R_k}^u\lambda_8-P_n\lambda_4}\right)^N\right\}\times\\&\left.\left\{1-\exp\left(-\frac{\gamma_{th}^S N_0}{P_{R_k}^u\lambda_7}\right)\left(\frac{P_{R_k}^u\lambda_7}{P_{R_k}^u\lambda_7+\gamma_{th}^S P_n\lambda_5}\right)^N\right\}\right]^K\end{aligned} \tag{4.82}$$

In the overlay transmission method, the received signal at the k^{th} relay from the transmission of S_{Tx} is expressed as:

$$y_{R_k}^o(t)=\sqrt{P_S^o}h_{SR_k}x_s(t)+\sqrt{P_{R_k}^o}h_k x_r(t)+n_o(t) \tag{4.83}$$

Therefore, in the overlay spectrum sharing method of transmission, the SINR expression at the k^{th} full-duplex (FD) relay is derived from the aforementioned expression as:

$$\gamma_1^o=\frac{P_S^o g_{SR_k}}{P_{R_k}^o g_k+N_o} \tag{4.84}$$

The signal received at S_{R_x} through the k^{th} FD relay when operating in overlay method is represented by:

$$y_{Rx}^o(t)=\sqrt{P_{R_k}^o}h_{R_k}x_r(t)+n_o(t) \tag{4.85}$$

Consequently, the SINR for the secondary receiver at the time of the overlay technique for transmission is expressed as:

$$\gamma_2^o = \frac{P_{R_k}^o g_{R_k}}{N_o} \tag{4.86}$$

Similarly, the SC method is utilized within the S_{R_x}, resulting in an end-to-end outage probability expression throughout the overlay transmission method, which is expressed as:

$$P_{out}^{over} = Pr\left[\left\{ \max_k \left(\min\left(\gamma_1^o, \gamma_2^o\right)\right)\right\} < \gamma_{th}^S\right] \tag{4.87}$$

Thus, the overlay mode end-to-end outage performance at S_{R_x} as described above can be written as follows:

$$\begin{aligned} P_{out}^{over} = & \left[1 - \exp\left(-\frac{\gamma_{th}^S N_0}{P_S^o \lambda_6}\right)\left(\frac{P_S^o \lambda_6}{P_S^o \lambda_6 + \gamma_{th}^S P_{R_k}^o \lambda_8}\right)\right. \\ & + \left\{\exp\left(-\frac{\gamma_{th}^S N_0}{P_S^o \lambda_6}\right)\left(\frac{P_S^o \lambda_6}{P_S^o \lambda_6 + \gamma_{th}^S P_{R_k}^o \lambda_8}\right)\right\} \times \\ & \left.\left\{1 - \exp\left(-\frac{\gamma_{th}^S N_0}{P_{R_k}^o \lambda_7}\right)\right\}\right]^K \end{aligned} \tag{4.88}$$

Finally, the outage probability for the full-duplex relaying approach within the combined underlay/overlay protocol is capable of being articulated as per:

$$P_{OUT}^{TOTAL} = [(1 - P_d) + \alpha P_d] P_{out}^{under} + (1 - \alpha) P_{out}^{over} \tag{4.89}$$

4.3.4 Result assessment and discussion

This section presents results and assessments of the system's performance using MATLAB simulation testbed. Proposed FD relay-supported adaptive spectrum access method, integrating underlay and overlay approaches, improves performance, as evidenced by the simulation results presented here. By employing FD relay instead of HD relay, spectrum efficiency enhances multi fold. The following parameters

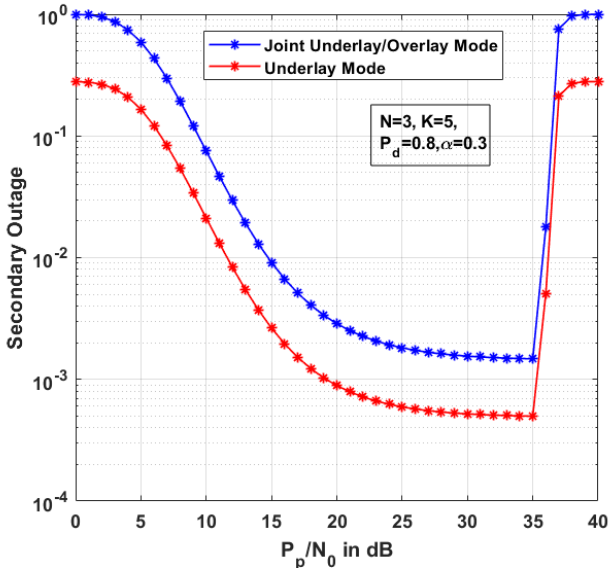

FIGURE 4.16: Comparison among the underlay, overlay, and joint underlay/overlay protocols for SU outages with reference to P_p/N_o (dB)

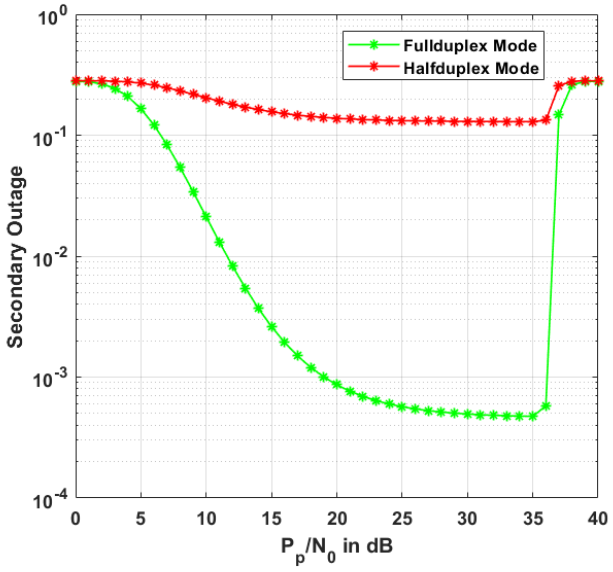

FIGURE 4.17: SU outage under joint underlay/overlay with FD relaying versus HD relaying approach with respect to P_p/N_o (dB)

are considered to evaluate system performance: PU transmission rate R_p=0.15 bits/s/Hz, SU transmission rate R_s=0.1 bits/s/Hz and primary user outage constraint $\varepsilon = 0.1$. The probability of detection, $P_d = 0.85$, normalised noise power is unity, the probability of channel occupancy $\alpha = 0.15$ and SI parameter of $\lambda_8 = 0.3$ is taken

into consideration.

Fig. 4.16 illustrates the end-to-end outage behaviour for different protocols, such as underlay and combined underlay/overlay under FD relaying, with primary users N=3. The overlay approach alone is impractical for SU communications, making it unsuitable for spectrum sharing. The combined underlay/overlay approach, however, outperforms the current underlay scenario for multiple PUs during outages. This improvement is due to the secondary transmitter switching to power restriction mode when the PU is active, and utilizing maximum power for data transmission when PU is inactive. The outage performance of secondary receiver deteriorates after 35 dB of P_p/N_0 due to the inclusion of a nonlinear EH circuit at SU transmitters and interference's from PU users.

Fig. 4.17 demonstrates that, compared to a HD relay network, the combined underlay/overlay mode in a full-duplex relay network has greater impact to the secondary network's outage behaviour. The findings clearly indicate that implementing an FD relay network, rather than an HD relay network, enhances outage performance when multiple primary users are present.

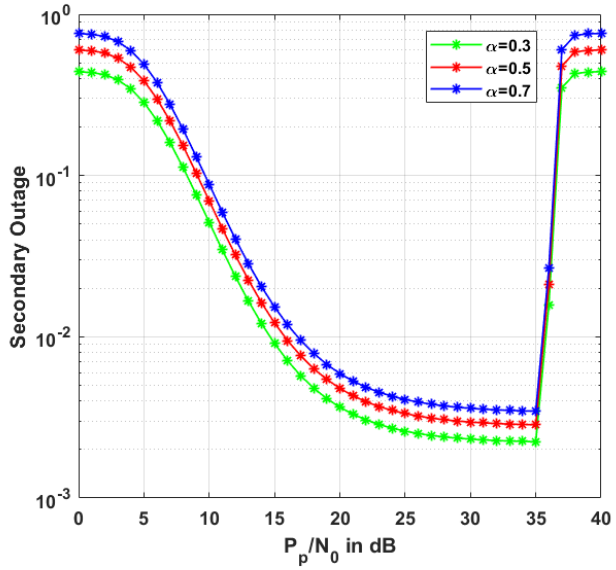

FIGURE 4.18: SU outage comparison for joint scheme FD relay mode with reference to P_p/N_o (dB), varying α

Fig. 4.18 shows the secondary network's outage behaviour in terms of P_p/N_o via

FD relay in adaptive underlay/overlay mode. The simulation assumes a fixed number of relays (K=5) and primary users (N=3), with varying channel occupancy $\alpha = 0.3, 0.5$ and 0.7. The normalized transmit power for the primary transmitter is set at 30 dB. The analysis indicates that the outage performance improves as α decreases, meaning lower channel occupancy results in better outage performance.

Fig. 4.19 demonstrates the secondary outage performance in terms of P_p/N_o in

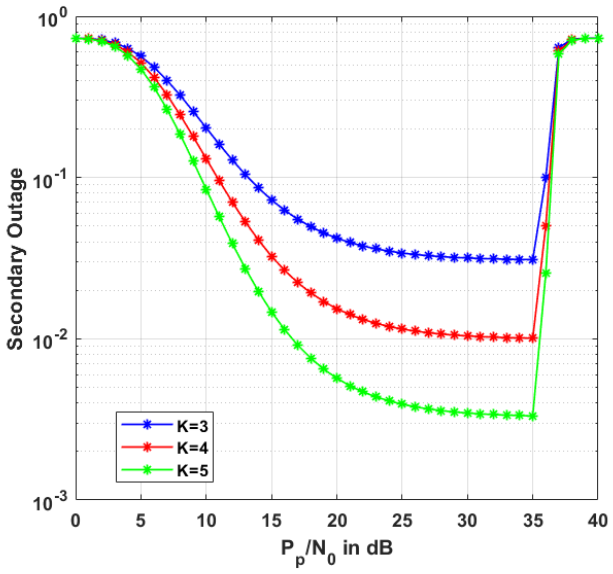

FIGURE 4.19: SU outage performance comparison in combined FD relaying mode based on P_p/N_o and K

dB through FD relay protocol in joint underlay/overlay transmission. The analysis considers fixed number of primary users ($N = 3$) with the variation of FD relays ($K = 3, 4, 5$). The study shows that increasing the number of FD relays improves the outage performance at the destination. This indicates that incorporating multiple FD relays in the system model enhances the diversity order and, consequently, the overall system performance.

Fig. 4.20 illustrates the secondary network's outage at S_{Rx} in relation to the detection probability P_d, using the FD relay protocol in adaptive underlay/overlay mode. The analysis indicates that outage performance improves as the detection probability increases.

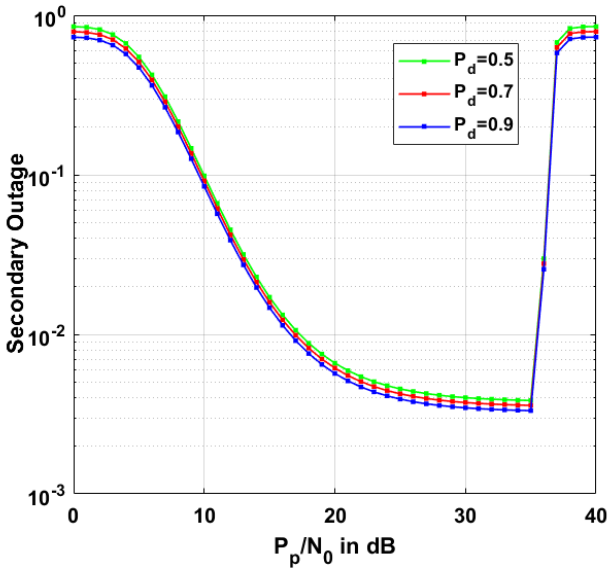

FIGURE 4.20: Performance comparison of SU outages in joint FD relaying mode in relation to detection probability P_d

4.4 Chapter summary

In this chapter, we have proposed and comprehensively analyzed an adaptive cognitive radio network (CRN) communication model that integrates full-duplex (FD) relaying with joint underlay/overlay transmission in a multi-user, multi-primary user environment under both linear and nonlinear energy harvesting (EH) scenarios. The findings of this chapter demonstrate an excellent method for integrating an FD relay network, which performs better than an HD relay network in terms of throughput and spectrum efficiency. System performance improves with dynamic switching between underlay and overlay modes based on real-time PU activity sensing, enabling efficient spectrum utilization. Through analytical and simulation-based evaluations, it is demonstrated that FD relaying significantly outperforms half-duplex (HD) relaying in terms of outage probability and throughput, even under high channel occupancy and low EH efficiency. In addition, the proposed model effectively balances energy harvesting, interference management, and throughput optimization. According to this study, an FD relaying CRN's nonlinear energy harvesting environment is significantly more realistic, which explains why the system provides a better outage

to its maximum permitted transmit power. The study concludes that the combination of FD relaying, cooperative diversity, and adaptive mode switching forms a robust and scalable solution to enhance overall performance (i.e., outage probability and system throughput) in future CRN deployments, with potential extensions of incorporating NOMA and intelligent reflecting surfaces (IRS) to further increase spectrum and energy efficiency.

Chapter 5

Performance analysis of NOMA-based hybrid cognitive radio network with full-duplex relay support

This chapter examines the throughput and outage performance of secondary users in a hybrid cognitive radio network (CRN) based on non-orthogonal multiple access (NOMA) technology. Based on channel occupancy, secondary transmitters in a hybrid CRN immediately switch between overlay or underlay mode in response to sensing results. If the primary user (PU) is not active, they operate in overlay mode with the maximum permitted transmit power; otherwise, they operate in underlay mode with a transmit power restriction. The secondary network employs the NOMA approach, in which the base station (BS) is assisted by a full-duplex (FD) relay network to send information to the secondary destinations. Secondary transmitters are equipped with an energy detector and harvesting circuit, which allows us to sense and store energy from the radio frequency of the multiple primary users. The benefit of using multiple FD relays along with the hybrid operation of joint

mode of transmission enables to increase the system throughput. Finally, an analytical formulation including closed form for the outage probability as encountered by the secondary users (SUs) in the presence of self interference (SI) and imperfect successive interference cancellation (i-SIC) under hybrid mode has been derived and validated through MATLAB simulation.

5.1 System model of NOMA-based hybrid cognitive radio network assist by full-duplex relay

In NOMA, individual user operates in same frequency band at the same time but they are distinguished by different power level intensities. Superposition signal is used at the transmitting section in such a way that successive interference cancellation (SIC) receiver can separate the users operating both in the uplink as well as downlink channels.

The system model assumed in this chapter is a cognitive radio network employing NOMA downlink scenario built up with multi primary users ($PU_{TX_n} - PU_{RX_n}; n = 1, 2, \ldots, N$) with PU_{TX_n}, PU_{RX_n} symbolized as n^{th} primary transmitter and primary receiver, respectively. A near secondary user destination (SU_1) and far secondary user destination (SU_2) receive signal from a secondary base station transmitter (BS) via FD relay network ($R_k; k = 1, 2, \ldots, K$) simultaneously. It is also assumed that the SUs require N licensed frequency bands each of which with the bandwidth, B1, B2, ... B_N. For simplicity, it has been assumed that B1=B2...=B_N=B (unit bandwidth); so SUs exploit a total bandwidth of NB from N number of primary users. Each FD relay and BS have an energy detector as well as EH circuit that can sense and collect energy from radio-frequency waves in the environment. The transmitting nodes at secondary are able to generate a portion of their energy from the N active PUs which create interference. The reason for adopting these EH circuits

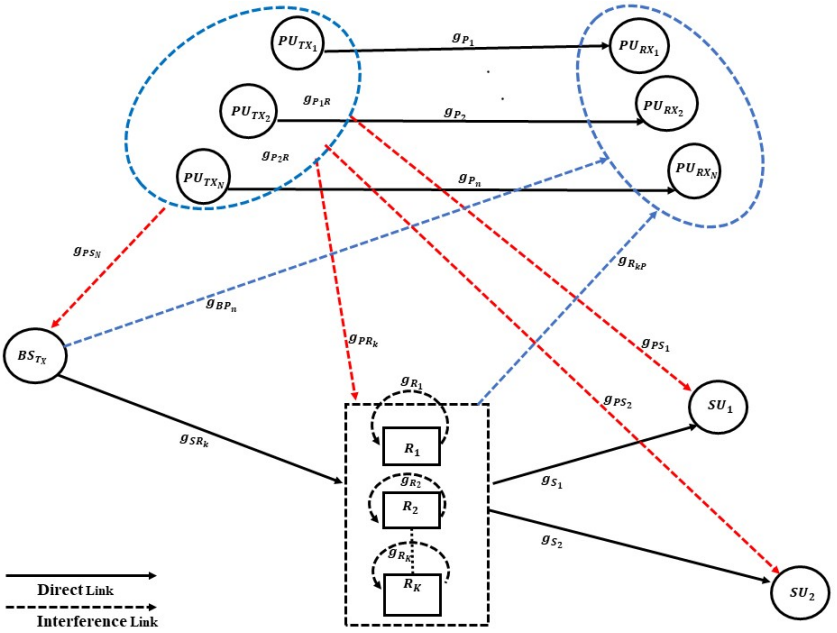

FIGURE 5.1: System model of FD relay based CRN under NOMA technique

as a component of the linear EH model in this proposed system is to avoid the intricate mathematical complexities and burdensome calculations associated with the non-linear EH model [137, 138]. Due to the significant shadowing effect, it is also considered that BS has no direct link to any of the SU destinations. Channel coefficients $h_{i,j}$ follow Rayleigh distribution with corresponding gains to be $g_{i,j}$ with exponential distribution of mean λ_a. TABLE 5.1 below provides link parameters in details.

However, a partial relay selection (PRS) mechanism is employed before the communication process begins. An efficient FD relay is selected by BS from the relay network based on estimated channel state information (CSI). This process is done by employing pilot symbols by BS to relay network [119]. After receiving the relevant pilot signals, each relay will then acknowledge the CSI of each of their respective links. Following the collection of the relevant CSI data, the BS chooses the selected R_k from relay network for transmission process. More specifically, the selected relay R_k is chosen on the basis of channel quality of the links and then the communication process starts from base station to the respective destinations via this selected relay.

TABLE 5.1: Path link- gain - parameter chart

Path link- gain - parameter chart		
Path,channel coefficient($h_{i,j}$)	gain $g_{i,j}$	Parameter λ_a
R_K-SU_1, h_{S_1}	g_{S_1}	λ_1
R_K-SU_2, h_{S_2}	g_{S_2}	λ_2
BS-R_K, h_{SR_k}	g_{SR_k}	λ_3
PU_{TX_N}-PU_{RX_N}, h_{P_n}	g_{P_n}	λ_4
R_K-PU_{RX_N}, h_{R_kP}	g_{R_kP}	λ_5
PU_{TX_N}-R_K, h_{PR_k}	g_{PR_k}	λ_6
PU_{TX_N}-SU_1, h_{PS_1}	g_{PS_1}	λ_7
PU_{TX_N}-SU_2, h_{PS_2}	g_{PS_2}	λ_8
R_K-R_K, h_{R_k}	g_{R_k}	λ_9
BS-PU_{RX_N}, h_{BP_n}	g_{BP_n}	λ_{10}

In order to transmit data to secondary destinations under this PRS scheme, the selected relay R_k needs to have the maximum channel gain from the BS to the relay network, which is represented as:

$$R_k = arg \max_{k=1,\ldots,K} |h_{SR_k}|^2 \tag{5.1}$$

The information is forwarded to both SU_1(S1) and SU_2(S2) simultaneously in the transmission process from BS via selected relay. This chapter describes an adaptive hybrid combination of underlay/overlay transmission technique to boost the CR network's spectrum efficiency. With the capability of the energy detector circuit embedded within the BS, it senses the activity of all PUs. After being sensed, BS and selected FD relay take part in monitoring the switching activity simultaneously to either underlay or overlay mode to communicate with the destinations. If the PU is busy after detecting, BS switches to its power restriction mode (underlay); if not, BS operates at its full power (overlay), helped by a selected active FD relay.

According to Federal Communications Commission (FCC) [128], the usual channel occupancy ranged between 15 percent to peak usage of close to 85 percent. Let, α be the probability of channel occupancy ($0 \leq \alpha \leq 1$), i.e., busy state of PU channel. Therefore, the probability for PU to be busy is αP_d and to be in inactive mode is

$(1-\alpha)P_d$, where, P_d is probability of detection of primary signal [16] and can be outlined as $P_d = \prod_{n=1}^{N} P_{d,n}$, where, $P_{d,n}$ is probability of detection of n^{th} primary user.

5.2 Energy harvesting and power management strategies

This has been assumed that T is the total amount of time it takes for the overall process including τ which is the length of time that secondary BS needs to harvest energy from the N-active PU network while sensing; transmission of data is done using the remaining $(T-\tau)$ time period.
Energy harvested at BS among all the N numbers of active PUs during time τ is formulated as:

$$E_{BS}^{H} = \eta\tau \left(\sum_{n=1}^{N} P_n g_{PS_N} \right) \tag{5.2}$$

where, P_n is defined as power transmitted from any $PU - TX_N$ with channel gain of g_{PS_N}. The in-built energy harvesting circuits have an efficiency factor of η.
During the transmission time of $(T-\tau)$, the accumulated power by EH circuit as driven by BS can be expressed as:

$$P_{BS}^{H} = \left(\frac{E_{BS}^{H}}{T-\tau} \right) \tag{5.3}$$

The harvested energy by an FD relay at time τ among N active PU is given by:

$$E_{SR_k}^{H} = \eta\tau \left(\sum_{n=1}^{N} P_n g_{PR_k} \right) \tag{5.4}$$

Similarly, during the transmission time of $(T-\tau)$, the accumulated power by EH circuit as driven by R_k can be expressed as:

$$P_{R_k}^H = \left(\frac{E_{SR_k}^H}{T-\tau}\right) \tag{5.5}$$

The peak interference parameter I_p of the primary network limits the simultaneous transmit power from BS and R_k as in the following equation

$$I_p \geq \left(P_s^0 g_{BP_n} + P_{R_k}^0 g_{R_k P}\right) \tag{5.6}$$

The primary unit's n^{th} receiver deals with signal to interference noise ratio,

$$\gamma_n = \frac{P_n g_{Pn}}{P_s^0 g_{BP_n} + P_{R_k}^0 g_{R_k P} + N_0} \tag{5.7}$$

From (5.7), assuming non-optimal conditions for P_s^0 and $P_{R_k}^0$ for simplicity, the BS and R_k transmit power should be maintained so that no PUs are subject to excessive interference from the communication of the SUs [29, 132] and $n_o(t) \sim \mathcal{N}(0, N_0)$ is defined as a complex Gaussian random signal with variance N_0 at each receiver node.

The transmitted power from the secondary transmitters must meet specific requirements in order to maintain the outage at the PU receiver and can be expressed as:

$$P_O^1 = Pr\left[\min_{n=1,\ldots,N}\left(\frac{P_n g_{Pn}}{P_s^0 g_{BP_n} + P_{R_k}^0 g_{R_k P} + N_0} \leq \gamma_{th}^P\right)\right] \leq \varepsilon \tag{5.8}$$

where, $\gamma_{th}^P = 2^{R_p} - 1$ signifies outage threshold (with R_p being the PU transmission rate), ε defines outage constraint at $PU - R_{XN}$.

The transmit power from both BS as well as from FD relay during underlay transmission must be either less than or equal to the primary outage constrain ε so as to maintain quality of service (QoS) of PUs. With the simplification of equal transmit

power, this primary outage can be rewritten as:

$$\begin{aligned} P_O^1 &= Pr\left[\min_{n=1,2,\ldots,N}\left(\frac{P_n g_{Pn}}{2P_s^0 g_{BP_n}+N_0}\leq \gamma_{th}^P\right)\right]\leq \varepsilon \\ &= 1-\sum_{n=1}^{N}\left[1-\underbrace{Pr\left(\frac{P_n g_{Pn}}{2P_s^0 g_{BP_n}+N_0}\leq \gamma_{th}^P\right)}_{P^o}\right]\leq \varepsilon \end{aligned} \tag{5.9}$$

where, P^o can be derived as:

$$P^o = 1-\exp\left(-\frac{\gamma_{th}^P N_0}{P_n\lambda_4}\right)\left(\frac{P_n\lambda_4}{P_n\lambda_4+2\gamma_{th}^P P_s^0\lambda_{10}}\right) \tag{5.10}$$

Substituting the value of P^o in equation (5.9) the outage expression P_O^1 can be simplified as:

$$P_O^1 = 1-\left[\exp\left(-\frac{\gamma_{th}^P N_0}{P_n\lambda_4}\right)\left(\frac{P_n\lambda_4}{P_n\lambda_4+2\gamma_{th}^P P_s^0\lambda_{10}}\right)\right]^N\leq \varepsilon \tag{5.11}$$

Therefore, the ability of the BS to transmit power under consideration of PU outage is written as:

$$P_s^0 = \frac{P_p\lambda_4}{2\gamma_{th}^P\lambda_{10}}\left[\frac{\exp\left(-\frac{\gamma_{th}^P N_0}{P_p\lambda_4}\right)}{(1-\varepsilon)^{\frac{1}{N}}}-1\right] \tag{5.12}$$

Similarly, the ability of the R_k to transmit power under consideration of PU outage is outlined by:

$$P_{R_k}^0 = \frac{P_p\lambda_4}{2\gamma_{th}^P\lambda_6}\left[\frac{\exp\left(-\frac{\gamma_{th}^P N_0}{P_p\lambda_4}\right)}{(1-\varepsilon)^{\frac{1}{N}}}-1\right] \tag{5.13}$$

At the underlay mode of transmission, the amount of power required by BS is provided by:

$$P_{S,u} = \min\left(P_{BS}^H, P_s^0\right) \tag{5.14}$$

Similarly, at the underlay mode of transmission, the amount of power required by R_k is shown as:

$$P_{R,u} = \min\left(P_{R_k}^H, P_{R_k}^0\right) \tag{5.15}$$

However, the base station can transmit with its maximum power while in overlay mode, and is expressed as:

$$P_{S,o} = P_{BS}^{H} \tag{5.16}$$

Similarly, the transmitted power by FD relay while in overlay mode is given by:

$$P_{R,o} = P_{R_k}^{H} \tag{5.17}$$

5.3 Performance and mathematical analysis

Let the message signals $s_1(t)$ and $s_2(t)$ correspond to SU_1 and SU_2 respectively. By assigning different power levels to SU_1 and SU_2, BS generates the NOMA signal $s(t)$ in the power domain. Because of the different channel characteristics that SU_1 and SU_2 have with BS and R_k, we classify SU_1 as the near user and SU_2 as the far user, where $|h_{R_k1}|^2 > |h_{R_k2}|^2$. This has been assumed that SU_1 and SU_2 are having a_1 and a_2 as their power allocation coefficients respectively as assigned by BS. Depending upon the mode of transmission as decided by BS to be either underlay or overlay, power allocated to SU_1 is $a_1P_{S,u}$ or $a_1P_{S,o}$ and $a_2P_{S,u}$ or $a_2P_{S,o}$, where $a_1 < a_2$, $\sum_{i=1}^{2} a_i = 1$. During the transmission process, the BS broadcasts the information to the relay network R_k, $k = 1, 2, ., K$. Simultaneously, the communication is performed by sending the information from selected FD relay to both SU_1 and SU_2. After the end of communication process, each of SU_1 and SU_2 individually uses a selection combination scheme to decode the information.

The transmitted signal $s(t)$ by the BS during underlay mode of transmission is given by:

$$s_u(t) = \sqrt{a_1P_{S,u}}s_1(t) + \sqrt{a_2P_{S,u}}s_2(t) \tag{5.18}$$

This base station's signal $s(t)$ during overlay mode of transmission changes and becomes:

$$s_o(t) = \sqrt{a_1P_{S,o}}s_1(t) + \sqrt{a_2P_{S,o}}s_2(t) \tag{5.19}$$

5.3.1 Outage analysis during underlay mode

During underlay mode of operation at the secondary node, the received signal at R_k transmitted from BS is given by:

$$y_{Rk}^{U}(t) = s_u(t)h_{SR_K} + \sqrt{P_{R_k}}h_{Rk}s_{ru}(t) + \sum_{n=1}^{N}\sqrt{P_n}h_{PR_k}x_n(t) + n_o(t) \tag{5.20}$$

where, $s(t)$, $s_{ru}(t)$ and $x_n(t)$ symbolize the signals from BS, R_k and n^{th} $PU-Tx$, respectively under the assumption that $\mathbb{E}|s(t)|^2 = 1$, $\mathbb{E}|s_{ru}(t)|^2 = 1$, $\mathbb{E}|x_n(t)|^2 = 1$ with $h_{i,j}$ is the channel coefficient with their standard meaning as already stated. The term $n_o(t)$ is defined as a complex Gaussian random signal with zero mean and variance N_0.

The relay R_k decodes the signal of SU_2 first followed by the signal of SU_1 using successive interference cancellation because of the fact that former signal is transmitted with more power for far user. The $SINR$ at R_k is given by $\gamma_{R,2}^{U}$ and $\gamma_{R,1}^{U}$ for $s_2(t)$ and $s_1(t)$, respectively which are calculated as:

$$\gamma_{R,2}^{U} = \frac{a_2 P_{S,u} g_{SR_k}}{a_1 P_{S,u} g_{SR_k} + P_{R_k} g_{R_k} + \sum_{n=1}^{N} P_n g_{PR_k} + N_o} \tag{5.21}$$

$$\gamma_{R,1}^{U} = \frac{a_1 P_{S,u} g_{SR_k}}{\phi a_2 P_{S,u} g_{SR_k} + P_{R_k} g_{R_k} + \sum_{n=1}^{N} P_n g_{PR_k} + N_o} \tag{5.22}$$

where, the terms ϕ $(0 \leq \phi \leq 1)$ and $(\phi a_2 P_{S,u} g_{SR_k})$ refer to the i-SIC factor and the residual i-SIC interference at R_k respectively.

In continuation to this, the information is sent to SU_1 and SU_2 simultaneously by the R_k. During underlay operation, the decoded signal at R_k forms a composite NOMA signal which is given by:

$$s_{ru}(t) = \sqrt{\alpha_1 P_{R,u}}s_1(t) + \sqrt{\alpha_2 P_{R,u}}s_2(t) \tag{5.23}$$

Now the received signal at SU_1 from relay can be expressed as:

$$y_{S_1}^U(t) = s_{ru}(t)h_{S1} + \sum_{n=1}^{N} \sqrt{P_n} h_{Ps_1} x_n(t) + n_o(t) \tag{5.24}$$

This has been assumed that α_1 and α_2 are power allocation coefficients for SU_1 and SU_2 respectively as assigned by FD relay, where, $\alpha_1 < \alpha_2$, $\sum_{i=1}^{2} \alpha_i = 1$. Since, the signal for the far user SU_2 is stronger than the signal for the near user SU_1; the signal from SU_2 is decoded first after receiving the composite signal from the relay by SU_1 using SIC. So, at underlay mode, the $(SINR)$ at SU_1 can be written as:

$$\gamma_{S1,2}^U = \frac{\alpha_2 P_{R,u} g_{s1}}{\alpha_1 P_{R,u} g_{s1} + \sum_{n=1}^{N} P_n g_{P_{S1}} + N_o} \tag{5.25}$$

$$\gamma_{S1,1}^U = \frac{\alpha_1 P_{R,u} g_{s1}}{\xi \alpha_2 P_{R,u} g_{s1} + \sum_{n=1}^{N} P_n g_{P_{S1}} + N_o} \tag{5.26}$$

where, the terms ξ $(0 \leq \xi \leq 1)$ and $(\xi \alpha_2 P_{R,u} g_{s1})$ refer to the i-SIC factor and the residual i-SIC interference at SU_1 respectively. Similarly, SU_2 by receiving the new NOMA composite signal from the FD relay, decodes its own high powered signal. Therefore, the received signal at SU_2 can be outlined as:

$$y_{S_2}^U(t) = s_{ru}(t)h_{S2} + \sum_{n=1}^{N} \sqrt{P_n} h_{Ps_2} x_n(t) + n_o(t) \tag{5.27}$$

So, at underlay mode, the $SINR$ at SU_2 can be written as:

$$\gamma_{S2,2}^U = \frac{\alpha_2 P_{R,u} g_{s2}}{\alpha_1 P_{R,u} g_{s2} + \sum_{n=1}^{N} P_n g_{P_{S2}} + N_o} \tag{5.28}$$

Now, the analytical models for evaluating the outage probability that SU_1 and SU_2 experienced in the system under consideration for CR-NOMA have been derived. Thus the condition for the end-to-end outage probability at SU_1 is given by:

$$P_{out,1}^{under} = Pr\Big[\max_k \gamma_{R,2}^U \leq u_2^{FD}, \max_k \gamma_{R,1}^U \leq u_1^{FD}, \gamma_{S1,2}^U \leq u_2^{FD}, \gamma_{S1,1}^U \leq u_1^{FD} \Big] \tag{5.29}$$

where, $u_1^{FD} = 2^{R_1/N} - 1$ and $u_2^{FD} = 2^{R_2/N} - 1$ denote the outage threshold of the selected destination for the given full-duplex communication. The transmission rate of SU_1 is R_1 and SU_2 is R_2.

Now, by substituting the values of $\gamma_{R,2}^U$, $\gamma_{R,1}^U$, $\gamma_{S1,2}^U$ and $\gamma_{S1,1}^U$, the above expression can be rewritten as:

$$\begin{aligned} P_{out,1}^{under} = \; & Pr\Big[\prod_{k=1}^{K} \frac{P_{S,u} g_{SR_k}}{P_{R_k} g_{R_k} + \sum_{n=1}^{N} P_n g_{PR_k} + N_o} \leq \gamma_{th}^1, \\ & \prod_{k=1}^{K} \frac{P_{S,u} g_{SR_k}}{P_{R_k} g_{R_k} + \sum_{n=1}^{N} P_n g_{PR_k} + N_o} \leq \gamma_{th}^2, \\ & \frac{P_{R,u} g_{S1}}{\sum_{n=1}^{N} P_n g_{P_{S1}} + N_o} \leq \gamma_{th}^3, \frac{P_{R,u} g_{S1}}{\sum_{n=1}^{N} P_n g_{P_{S1}} + N_o} \leq \gamma_{th}^4\Big] \end{aligned} \tag{5.30}$$

where,

$$\begin{aligned} \gamma_{th}^1 = \frac{u_2^{FD}}{a_2 - a_1 u_2^{FD}}, \gamma_{th}^2 = \frac{u_1^{FD}}{a_1 - \phi a_2 u_1^{FD}}, \\ \gamma_{th}^3 = \frac{u_2^{FD}}{\alpha_2 - \alpha_1 u_2^{FD}}, \gamma_{th}^4 = \frac{u_1^{FD}}{\alpha_1 - \xi \alpha_2 u_1^{FD}} \end{aligned}$$

The condition for the end-to-end outage probability at SU_2 is given by:

$$P_{out,2}^{under} = Pr\Big[\max_k \gamma_{R,2}^U \leq u_2^{FD}, \max_k \gamma_{R,1}^U \leq u_1^{FD}, \gamma_{S2,2}^U \leq u_2^{FD}\Big] \tag{5.31}$$

Now, by substituting the values of $\gamma_{R,2}^U$, $\gamma_{R,1}^U$ and $\gamma_{S2,2}^U$, the above expression can be rewritten as:

$$\begin{aligned} P_{out,2}^{under} = \; & Pr\Big[\prod_{k=1}^{K} \frac{P_{S,u} g_{SR_k}}{P_{R_k} g_{R_k} + \sum_{n=1}^{N} P_n g_{PR_k} + N_o} \leq \gamma_{th}^1, \\ & \prod_{k=1}^{K} \frac{P_{S,u} g_{SR_k}}{P_{R_k} g_{R_k} + \sum_{n=1}^{N} P_n g_{PR_k} + N_o} \leq \gamma_{th}^2, \frac{P_{R,u} g_2}{\sum_{n=1}^{N} P_n g_{P_{S2}} + N_o} \leq \gamma_{th}^3\Big] \end{aligned} \tag{5.32}$$

The closed form expression for end-to-end outage probability at SU_1 and SU_2 during underlay transmission protocol can be evaluated as:

$$P_{out,1}^{under} = \Bigg[\underbrace{\left\{1-\exp\left(-\frac{\gamma_{th}^{1}N_0}{P_{S,u}\lambda_3}\right)\left(\frac{P_{S,u}\lambda_3}{P_{S,u}\lambda_3+\gamma_{th}^{1}P_{R,u}\lambda_9}\right)\left(\frac{P_{R,u}\lambda_9}{P_{R,u}\lambda_9-P_n\lambda_6}\right)^N\right\}^K}_{U}\times$$
$$\underbrace{\left\{1-\exp\left(-\frac{\gamma_{th}^{2}N_0}{P_{S,u}\lambda_3}\right)\left(\frac{P_{S,u}\lambda_3}{P_{S,u}\lambda_3+\gamma_{th}^{2}P_{R,u}\lambda_9}\right)\left(\frac{P_{R,u}\lambda_9}{P_{R,u}\lambda_9-P_n\lambda_6}\right)^N\right\}^K}_{V}\times$$
$$\left\{1-\exp\left(-\frac{\gamma_{th}^{3}N_0}{P_{R,u}\lambda_1}\right)\left(\frac{P_{R,u}\lambda_1}{P_{R,u}\lambda_1+\gamma_{th}^{3}P_n\lambda_7}\right)^N\right\}\times$$
$$\left\{1-\exp\left(-\frac{\gamma_{th}^{4}N_0}{P_{R,u}\lambda_1}\right)\left(\frac{P_{R,u}\lambda_1}{P_{R,u}\lambda_1+\gamma_{th}^{4}P_n\lambda_7}\right)^N\right\}\Bigg] \tag{5.33}$$

Proof: Refer to Appendix C, D for proof of U and V.

$$P_{out,2}^{under} = \left[U\times V\times\left\{1-\exp\left(-\frac{\gamma_{th}^{3}N_0}{P_{R,u}\lambda_2}\right)\left(\frac{P_{R,u}\lambda_2}{P_{R,u}\lambda_2+\gamma_{th}^{3}P_n\lambda_8}\right)^N\right\}\right] \tag{5.34}$$

5.3.2 Outage analysis during overlay mode

Considering the overlay transmission mode in which the secondary transmitters are allowed to transmit with their maximum power, the received signal at FD relay from BS is given by:

$$y_{Rk}^{O}(t) = s_o(t)h_{SR_K} + \sqrt{P_{R_k}}h_{Rk}s_{ro}(t) + n_o(t) \tag{5.35}$$

The composite new NOMA signal during overlay operation is given by:

$$s_{ro}(t) = \sqrt{\alpha_1 P_{S,o}}s_1(t) + \sqrt{\alpha_2 P_{S,o}}s_2(t) \tag{5.36}$$

FD relay, after receiving the composite NOMA signal from BS, decodes the SU_2's signal first followed by SU_1's signal using SIC technique. Therefore, at overlay mode,

the $SINR$ at relay for $s_2(t)$ and $s_1(t)$, can be written respectively as:

$$\gamma_{R,2}^{O} = \frac{a_2 P_{S,o} g_{SR_k}}{a_1 P_{S,o} g_{SR_k} + P_{R_k} g_{R_k} + N_o} \tag{5.37}$$

$$\gamma_{R,1}^{O} = \frac{a_1 P_{S,o} g_{SR_k}}{\phi a_2 P_{S,o} g_{SR_k} + P_{R_k} g_{R_k} + N_o} \tag{5.38}$$

where, the terms ϕ $(0 \leq \phi \leq 1)$ and $(\phi a_2 P_{S,o} g_{SR_k})$ refer to the i-SIC factor and the residual i-SIC interference at R_k, respectively.

The received signal at SU_1 during overlay transmission process can be expressed as:

$$y_{S_1}^{O}(t) = s_{ro}(t) h_{S1} + n_o(t) \tag{5.39}$$

So, at overlay mode, the $SINR$ at SU_1 for $s_2(t)$ and $s_1(t)$ can be written respectively as:

$$\gamma_{S1,2}^{O} = \frac{\alpha_2 P_{R,o} g_{S1}}{\alpha_1 P_{R,o} g_{S1} + N_o} \tag{5.40}$$

$$\gamma_{S1,1}^{O} = \frac{\alpha_1 P_{R,o} g_{S1}}{\xi \alpha_2 P_{R,o} g_{S1} + N_o} \tag{5.41}$$

where, the terms ξ $(0 \leq \xi \leq 1)$ and $(\xi \alpha_2 P_{R,o} g_{S1})$ refer to the i-SIC factor and the residual i-SIC interference at SU_1, respectively. Similarly, SU_2 after receiving the new NOMA composite signal from the FD relay, decodes its own high powered signal. Therefore, the received signal at SU_2 is represented by:

$$y_{S_2}^{O}(t) = s_{ro}(t) h_{S2} + n_o(t) \tag{5.42}$$

So, at overlay mode, the $SINR$ at SU_2 can be written from the above expression as:

$$\gamma_{S2,2}^{O} = \frac{\alpha_2 P_{R,o} g_{S2}}{\xi \alpha_2 P_{R,o} g_{S2} + N_o} \tag{5.43}$$

The condition for the end-to-end outage performance at SU_1 under overlay mode is given by:

$$P_{out,1}^{over} = Pr\Big[\max_k \gamma_{R,2}^{O} \leq u_2^{FD}, \max_k \gamma_{R,1}^{O} \leq u_1^{FD}, \gamma_{S1,2}^{O} \leq u_2^{FD}, \gamma_{S1,1}^{O} \leq u_1^{FD}\Big] \quad (5.44)$$

Now, by substituting the values of $\gamma_{R,2}^{O}$, $\gamma_{R,1}^{O}$, $\gamma_{S1,2}^{O}$ and $\gamma_{S1,1}^{O}$ the above expression can be rewritten as:

$$\begin{aligned} P_{out,1}^{over} = \; & Pr\Big[\prod_{k=1}^{K} \frac{P_{S,o}g_{SR_k}}{P_{R_k}g_{R_k}+N_o} \leq \gamma_{th}^{1}, \prod_{k=1}^{K} \frac{P_{S,o}g_{SR_k}}{P_{R_k}g_{R_k}+N_o} \leq \gamma_{th}^{2}, \frac{P_{R,o}g_{S1}}{N_o} \leq \gamma_{th}^{3}, \\ & \frac{P_{R,o}g_{S1}}{N_o} \leq \gamma_{th}^{4}\Big] \end{aligned} \quad (5.45)$$

The condition for the end-to-end outage probability at SU_2 under overlay mode is given by:

$$P_{out,2}^{over} = Pr\Big[\max_k \gamma_{R,2}^{O} \leq u_2^{FD}, \max_k \gamma_{R,1}^{O} \leq u_1^{FD}, \gamma_{S2,2}^{O} \leq u_2^{FD}\Big] \quad (5.46)$$

Now, by substituting the values of $\gamma_{R,2}^{O}$, $\gamma_{R,1}^{O}$ and $\gamma_{S2,2}^{O}$, the above expression can be rewritten as:

$$P_{out,2}^{over} = Pr\Big[\prod_{k=1}^{K} \frac{P_{S,o}g_{SR_k}}{P_{R_k}g_{R_k}+N_o} \leq \gamma_{th}^{1}, \prod_{k=1}^{K} \frac{P_{S,o}g_{SR_k}}{P_{R_k}g_{R_k}+N_o} \leq \gamma_{th}^{2}, \frac{P_{R,o}g_{S2}}{N_o} \leq \gamma_{th}^{3}\Big] \quad (5.47)$$

The closed form expression for end-to-end outage probability at SU_1 and SU_2 during overlay transmission protocol can be evaluated as:

$$\begin{aligned} P_{out,1}^{over} = \; & \Bigg[\underbrace{\left\{1-\exp\left(-\frac{\gamma_{th}^{1}N_0}{P_{S,o}\lambda_3}\right)\left(\frac{P_{S,o}\lambda_3}{P_{S,o}\lambda_3+\gamma_{th}^{1}P_{R,o}\lambda_9}\right)\right\}^{K}}_{W} \times \\ & \underbrace{\left\{1-\exp\left(-\frac{\gamma_{th}^{2}N_0}{P_{S,o}\lambda_3}\right)\left(\frac{P_{S,o}\lambda_3}{P_{S,o}\lambda_3+\gamma_{th}^{2}P_{R,o}\lambda_9}\right)\right\}^{K}}_{Q} \times \\ & \left\{1-\exp\left(-\frac{\gamma_{th}^{3}N_0}{P_{R,o}\lambda_1}\right)\right\} \times \left\{1-\exp\left(-\frac{\gamma_{th}^{4}N_0}{P_{R,o}\lambda_1}\right)\right\}\Bigg] \end{aligned} \quad (5.48)$$

Proof: Refer to Appendix C, D for proof of W and Q.

$$P_{out,2}^{over} = \left[W \times Q \times \left\{ 1 - \exp\left(-\frac{\gamma_{th}^{3} N_0}{P_{R,o} \lambda_2} \right) \right\} \right] \tag{5.49}$$

5.3.3 Outage analysis and system throughput during joint underlay/overlay mode

Simultaneous underlay or overlay mode switching procedure is determined by secondary transmitters, which detect PU activity using an energy detector technology. After sensing, SU initiates its power limitation mode (underlay) if the PU is busy; otherwise, SU operates at its maximum power (overlay), assisted by a number of FD relays. The probability that the primary signal will be detected is known as the probability of detection (Pd). Let, α be the probability of channel occupancy ($0 \leq \alpha \leq 1$). Total outage probability at SU_1 and SU_2 during combination of underlay/overlay is given respectively as:

$$P_{out,1}^{TOTAL} = \left[\left\{ \Big(1 - P_d\Big) + \alpha P_d \right\} P_{out,1}^{under} + \Big(1 - \alpha\Big) P_{out,1}^{over} \right] \tag{5.50}$$

$$P_{out,2}^{TOTAL} = \left[\left\{ \Big(1 - P_d\Big) + \alpha P_d \right\} P_{out,2}^{under} + \Big(1 - \alpha\Big) P_{out,2}^{over} \right] \tag{5.51}$$

Secondary network's total system throughput (T_t) is determined by:

$$T_t = \left\{ R_1 \Big(1 - P_{out,1}^{TOTAL}\Big) + R_2 \Big(1 - P_{out,2}^{TOTAL}\Big) \right\} \tag{5.52}$$

5.4 Results and discussion

The discussion and analysis of the system performance proposed in this chapter are covered in this part. The MATLAB simulation is used to validate the simulation

of the numerical mathematical expressions. Analytical results are represented by continuous curves whereas simulation results are projected as discrete marks on the curves in this section. Numerical results obtained for FD relay based CR-NOMA exhibit improved performance as compared to conventional HD relaying protocol operating in underlay mode. Concerning interference, variables including SI, primary interference, and i-SIC have all been handled. Opportunistically switching of joint underlay/overlay FD relaying mechanism improves the spectral efficiency of CRN shown in this section. In order to model the system performance, the following parameters are assumed: the primary transmission rate R_p=0.15 bits/s/Hz and the secondary transmission rate, R_1=R_2=R_s=0.1 bits/s/Hz. The PU outage constraint, $\varepsilon = 0.1$. The probability of detection, P_d is assumed to be 0.85. The efficiency factor of the EH circuit $\eta = 0.3$ and the probability of channel occupancy $\alpha = 0.15$. The total time involved $T = 100\ ms$ with harvesting and sensing time $\tau = 20\ ms$.

Fig. 5.2 displays the BS to SU_1 as well as SU_2 outage probability as a function of

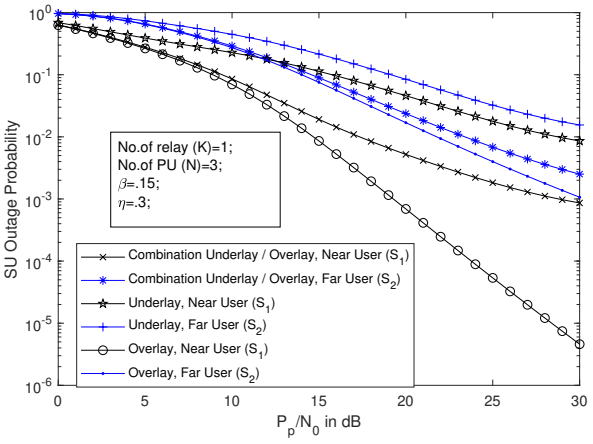

FIGURE 5.2: Comparison of SU outage performance in underlay, overlay and joint underlay/overlay mode in comparison to P_p/N_o in dB

P_p/N_o for all theses protocols, including underlay, overlay and joint underlay/overlay with number of primary users N=3 and a single FD relay i.e. K=1. It has been found that the overlay mode's outage performance is independent of the transmitting power of PU, P_p (i.e., the SUs do not maintain the QoS of PU). Therefore, this overlay technique alone is ineligible to participate in the spectrum sharing paradigm.

Additionally, it has been demonstrated that the combined underlay/overlay scheme performs better during outages than the existing underlay mode for a single PU [119]. This is because of the fact that if PU is busy, secondary base station adapts power restriction mode; otherwise can transmit power by its benefit.

Fig. 5.3 demonstrates the impact of the secondary network's performance on the

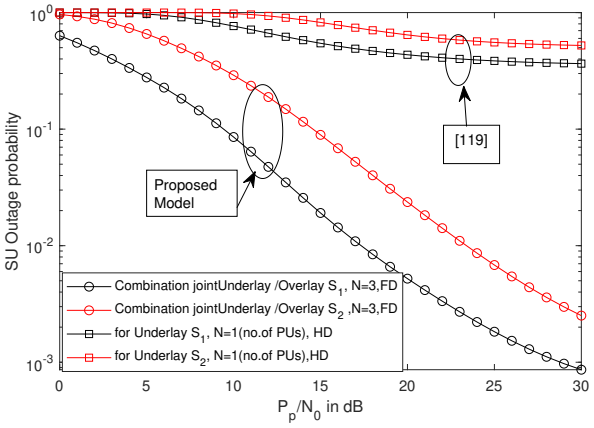

FIGURE 5.3: SU_1 and SU_2 outage behaviour under joint FD relaying mode compared with underlay HD relaying with respect to P_p/N_o in dB

outage behavior serving destinations SU_1 and SU_2 under both HD and FD relay networks. It has been shown that FD relay network outperforms the HD relay network. A comparison is carried out with [119], where the outage performance is described for underlay mode only with single primary user and under joint underlay/overlay with multiple primary users i.e. N=3. Additionally, EH circuit is employed at each secondary transmitter nodes to boost the system performance by allowing relay to transmit with its maximum power during overlay protocol. This has been found that our proposed model shows a better outage performance than that of the existing work in [119].

Fig. 5.4 demonstrates the impact of the secondary network's performance on the outage behavior serving destinations SU_1 and SU_2 versus P_p/N_o for FD relaying protocol under adaptive joint underlay/overlay mode. For this simulation, we assume $\lambda_9 = 0.3$ and $\eta = 0.3$. The analysis of outage behavior for K=1 and N =1 in [122] has been compared with our proposed model with K=2 and N =3. The investigation

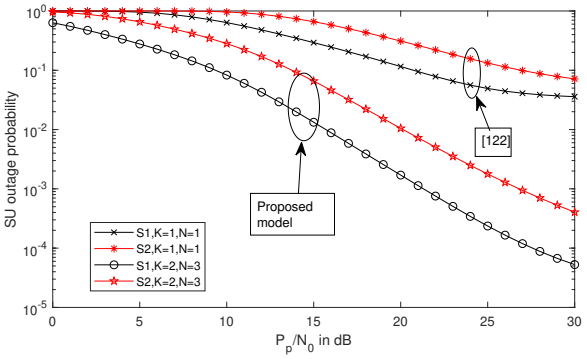

FIGURE 5.4: SU_1 and SU_2 outage behaviour under joint FD relaying scheme with respect to P_p/N_o in dB, varying K

shows that the outage behaviour gets better for the increase in number of FD relays as well as number of PUs. This reflects that by taking multiple FD relays in our discussion increases the diversity order, and multi PUs increases spectrum efficiency, which in turn, enhances the system performance.

Fig. 5.5 shows the impact of the secondary network's performance on the out-

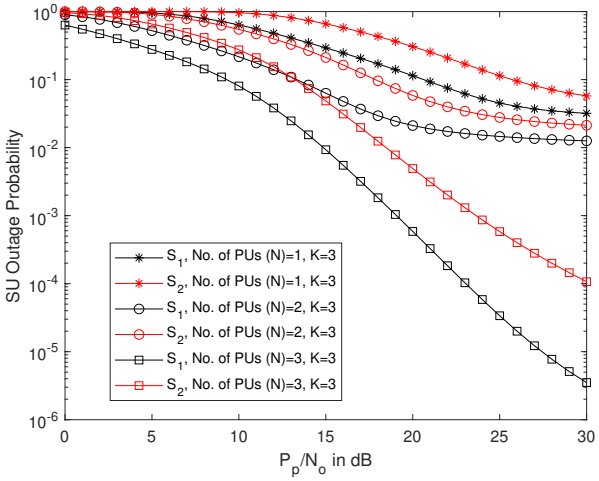

FIGURE 5.5: SU_1 and SU_2 outage behaviour under joint FD relaying scheme with respect to P_p/N_o in dB, fixed K and varying N

age behavior serving destinations SU_1 and SU_2 versus P_p/N_o in dB for FD relaying protocol under adaptive joint underlay/overlay mode. Outage behaviour analysis has been carried out with constant number of FD relays ($K = 3$) and with variable number of primary users ($N = 1, 2, 3$). The investigation shows that the outage

behaviour for both SU_1 and SU_2 gets better for the increase in number of primary users. This is because of the fact that due to increase in number of primary users, the available bandwidth gets increased and this results in an increase in throughput. Whereas, **Fig. 5.6** explains the outage analysis with variable number of FD relays ($K = 3, 4, 5$) assuming fixed number of primary users ($N = 3$). This result depicts that more the diversity, the outage behaviour for both SU_1 and SU_2 gets better for the increase in number of FD relays.

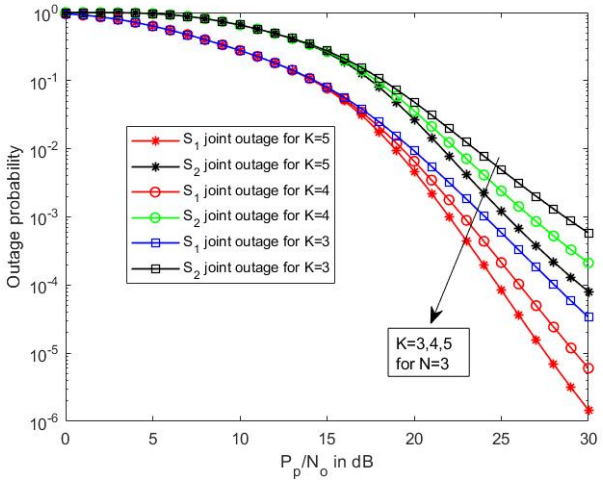

FIGURE 5.6: SU_1 and SU_2 outage behaviour under joint FD relaying scheme with respect to P_p/N_o in dB, fixed N and varying K

Fig. 5.7 shows the system throughput with respect to P_p/N_o for FD relaying protocol under adaptive joint underlay/overlay mode with different values of η. In our analysis, while maintaining QoS of PUs, the secondary transmitter power gets additional power requirement benefit with the increase in energy harvesting efficiency factor, which makes an improvement in SINR and results in better outage probability for both the users. Whereas, equation (5.52), describes the system throughput which is a function of outage probability. Higher value of η dictates more energy to be harvested at transmitter nodes which will enhance the transmitter power. As a result, this has been shown in **Fig. 5.7** that the system throughput is gradually improved with higher values of energy harvesting efficiency factor. The investigation reflects that the system throughput gets better and better with the increase

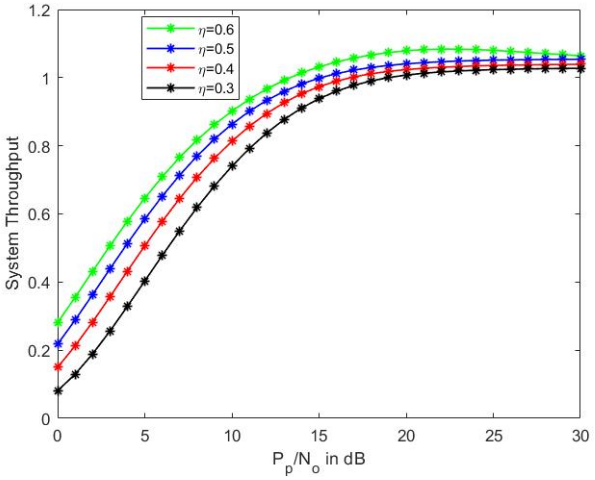

FIGURE 5.7: Normalized system throughput with respect to P_p/N_o

in energy harvesting efficiency factor. Finally, our results present a better system throughput with the inclusion of EH circuit.

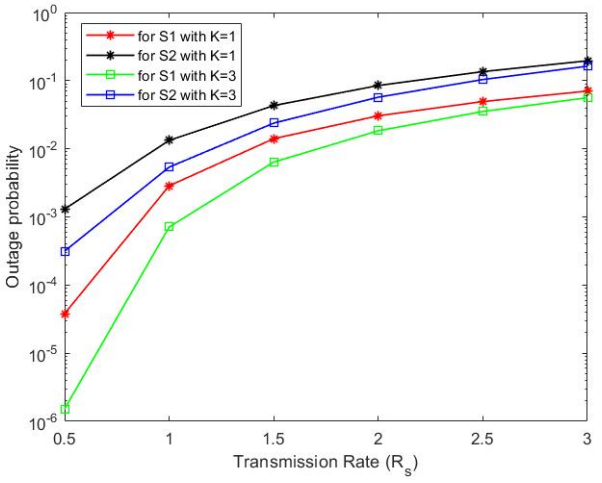

FIGURE 5.8: Outage probability with respect to transmission rate

The analysis of secondary users' outage behavior in relation to transmission rates R_s, has been presented in **Fig. 5.8**. It reveals that the outage behavior deteriorates as the transmission rate increases. It can be reminded that radio transmissions are constantly subject to bandwidth constraints while maximum SI cancellation is limited.

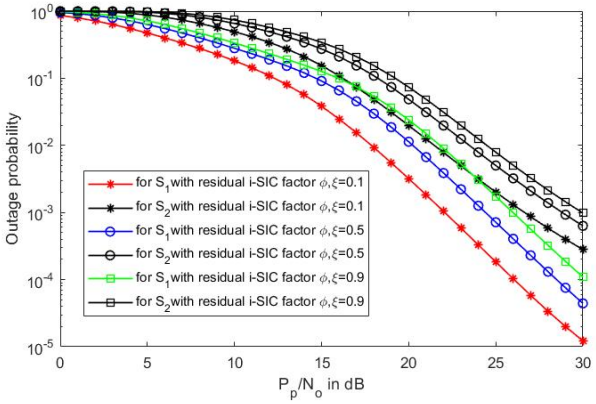

FIGURE 5.9: Outage probability with respect to P_p/N_o in terms of residual i-SIC

Fig. 5.9 depicts the effect of the secondary network's outage behavior for destinations SU_1 and SU_2 as a function of P_p/N_o, based on the residual i-SIC factor in a full-duplex relaying protocol under an adaptive joint underlay/overlay mode. The outage performance worsens as the residual i-SIC factor increases, with values ranging from $\phi = \xi = 0.1, 0.5, 0.9$.

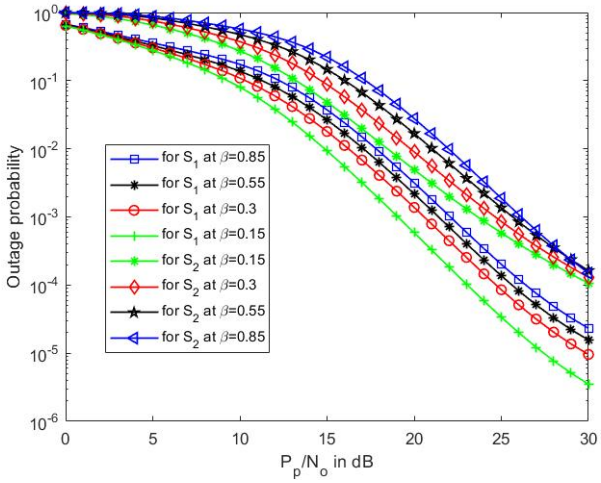

FIGURE 5.10: Outage probability with respect to P_p/N_o in terms of α

Fig. 5.10 describes the outage performance at both the NOMA users end with the effect of channel occupancy factor α. The outage performance deteriorates as the α value increases from 0.15 to 0.85. This occurs because, at lower α values, the system predominantly functions in overlay mode, while at higher α values, it shifts to underlay mode.

5.5 Chapter summary

This chapter investigates the outage performance of cognitive radio networks under total power management constraints and introduces opportunistic joint underlay/overlay full-duplex (FD) relaying techniques. Specifically, we propose practical and easily implementable FD relaying strategies within a NOMA-enabled cognitive radio framework, accounting for residual self-interference (SI) and energy harvesting (EH) conditions. As expected, the study demonstrates that full-duplex (FD) relaying significantly enhances system throughput compared to conventional half-duplex (HD) relaying. Furthermore, the adaptive switching mechanism between the underlay or overlay improves the spectrum utility in a CR-NOMA network. The outage performance at secondary, considering SI, i-SIC and more interferences from primary network, even with a low energy harvesting efficiency factor, achieves the expected results. In addition, it is also found that the proposed joint underlay/overlay mode significantly improves the secondary network's throughput and the outage probability of the SUs as compared to underlay allocation strategy.

Chapter 6

Performance analysis of full-duplex relay based cognitive radio network assisted by intelligent reflecting surface network

This chapter investigates the throughput and outage performance of an intelligent reflecting surface (IRS)-assisted full-duplex relay node in a cognitive radio network (CRN), considering m-Nakagami fading channels. In particular, a secondary source transmitter (S) broadcasts an information to secondary destination (D) via IRS network as well as full-duplex (FD) relay network which practices decode-and-forward protocol. This chapter examines how effectively the IRS network supports the joint intermediate FD relaying node in maintaining the primary users' (PUs) interference threshold. In order to do this, we precisely derive closed-form analytical mathematical equations for the secondary users' throughput and outage probability. When compared to a traditional FD relaying network, the IRS-assisted system exhibits a

significant performance gain for the proposed model. The overall analytical closed form solution has been performed and verified via MATLAB simulation testbed.

6.1 System model of cognitive radio network assisted by full-duplex relay and intelligent reflecting surface network

To improve communication reliability, a cognitive radio network (CRN) model has been developed in which an intelligent reflecting surface (IRS) supports a full-duplex relay node. With the goal of enhancing signal quality and spectrum utilization, the system functions in m-Nakagami fading conditions. To control interference and strengthen the received signal, the IRS dynamically modifies reflections.

We have considered a full-duplex (FD) downlink transmission scenario where a source node (S) communicates with a destination node (D) with the assistance of an intelligent reflecting surface (IRS) equipped with N reflecting elements as well as full-duplex relay network (R) as shown in **Fig. 6.1**. It is assumed that all FD relays with the capacity to transceive simultaneously have been installed with separate transmit and receive antennas, while S and D are configured with a single antenna. Furthermore, because of environmental barriers, messages are transmitted from source to destination via R and IRS rather than direct link.

Assuming we know every detail of the channel state information, the channel coefficients between the i^{th} element of the IRS and the S/D are represented by h_{1i}/h_{2i}, where $i \in 1, 2, 3, \ldots N$. For every reflecting element in IRS, the phase shift and reflection amplitude are $\tilde{\theta} \in [0, 2\pi]$ and $\eta \in [0, 1]$, respectively. Rest all the channel coefficients $h_{x,y}$ follow Nakagami-m distribution with corresponding square of coefficient to be Gamma distribution of mean parameter Ω_x, integer fading factor m_x and scale parameter β_x. Probability density function of Nakagami-m distribution

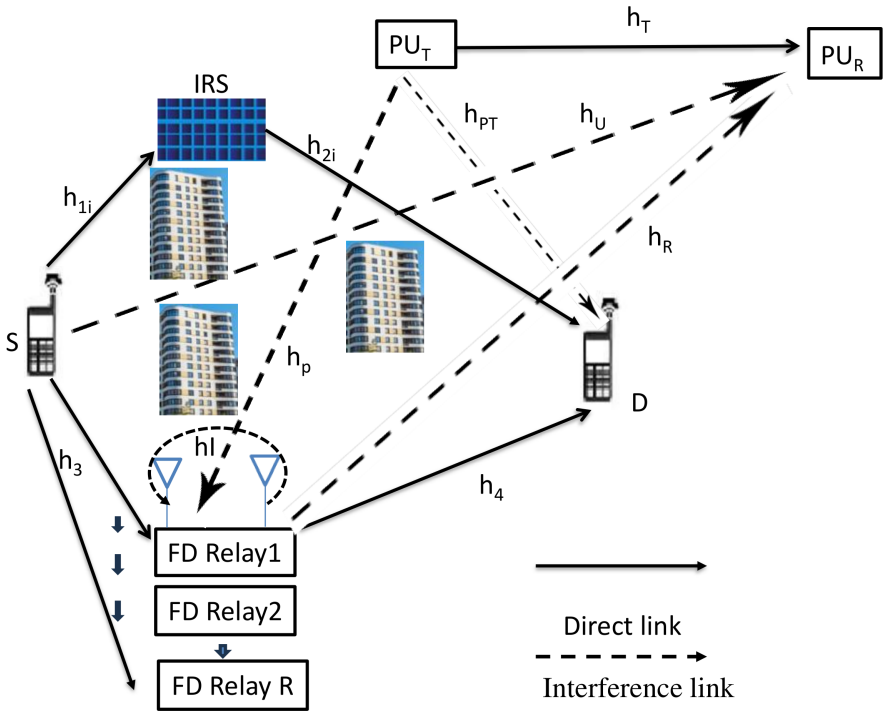

FIGURE 6.1: System Model on IRS-FD relay network based CRN

model random variable is outlined by:

$$f_X(x) = \frac{2x^{2m_x-1}}{\Gamma m_x \Omega_x^{m_x}} \exp \frac{-x^2}{\Omega_x} \tag{6.1}$$

where, $\Gamma()$ is the Gamma function. TABLE 6.1 below describes link parameters in details.

By using a spectrum sharing strategy, information from both S and R is transmitted at a specific power without alerting any primary user subjected to the peak interference threshold I_P as follows:

$$I_P \geq \left(P_s|h_u|^2 + P_r|h_r|^2\right) \tag{6.2}$$

TABLE 6.1: Path-link with parameter list

Channel- link with particular parameters				
Node to node link (x, y)	coefficient (h_x)	spread parameter (Ω_x)	shape fading factor (m_x)	Scale parameter (β_x)
$PU_{TX} \rightarrow PU_{RX}$	h_T	Ω_T	m_T	β_T
$S \rightarrow IRS$	$h_{1,i}$	Ω_1	m_1	β_1
$IRS \rightarrow D$	$h_{i,2}$	Ω_2	m_2	β_2
$S \rightarrow R$	h_3	Ω_3	m_3	β_3
$R \rightarrow D$	h_4	Ω_4	m_4	β_4
$PU_{TX} \rightarrow R$	h_p	Ω_p	m_p	β_p
$PU_{TX} \rightarrow D$	h_{PT}	Ω_T	m_y	β_T
$S \rightarrow PU_{RX}$	h_u	Ω_u	m_u	β_u
$R \rightarrow PU_{RX}$	h_r	Ω_r	m_r	β_r
$R \rightarrow R$	h_I	Ω_I	m_I	β_I

The non-optimal power allocation for P_s and P_r can be formulated as :

$$P_s = \frac{I_P}{2|h_u|^2} \tag{6.3}$$

$$P_r = \frac{I_P}{2|h_r|^2} \tag{6.4}$$

where, P_s and P_r are transmitted power from source and each FD relay.

Before communication between the source and destination starts, a partial relay selection mechanism is employed. The source selects an optimal FD relay from the network based on the estimated channel state information. To facilitate this, the source sends pilot symbols to the relay network, and each relay evaluates the CSI of its respective links upon receiving these signals. Depending on the quality of channel, the relay R is chosen from the relay network for communication purpose from the source to the destination as follows:

$$R = arg \max_{k=1,\ldots,K} |h_k|^2 \tag{6.5}$$

Any one of the numerous transmissions that have been examined may be regarded as the optimum link, with an example, $h_k = h_3$, the best link at that time frame and R is selected as the optimal relay. For mathematical simplicity, it has been assumed that the system model avoids IRS reflection from the primary transmitter and the relay node to the destination, as well as any direct communication between the source and the destination.

6.2 Channel model and mathematical analysis

The IRS creates an additional path for the signal, allowing it to be reflected and possibly enhancing the overall signal strength at the destination. The signal received at the destination D through the IRS is often expressed mathematically:

$$y_D(t) = \sum_{i=1}^{N} \sqrt{P_s}\eta_i \exp(j\theta_i) h_{1i} h_{2i} x_1(t) + \sqrt{P_T} h_{PT} x_P(t) + n_o(t) \tag{6.6}$$

where, P_s and P_T are defined as transmitted power from S and PU_{TX}, respectively. $n_o(t)$ is defined as additive white gaussian noise (AWGN) with zero mean and variance N_0, respectively with $\eta_i \in [0, 1]$ and $\tilde{\theta}_i \in [0, 2\pi]$ defining the reflected amplitude coefficient and the effective phase shift present by the IRS's i^{th} element, respectively. Therefore, the signal to interference ratio at D for the received signal $y_D(t)$ via IRS can be outlined as:

$$\gamma_1 = \frac{\left| \sum_{i=1}^{N} P_s \eta_i h_{1i} h_{2i} \right|^2}{P_T \left| h_{PT} \right|^2 + N_o} \tag{6.7}$$

where, $x_1(t)$ and $x_P(t)$ symbolize the signals from S and PU_{TX}, respectively under the assumption that $\mathbb{E}|x_1(t)|^2 = 1$, $\mathbb{E}|x_P(t)|^2 = 1$ with $h_{x,y}$ is the channel coefficient with their standard meaning as already stated earlier.

The relay R receives the information from the secondary source S which is given as:

$$y_r(t) = \sqrt{P_s} h_3 x_1(t) + \sqrt{P_r} h_I x_r(t) + \sqrt{P_T} h_P x_P(t) + n_o(t) \tag{6.8}$$

Therefore, the signal to interference noise ratio (SINR) at secondary FD relay R is expressed as:

$$\gamma_2 = \frac{P_s \left|h_3\right|^2}{P_r \left|h_I\right|^2 + P_T \left|h_P\right|^2 + N_o} \tag{6.9}$$

where, $x_r(t)$ and P_r respectively symbolize the signal and transmitted power from R under the assumption that $\mathbb{E}|x_r(t)|^2 = 1$.

After being decoded at FD relay, the information is forwarded to D, where the received signal is given as:

$$y_{R-D}(t) = \sqrt{P_r} h_4 x_r(t-\tau) + \sqrt{P_T} h_{PT} x_P(t-\tau) + n_o(t-\tau) \tag{6.10}$$

where, time τ signifies the propagation delay.

SINR expression at D via FD relay simplifies to:

$$\gamma_3 = \frac{P_r \left|h_4\right|^2}{P_T \left|h_{PT}\right|^2 + N_o} \tag{6.11}$$

It is possible to evaluate the communication link's dependability using the outage performance. When the instantaneous signal to interference noise ratio falls below a predetermined threshold, γ_{th}, the outage performance occurs. Hence end-to-end outage probability at D can be found out to be:

$$P_0^{total} = Pr\left[\max_{i=1,2,\ldots,N} \underbrace{(\gamma_1 \leq \gamma_{th})}_{A}, \max_{k=1,2,\ldots,K} \underbrace{\left(min(\gamma_2, \gamma_3 \leq \gamma_{th})\right)}_{B}\right] \tag{6.12}$$

where, $\gamma_{th} = 2^{R_s} - 1$, is described by the outage threshold at D for the given full-duplex communication. The transmission rate for secondary is given by R_s.

Now, from equation (6.12), solving for A is given below:

$$Pr(\gamma_1 \leq \gamma_{th}) = Pr\left[\frac{P_s \eta_i \left|\sum_{i=1}^{N} h_{1i} h_{2i}\right|^2}{P_T \left|h_{PT}\right|^2} \leq \gamma_{th}\right] \tag{6.13}$$

The CDF, $F_{\gamma_1}(\gamma_{th})$ of above expression for maximum signal to interference ratio can be written in the form as:

$$F_{\gamma_1}(\gamma_{th}) = Pr\left[\frac{W}{Y} < \gamma_{th}\right] \tag{6.14}$$

where, $W = \eta P_s Q^2$, $Q = \sum_{i=1}^{N} X$, $X = h_{1i}h_{2i}$

Moreover, $Y = P_T\left|h_{PT}\right|^2$, is a Gamma random variable $(m_y, \bar{\beta}_y)$,where, $\bar{\beta}_y = P_T\beta_T$, $\beta_T = \frac{\Omega_T}{m_y}$

The PDF of double Nakagami m distribution random variable Q can be expressed over KG distribution as [139],

$$f_Q(q) = \frac{4\phi^{m_1+m_2}q^{m_1+m_2-1}K_{m_1-m_2}(2\phi q)}{\Gamma m_1 \Gamma m_2} \tag{6.15}$$

where, $\phi = \sqrt{\frac{m_1 m_2}{\Omega_m}}$, with $\Omega_1\Omega_2 = \Omega_m$

The PDF of random variable W, can be expressed by squared KG distribution as [139]:

$$f_W(w) = \frac{2\bar{\phi}^{m_1+m_2}w^{\frac{m_1+m_2}{2}-1}K_{m_1-m_2}(2\bar{\phi}\sqrt{w})}{\Gamma m_1 \Gamma m_2} \tag{6.16}$$

The closed form expression for CDF, $F_{\gamma_1}(\gamma_{th})$ is therefore is given as:

$$F_{\gamma_1}(\gamma_{th}) = Pr\left[\frac{W}{Y} < \gamma_{th}\right] = \frac{1}{\Gamma m_1 \Gamma m_2 \Gamma m_y} G_{2,3}^{2,2}\left[\gamma_{th}\bar{\phi}^2\bar{\beta}_y\middle|\begin{matrix}1 & 1-m_y \\ m_1, & m_2, \quad 0\end{matrix}\right] \tag{6.17}$$

where, $\bar{\phi} = \sqrt{\frac{\phi}{\eta_i P_S}}$, and $G[\cdot,\cdot]$ defines Meijer G-function [131].

Now, solving for B in equation (6.12), the outage probability at destination D via relay network from source S is defined by the expression given below:

$$Pr\left[min(\gamma_2, \gamma_3 \leq \gamma_{th})\right\}\Big] = F_{\gamma_2}(\gamma_{th}) + F_{\gamma_3}(\gamma_{th}) - F_{\gamma_2}(\gamma_{th})F_{\gamma_3}(\gamma_{th}) \tag{6.18}$$

where, $F_{\gamma_2}(\gamma_{th})$ and $F_{\gamma_3}(\gamma_{th})$ respectively denote the CDF function at relay and destination. The required derivations for these CDF are given below:

$$\begin{aligned} F_{\gamma_2}(\gamma_{th}) &= Pr\left[\left(\frac{P_s\left|h_3\right|^2}{P_r\left|h_I\right|^2+P_T\left|h_P\right|^2+N_o}\leq\gamma_{th}\right)\right] \\ &= \Bigg[1-\Bigg[\exp\left(-\frac{\gamma_{th}N_0}{P_s\Omega_3}\right)\sum_{n=0}^{m_3-1}\sum_{n_1=0}^{n}\sum_{n_2=0}^{n_1}\binom{n}{n_1}\binom{n_1}{n_2}\left(\frac{1}{n!\Omega_3^n}\right) \\ &\quad\times\left(\frac{\gamma_{th}N_0}{P_s}\right)^n\frac{1}{\Gamma m_p\Omega_P^{m_p}}\left(\frac{\gamma_{th}P_T}{P_s\Omega_3}+\frac{1}{\Omega_P}\right)^{-n_2-m_p} \\ &\quad\times\Gamma(n_2+m_p)\Gamma(n_1-n_2+m_I)\left(\frac{P_T}{N_0}\right)^{n_2}\left(\frac{P_r}{N_0}\right)^{n_1-n_2} \\ &\quad\times\frac{1}{\Gamma m_I\Omega_I^{m_I}}\left(\frac{\gamma_{th}P_r}{P_s\Omega_3}+\frac{1}{\Omega_I}\right)^{-n_1+n_2-m_I}\Bigg]\Bigg] \end{aligned} \tag{6.19}$$

Similarly, to find for $F_{\gamma_3}(\gamma_{th})$ the required expression is given below:

$$\begin{aligned} F_{\gamma_3}(\gamma_{th}) &= Pr\left[\left(\frac{P_R\left|h_4\right|^2}{P_T\left|h_P\right|^2+N_0}\leq\gamma_{th}\right)\right] \\ &= \Bigg[1-\Bigg[\exp\left(-\frac{\gamma_{th}N_0}{P_R\Omega_4}\right)\sum_{n=0}^{m_4-1}\sum_{n_1=0}^{n}\binom{n}{n_1}\left(\frac{1}{n!\Omega_4^n}\right)\left(\frac{\gamma_{th}N_0}{P_R\Omega_4}\right)^n \\ &\quad\times\frac{\Gamma(n_1+m_p)}{\Gamma m_p\Omega_P^{m_p}}\left(\frac{P_T}{N_0}\right)^{n_1}\left(\frac{\gamma_{th}P_T}{P_R\Omega_4}+\frac{1}{\Omega_P}\right)^{-n_1-m_p}\Bigg]\Bigg] \end{aligned} \tag{6.20}$$

Finally, the end-to-end outage performance at D from both IRS network as well as from FD relay network can be rewritten as:

$$P_0^{total}=\left[\prod_{i=1}^{N}F_{\gamma_1}(\gamma_{th})\times\prod_{k=1}^{K}\Big\{F_{\gamma_2}(\gamma_{th})+F_{\gamma_3}(\gamma_{th})-F_{\gamma_2}(\gamma_{th})F_{\gamma_3}(\gamma_{th})\Big\}\right] \tag{6.21}$$

The end-to-end throughput T_h of the secondary network refers to the overall data transmission rate from the source to the destination in a cognitive radio system. In the context of the considered system model, it represents how efficiently data can be transferred across the entire network, taking into account the influence of the IRS

and FD relay nodes. The throughput calculation T_h can be evaluated as follows:

$$T_h = \left\{ R_s \left(1 - P_0^{total} \right) \right\} \tag{6.22}$$

6.3 Results and discussion

This section presents mathematical results to investigate how significantly system parameters affect the system's overall end-to-end performance. Theoretical expressions of the proposed model for throughput and outage are validated using the MATLAB simulation method. When compared to traditional FD relaying protocol operating in underlay mode, numerical findings for IRS-based cognitive radio networks and FD relay networks exhibit improved performance.

Fig. 6.2 shows the S to D outage probability as a function of transmitted power

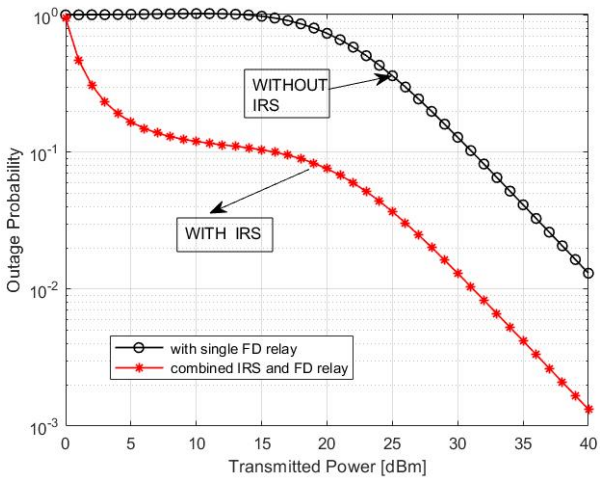

FIGURE 6.2: Comparison of outage probability at D versus transmitted power in terms of with/without IRS FD relay network

P_T via single FD relay including IRS network with number of IRS elements N=3 and a single FD relay i.e. K=1. It has been found that system outages perform better when both the IRS and FD relay networks are involved in the communication process, compared to when only FD relay transmission is used without the IRS.

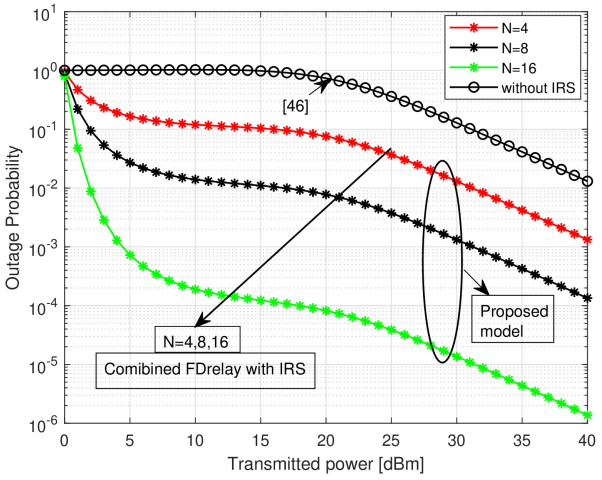

FIGURE 6.3: Outage comparison at D for combined FD relay with variable numbers of IRS elements and sole FD relay with respect to P_T in dBm

Fig. 6.3 investigates the S to D outage probability as a function of transmitted power P_T via single FD relay and for combined FD relay with variable numbers of IRS elements N=4, 8 and 16. The investigation shows that system outages perform better with combined FD relay and IRS network. Additionally, it has been noted that as the number of IRS elements increases, system performance progressively improves.

Fig. 6.4 depicts the outage at D versus transmitted power P_T via multiple FD

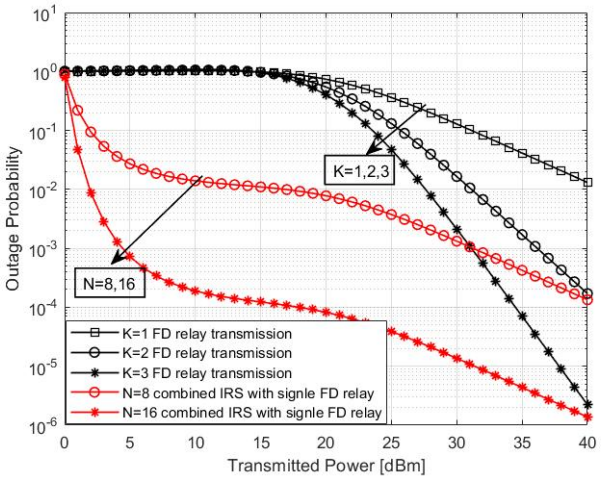

FIGURE 6.4: Outage comparison at D with variable K and variable N with respect to P_T in dBm

relays and for combined single FD relay with multiple numbers of elements i.e. N=8 and 16 in an IRS network. The result clearly underscores that using combined network with K=1,2,3 and N=8,16 the outage performance shows an improvement as the number of reflecting elements N for IRS gets increased. The improved outage and spectral efficiency resulting in the FD-IRS model setup, however, demonstrates the benefit of combining the FD relay node and IRS network.

The analysis of destination outage behavior in relation to transmission rates R_s,

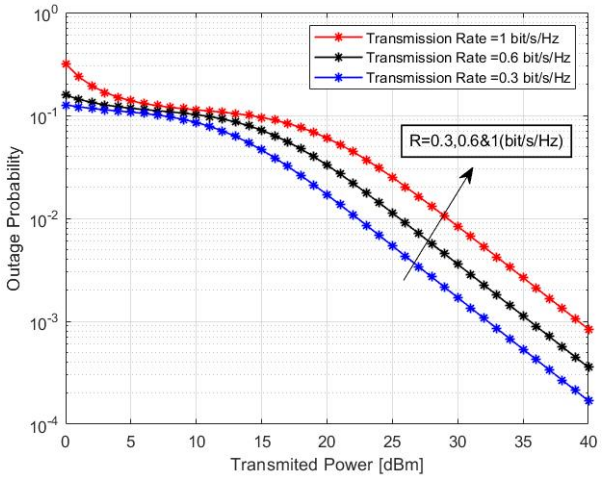

FIGURE 6.5: Outage comparison at D versus P_T in dBm in terms of transmission rates

has been presented in **Fig. 6.5**. It reveals that the outage behavior deteriorates as the transmission rate increases. It can be reminded that radio transmissions are constantly subject to bandwidth constraints while maximum SI cancellation is limited.

Fig. 6.6 shows the outage probability at D as a function of transmitted power P_T via combined FD relay with IRS network in terms of throughput analysis. When comparing the results obtained with the combined network to the traditional sole FD relaying protocol, it is evident that the throughput performance improves for N = 4 and 8. Nonetheless, the enhanced throughput performance outcomes for the FD-IRS model configuration highlight the advantages of applying the IRS.

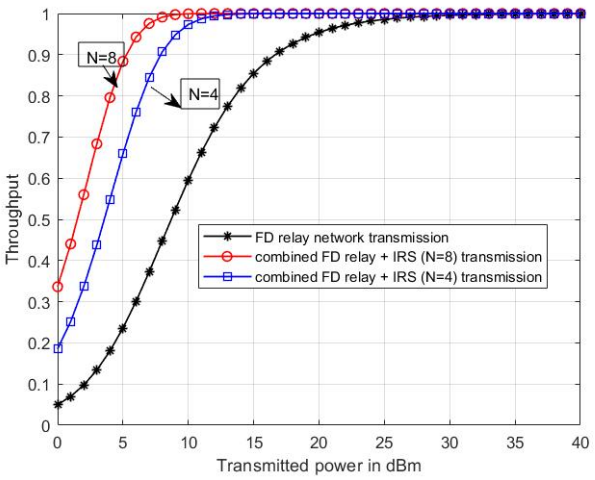

FIGURE 6.6: Normalized throughput comparison without IRS and with varying elements in IRS network

6.4 Chapter summary

This study focuses on analyzing two key performance metrics namely, system throughput and outage performance for a secondary destination in a cognitive radio network that uses FD relaying and is integrated with an IRS network. A mathematical closed form analysis for secondary throughput and outage validation is examined, taking into account the primary and self interference parameters. According to this study, the combined effect of the FD relay and IRS network results in a better outage performance than the FD relay network working alone. The combined impact of the IRS network and FD relay is taken into consideration as the study looks at how secondary transmission rates affected outage performance at secondary destinations. Combining FD relaying with IRS technology results in improved system throughput compared to using FD relaying alone. In a full-duplex relay system, the relay can transmit and receive signals simultaneously, which boosts data transmission rates. However, adding an IRS, which can reflect and optimize signal paths, further enhances the efficiency of the communication system. The observation highlights that increasing the number of IRS elements and relays significantly improves the overall data rate or throughput of the system. This is because more IRS elements provide

greater control over the signal's path and strength, and additional relays improve signal transmission, especially in challenging environments with interference or obstacles. In summary, the combination of IRS and FD relaying significantly boosts system performance by optimizing signal propagation and transmission capacity.

Chapter 7

Summary and future scope

7.1 Summary

A detailed study on cognitive radio network where the secondary users share their information through half-duplex and full-duplex relay network in presence of various environment has been discussed in this thesis.

Chapter 3 is described by a system architecture where the HD relays are equipped with multiple antennas in CRN setup and the secondary users adaptively switch between underlay or overlay mode based on the sensing activity of the secondary users' transmitters. The analysis done in this chapter reveals that outage performance, spectral efficiency and system throughput are better in all the cases as compared to other models considering HD relay network. The next part of this chapter encompasses a detailed study based on AF, DF and AHR half-duplex relay network being incorporated in between source and destination of secondary users in a CRN. The system model of CRN setup is shown where the secondary relays adaptively switch between AF or DF mode i.e., AHR mode based on successful decoding activity of relays. It is also assumed that the secondary user transmitters are equipped with energy harvesting circuit, that can harvest energy from the surroundings including co- channel interference environment.

In chapter 4, an extensive analysis is carried out based on the performance of full-duplex relay network, serving to transfer the information from secondary source to destination in a multi user CRN. Out of three system models developed in this chapter, first and second models deal with multi-user scenario CRN with single and multiple secondary destination in presence of linear energy harvesting environment and the last one is discussed with non-linear EH circuit. The analysis carried in this chapter exhibits a better outage performance and throughput in FD relay network than HD relay network eventually in all of these cases. Consideration of non-linear EH environment in CRN makes more realistic approach in full-duplex communication process.

Leaving behind the traditional OMA technology in wireless communication, a new approach towards NOMA technique is adapted in an FD relay network-based CRN with system model and analysis carried out in chapter 5. A joint underlay/ overlay mode of communication by the secondary users has been discussed under FD relay network. NOMA based CRN describes a better performance in terms of system outage and overall throughput for both the end users with respect to conventional OMA technology CRN equipped with HD relay network.

Finally, an FD relay network-based CRN is built up with addition of intelligent reflecting surface providing a significant improvement in performance. The secondary users in CRN communicate among themselves via FD relay network as well as via IRS network. The approach towards incorporating IRS network in addition to FD communication significantly outperforms the sole FD relay network.

7.2 Proposed future research works

The work presented in this thesis may further be extended in the following areas as listed below:

(i) The approach towards incorporating IRS network with FD communication can be extended further by opportunistically switching between underlay and overlay CRN based on channel occupancy.

(ii) Additionally, in a NOMA context, a method can be implemented to integrate the IRS network with the FD communication in CRN.

(iii) IRS network integrated with Unmanned Aerial Vehicles (UAVs) can be further expanded through the use of combined underlay/overlay protocols.

(iv) The approach for combining the IRS network with Unmanned Aerial Vehicles (UAVs) can be further expanded in the framework of NOMA using the underlay protocol of CRN.

Appendix A

Proof of CDF for $F(\gamma_1)$

We considered that the channel interference is originated from N number of primary sources to destination and relay with channel gain as $g_{P_{nD}}$ and $g_{P_{nR}}$ respectively, defined as $Z = \sum_{n=1}^{N} G'_n$, where, Z is the sum of independent exponential random variables G'_n for n=1 to N. All other channel gains are assumed to be exponentially distributed.

The PDF of Z with parameter λ is given by [73]:

$$f_Z(z) = \frac{z^{n-1} exp(\frac{-z}{\lambda})}{\Gamma n \lambda^n} \tag{A.1}$$

We have considered X and Y to be exponential random variable with parameter λ_a and λ_b respectively.

$$Pr\Big(\frac{P_1 X}{\underbrace{P_3 Y + P_2 Z}_{G'} + N_0} \leq m\Big) \tag{A.2}$$

Now considering the above expression of $G^{'}$,

$$\begin{aligned} F_{G'}(g^{'}) &= Pr\Big(G^{'} \leq g^{'}\Big) \\ & Pr\Big(P_3 Y + P_2 Z \leq g^{'}\Big) \end{aligned} \tag{A.3}$$

$$
\begin{aligned}
F_{G'}(g') = & \int_{z=0}^{+\infty} \int_{y=0}^{\frac{(g'-P_2 z)}{P_3}} f_Y(y) f_Z(z)\, dy\, dz \\
& = \int_{z=0}^{+\infty} f_Z(z)\, dz \int_{y=0}^{\frac{(g'-P_2 z)}{P_3}} (\frac{1}{\lambda_b}) exp(\frac{-y}{\lambda_b})\, dy \\
& = \int_{z=0}^{+\infty} f_Z(z)[1 - exp(\frac{-(g'-P_2 z)}{P_3 \lambda_b})]\, dz \\
& = 1 - exp(\frac{-g'}{P_3 \lambda_b}) \times \\
& \left[\int_{z=0}^{+\infty} exp(\frac{P_2 z}{P_3 \lambda_b}) \frac{z^{n-1} exp(\frac{-z}{\lambda})}{\Gamma n \lambda^n}\, dz \right] \\
& F_{G'}(g') = 1 - exp(\frac{-g'}{P_3 \lambda_b}) \left(\frac{P_3 \lambda_b}{P_3 \lambda_b - P_2 \lambda} \right)^n \\
& f_{G'}(g') = (\frac{1}{P_3 \lambda_b}) exp(\frac{-g'}{P_3 \lambda_b}) \left(\frac{P_3 \lambda_b}{P_3 \lambda_b - P_2 \lambda} \right)^n
\end{aligned}
\tag{A.4}
$$

Now from equation (A.2), we get,

$$
Pr\Big(\frac{P_1 X}{G' + N_0} \leq m\Big) \tag{A.5}
$$

$$
\begin{aligned}
F_M(m) = & \int_{g'=0}^{+\infty} \int_{x=0}^{\frac{(mg' + mN_0)}{P_1}} f_{G'}(g') f_X(x)\, dx\, dg' \\
& = \int_{g'=0}^{+\infty} \int_{x=0}^{\frac{(mg' + mN_0)}{P_1}} (\frac{1}{\lambda_a}) exp(\frac{-x}{\lambda_a}) f_{G'}(g')\, dx\, dg' \\
& = \int_{g'=0}^{+\infty} \Big[1 - exp\big(\frac{-(mg' + mN_0)}{P_1 \lambda_a}\big)\Big] f_{G'}(g')\, dg' \\
& = 1 - exp(\frac{-mN_0}{P_1 \lambda_a}) \Big(\frac{P_1 \lambda_a}{P_1 \lambda_a + mP_3 \lambda_b} \Big) \\
& \Big(\frac{P_3 \lambda_b}{P_3 \lambda_b - P_2 \lambda} \Big)^n
\end{aligned}
\tag{A.6}
$$

Appendix B

Proof of CDF for $F(\gamma_2)$

We have considered Ψ and Z to be exponential and gamma distributed random variable with parameter λ_c and λ respectively,

$$Pr\Big(\frac{P_4\Psi}{P_5Z+N_0} \leq q\Big) \tag{B.1}$$

$$\begin{aligned} F_Q(q) = & \int_{z=0}^{+\infty}\int_{\psi=0}^{\frac{(qP_5Z+qN_0)}{P_4}} (\frac{1}{\lambda_c})exp(\frac{-\psi}{\lambda_c})f_Z(z)\,d\psi\,dz \\ & = 1-exp(\frac{-qN_0}{P_4\lambda_c}) \\ & \int_{z=0}^{+\infty} exp(\frac{-qP_5z}{P_4\lambda_c})\frac{z^{n-1}exp(\frac{-z}{\lambda})}{\Gamma n\lambda^n}\,dz \\ & = 1-exp(\frac{-qN_0}{P_4\lambda_c})\left(\frac{P_4\lambda_c}{P_4\lambda_c+qP_5\lambda}\right)^n \end{aligned} \tag{B.2}$$

Also from [119], we get if

$$Pr\Big(\max_{k=1,2,\ldots,K}\frac{P_4\Psi}{P_5Z+N_0} \leq q\Big)$$

then the above expression can be written as,

$$\begin{aligned} F_Q(q) = & \prod_{k=1}^{K} Pr\Big(\frac{P_4\Psi}{P_5Z+N_0} \leq q\Big) \\ & = \left[1-exp(\frac{-qN_0}{P_4\lambda_c})\left(\frac{P_4\lambda_c}{P_4\lambda_c+qP_5\lambda}\right)^n\right]^K \end{aligned} \tag{B.3}$$

Appendix C

Proof for equation (5.33)

The proof for U and V in equation (5.33) can be derived as follows. The channel gain parameter of the primary network source to FD relay is considered as $g_{P_{nR}}$, defined as $Z = \sum_{n=1}^{N} G'_n$ where, Z is the sum of independent exponential random variables G'_n for n=1 to N. This has been assumed that the power is symbolized here as P_i for all $i = 1, 2..$ and other gains be exponentially distributed.
The PDF of Z with parameter λ is given by [73]:

$$f_Z(z) = \frac{z^{n-1} exp(\frac{-z}{\lambda})}{\Gamma n \lambda^n} \tag{C.1}$$

We assume that both X and Y are random variables with exponential distribution and with parameters λ_a and λ_b, respectively.

$$Pr\Big(\frac{P_1 X}{\underbrace{P_3 Y + P_2 Z}_{G'} + N_0} \leq m\Big) \tag{C.2}$$

The term $G^{'}$ is now being evaluated as,

$$\begin{aligned} F_{G'}(g^{'}) &= Pr\Big(G^{'} \leq g^{'}\Big) \\ &Pr\Big(P_3 Y + P_2 Z \leq g^{'}\Big) \end{aligned} \tag{C.3}$$

$$
\begin{aligned}
F_{G'}(g^{'}) = & \int_{z=0}^{+\infty} \int_{y=0}^{\frac{(g^{'}-P_2 z)}{P_3}} f_Y(y) f_Z(z)\, dy\, dz \\
& = \int_{z=0}^{+\infty} f_Z(z)\, dz \int_{y=0}^{\frac{(g^{'}-P_2 z)}{P_3}} (\frac{1}{\lambda_b}) exp(\frac{-y}{\lambda_b})\, dy \\
& = \int_{z=0}^{+\infty} f_Z(z)[1 - exp(\frac{-(g^{'}-P_2 z)}{P_3 \lambda_b})]\, dz \\
& = 1 - exp(\frac{-g^{'}}{P_3 \lambda_b}) \times \left[\int_{z=0}^{+\infty} exp(\frac{P_2 z}{P_3 \lambda_b}) \frac{z^{n-1} exp(\frac{-z}{\lambda})}{\Gamma n \lambda^n}\, dz \right] \\
& F_{G'}(g^{'}) = 1 - exp(\frac{-g^{'}}{P_3 \lambda_b}) \left(\frac{P_3 \lambda_b}{P_3 \lambda_b - P_2 \lambda} \right)^n \\
& f_{G'}(g^{'}) = (\frac{1}{P_3 \lambda_b}) exp(\frac{-g^{'}}{P_3 \lambda_b}) \left(\frac{P_3 \lambda_b}{P_3 \lambda_b - P_2 \lambda} \right)^n
\end{aligned}
\tag{C.4}
$$

The equation C.2 can now be expressed as:

$$
Pr\Big(\frac{P_1 X}{G' + N_0} \leq m \Big) \tag{C.5}
$$

$$
\begin{aligned}
F_M(m) = & \int_{g'=0}^{+\infty} \int_{x=0}^{\frac{(mg^{'}+mN_0)}{P_1}} f_{G'}(g^{'}) f_X(x)\, dx\, dg^{'} \\
& = \int_{g'=0}^{+\infty} \int_{x=0}^{\frac{(mg^{'}+mN_0)}{P_1}} (\frac{1}{\lambda_a}) exp(\frac{-x}{\lambda_a}) f_{G'}(g^{'})\, dx\, dg^{'} \\
& = \int_{g'=0}^{+\infty} \Big[1 - exp\big(\frac{-(mg^{'}+mN_0)}{P_1 \lambda_a}\big) \Big] f_{G'}(g^{'})\, dg^{'} \\
& = 1 - exp(\frac{-mN_0}{P_1 \lambda_a}) \Big(\frac{P_1 \lambda_a}{P_1 \lambda_a + m P_3 \lambda_b} \Big) \Big(\frac{P_3 \lambda_b}{P_3 \lambda_b - P_2 \lambda} \Big)^n
\end{aligned}
\tag{C.6}
$$

Appendix D

Proof for equation (5.48) The proof for W and Q in equation (5.48) can be derived as follows. Similarly, Ψ is exponentially distributed and Z is Gamma distributed random variable, with parameters λ_c and λ, respectively,

$$Pr\Big(\frac{P_4\Psi}{P_5Z+N_0} \leq q\Big) \tag{D.1}$$

$$\begin{aligned} F_Q(q) = & \int_{z=0}^{+\infty}\int_{\psi=0}^{\frac{(qP_5Z+qN_0)}{P_4}} (\frac{1}{\lambda_c})exp(\frac{-\psi}{\lambda_c})f_Z(z)\,d\psi\,dz \\ & = 1-exp(\frac{-qN_0}{P_4\lambda_c})\int_{z=0}^{+\infty} exp(\frac{-qP_5z}{P_4\lambda_c})\frac{z^{n-1}exp(\frac{-z}{\lambda})}{\Gamma n\lambda^n}\,dz \\ & = 1-exp(\frac{-qN_0}{P_4\lambda_c})\left(\frac{P_4\lambda_c}{P_4\lambda_c+qP_5\lambda}\right) \end{aligned} \tag{D.2}$$

From [119], we get if

$$Pr\Big(\max_{k=1,2,\ldots,K}\frac{P_4\Psi}{P_5Z+N_0} \leq q\Big) \tag{D.3}$$

then the equation can be expressed as:

$$\begin{aligned} F_Q(q) = & \prod_{k=1}^{K} Pr\Big(\frac{P_4\Psi}{P_5Z+N_0} \leq q\Big) \\ & = \left[1-exp(\frac{-qN_0}{P_4\lambda_c})\left(\frac{P_4\lambda_c}{P_4\lambda_c+qP_5\lambda}\right)\right]^K \end{aligned} \tag{D.4}$$

Bibliography

[1] A. Goldsmith, S. A. Jafar, I. Maric, and S. Srinivasa, "Breaking spectrum gridlock with cognitive radios: An information theoretic perspective," *Proceedings of the IEEE*, vol. 97, no. 5, pp. 894–914, 2009.

[2] S. Haykin, "Cognitive radio: brain-empowered wireless communications," *IEEE journal on selected areas in communications*, vol. 23, no. 2, pp. 201–220, 2005.

[3] J. Mitola and G. Q. Maguire, "Cognitive radio: making software radios more personal," *IEEE personal communications*, vol. 6, no. 4, pp. 13–18, 1999.

[4] R. Zhang and Y.-C. Liang, "Optimal power allocation for cognitive radio networks under coupled interference constraints: A cooperative game-theoretic perspective," *IEEE Transactions on Wireless Communications*, vol. 8, no. 11, pp. 5748–5757, 2009.

[5] M.-S. Alouini and A. J. Goldsmith, "Capacity of mrc diversity systems with amplify-and-forward relaying over rayleigh fading channels," *IEEE Transactions on Vehicular Technology*, vol. 49, no. 5, pp. 1992–1997, 2000.

[6] M. O. Hasna and M.-S. Alouini, "Performance of amplify-and-forward and decode-and-forward relaying over fading channels," *IEEE Transactions on Communications*, vol. 51, no. 6, pp. 982–989, 2003.

[7] S. Haykin and M. Moher, *Modern Wireless Communications*. Pearson Education, 2005.

[8] T. S. Rappaport, *Wireless Communications: Principles and Practice*, 2nd ed. Prentice Hall, 2002.

[9] Z. Ding, M. Peng, and H. V. Poor, "Cooperative non-orthogonal multiple access in 5g systems," *IEEE Communications Letters*, vol. 19, no. 8, pp. 1462–1465, 2015.

[10] X. Lu, D. Niyato, P. Wang, D. I. Kim, and Z. Han, "Wireless networks with rf energy harvesting: A contemporary survey," *IEEE Communications Surveys & Tutorials*, vol. 17, no. 2, pp. 757–789, 2015.

[11] R. Jiang, "Rf-based energy harvesting: Nonlinear models, applications and challenges," *arXiv preprint arXiv:2405.04976*, 2024.

[12] E. Boshkovska, D. W. K. Ng, N. Zlatanov, and R. Schober, "Practical non-linear energy harvesting model and resource allocation for swipt systems," *arXiv preprint arXiv:1509.02956*, 2015.

[13] P. N. Alevizos and A. Bletsas, "Sensitive and nonlinear far field rf energy harvesting in wireless communications," *arXiv preprint arXiv:1707.07041*, 2017.

[14] Q. Wu and R. Zhang, "Intelligent reflecting surface (irs)-aided wireless communications: A tutorial," *IEEE Transactions on Communications*, vol. 69, no. 5, pp. 3313–3351, 2021.

[15] V. Chakravarthy, X. Li, R. Zhou, Z. Wu, and M. Temple, "A novel hybrid overlay/underlay cognitive radio waveform in frequency selective fading channels," in *2009 4th International Conference on Cognitive Radio Oriented Wireless Networks and Communications*. IEEE, 2009, pp. 1–6.

[16] J. Oh and W. Choi, "A hybrid cognitive radio system: A combination of underlay and overlay approaches," in *2010 IEEE 72nd Vehicular Technology Conference-Fall*. IEEE, 2010, pp. 1–5.

[17] X. Bao, P. Martins, T. Song, and L. Shen, "Capacity of hybrid cognitive network with outage constraints," *IET communications*, vol. 5, no. 18, pp. 2712–2720, 2011.

[18] J. Zuo, L. Zhao, Y. Bao, and C. Zou, "Energy-efficient power allocation for cognitive radio networks with joint overlay and underlay spectrum access mechanism," *ETRI Journal*, vol. 37, no. 3, pp. 471–479, 2015.

[19] S. Sharma, S. Dhar Roy, and S. Kundu, "Secure communication with energy harvesting multiple half-duplex df relays assisted with jamming," *Wireless Networks*, vol. 26, no. 2, pp. 1151–1164, 2020.

[20] M. Mao, N. Cao, Y. Chen, and Y. Zhou, "Multi-hop relaying using energy harvesting," *IEEE Wireless Communications Letters*, vol. 4, no. 5, pp. 565–568, 2015.

[21] Y. Gu and S. Aissa, "Rf-based energy harvesting in decode-and-forward relaying systems: Ergodic and outage capacities," *IEEE Transactions on Wireless Communications*, vol. 14, no. 11, pp. 6425–6434, 2015.

[22] S. Mondal, S. Roy, and S. Kundu, "On performance of multihop energy harvesting crn in the presence of co-channel interferers," *International Journal of Electronics Letters*, vol. 10, no. 1, pp. 1–15, 2022.

[23] H. W. Merino, C. E. Camara, and C. de Almeida, "Uplink spectral efficiency for small-cells with dual-hop amplify-and-forward relaying at 28 ghz," *IET communications*, vol. 13, no. 5, pp. 496–504, 2019.

[24] P. M. Nam, T. T. Duy, and P. V. Ca, "Performance of cluster-based cognitive multihop networks under joint impact of hardware noises and non-identical primary co-channel interference," *TELKOMNIKA Telecommunication Computing Electronic and Control*, vol. 17, no. 1, pp. 49–59, 2019.

[25] D. S. Michalopoulos, J. Schlenker, J. Cheng, and R. Schober, "Error rate analysis of full-duplex relaying," in *2010 International Waveform Diversity and Design Conference*. IEEE, 2010, pp. 000 165–000 168.

[26] S. Poornima and A. Babu, "Power adaptation for enhancing spectral efficiency and energy efficiency in multi-hop full duplex cognitive wireless relay networks," *IEEE Transactions on Mobile Computing*, 2020.

[27] I. Krikidis and H. A. Suraweera, "Full-duplex cooperative diversity with alamouti space-time code," *IEEE Wireless Communications Letters*, vol. 2, no. 5, pp. 519–522, 2013.

[28] T. Riihonen, S. Werner, and R. Wichman, "Hybrid full-duplex/half-duplex relaying with transmit power adaptation," *IEEE Transactions on Wireless Communications*, vol. 10, no. 9, pp. 3074–3085, 2011.

[29] M. Babaei, Ü. Aygölü, M. Başaran, and L. Durak-Ata, "Ber performance of full-duplex cognitive radio network with nonlinear energy harvesting," *IEEE Transactions on Green Communications and Networking*, vol. 4, no. 2, pp. 448–460, 2020.

[30] Z. Ding, Y. Liu, J. Choi, Q. Sun, M. Elkashlan, I. Chih-Lin, and H. V. Poor, "Application of non-orthogonal multiple access in lte and 5g networks," *IEEE Communications Magazine*, vol. 55, no. 2, pp. 185–191, 2017.

[31] L. Zhang, Y.-C. Liang, and M. Xiao, "Spectrum sharing for internet of things: A survey," *IEEE Wireless Communications*, vol. 26, no. 3, pp. 132–139, 2018.

[32] Z. Ding, X. Lei, G. K. Karagiannidis, R. Schober, J. Yuan, and V. K. Bhargava, "A survey on non-orthogonal multiple access for 5g networks: Research challenges and future trends," *IEEE Journal on Selected Areas in Communications*, vol. 35, no. 10, pp. 2181–2195, 2017.

[33] L. Lv, J. Chen, Q. Ni, and Z. Ding, "Design of cooperative non-orthogonal multicast cognitive multiple access for 5g systems: User scheduling and performance analysis," *IEEE Transactions on Communications*, vol. 65, no. 6, pp. 2641–2656, 2017.

[34] Z. Zhang, Z. Ma, M. Xiao, Z. Ding, and P. Fan, "Full-duplex device-to-device-aided cooperative nonorthogonal multiple access," *IEEE Transactions on Vehicular Technology*, vol. 66, no. 5, pp. 4467–4471, 2016.

[35] L. Zhang, J. Liu, M. Xiao, G. Wu, Y.-C. Liang, and S. Li, "Performance analysis and optimization in downlink noma systems with cooperative full-duplex relaying," *IEEE Journal on Selected Areas in Communications*, vol. 35, no. 10, pp. 2398–2412, 2017.

[36] X. Yue, Y. Liu, S. Kang, A. Nallanathan, and Z. Ding, "Exploiting full/half-duplex user relaying in noma systems," *IEEE Transactions on Communications*, vol. 66, no. 2, pp. 560–575, 2017.

[37] Q. Wu and R. Zhang, "Intelligent reflecting surface enhanced wireless network via joint active and passive beamforming," *IEEE transactions on wireless communications*, vol. 18, no. 11, pp. 5394–5409, 2019.

[38] X. Yu, D. Xu, and R. Schober, "Miso wireless communication systems via intelligent reflecting surfaces," in *2019 IEEE/CIC International Conference on Communications in China (ICCC)*. IEEE, 2019, pp. 735–740.

[39] D. Xu, X. Yu, Y. Sun, D. W. K. Ng, and R. Schober, "Resource allocation for secure irs-assisted multiuser miso systems," in *2019 IEEE Globecom Workshops (GC Wkshps)*. IEEE, 2019, pp. 1–6.

[40] C. Pan, H. Ren, K. Wang, M. Elkashlan, A. Nallanathan, J. Wang, and L. Hanzo, "Intelligent reflecting surface aided mimo broadcasting for simultaneous wireless information and power transfer," *IEEE Journal on Selected Areas in Communications*, vol. 38, no. 8, pp. 1719–1734, 2020.

[41] S. Zhang and R. Zhang, "Capacity characterization for intelligent reflecting surface aided mimo communication," *IEEE Journal on Selected Areas in Communications*, vol. 38, no. 8, pp. 1823–1838, 2020.

[42] K. Tian, B. Duo, S. Li, Y. Zuo, and X. Yuan, "Hybrid uplink and downlink transmissions for full-duplex uav communication with ris," *IEEE Wireless Communications Letters*, vol. 11, no. 4, pp. 866–870, 2022.

[43] H. Shen, T. Ding, W. Xu, and C. Zhao, "Beamformig design with fast convergence for irs-aided full-duplex communication," *IEEE Communications Letters*, vol. 24, no. 12, pp. 2849–2853, 2020.

[44] Z. Abdullah, G. Chen, S. Lambotharan, and J. A. Chambers, "Optimization of intelligent reflecting surface assisted full-duplex relay networks," *IEEE Wireless Communications Letters*, vol. 10, no. 2, pp. 363–367, 2020.

[45] Y. Ge and J. Fan, "Robust secure beamforming for intelligent reflecting surface assisted full-duplex miso systems," *IEEE Transactions on Information Forensics and Security*, vol. 17, pp. 253–264, 2021.

[46] Q. Ding, J. Yang, Y. Luo, and C. Luo, "Intelligent reflecting surface vs. conventional full-duplex relay in mmwave mimo networks: A comprehensive performance comparison," *IEEE Transactions on Vehicular Technology*, 2024.

[47] L. Zhang, M. Xiao, G. Wu, M. Alam, Y.-C. Liang, and S. Li, "A survey of advanced techniques for spectrum sharing in 5g networks," *IEEE Wireless Communications*, vol. 24, no. 5, pp. 44–51, 2017.

[48] J. G. Proakis, *Digital Communications*. McGraw-Hill, 2001.

[49] N. M. Sekulović and M. Č. Stefanović, "Performance analysis of system with micro- and macrodiversity reception in correlated gamma shadowed rician fading channels," *Wireless Personal Communications*, vol. 65, p. 143–156, 2012, analyzes micro- and macro-diversity combining (antenna diversity and multiple BSs) under fading and shadowing :contentReference[oaicite:2]index=2.

[50] T. S. Rappaport, *Wireless communications: principles and practice*. Cambridge University Press, 2024.

[51] N. M. Sekulović and M. Stefanović, "Relay selection in cognitive radio networks with interference constraints," *IET Communications*, 2013, defines PU interference threshold and limits SU/relay power accordingly :contentReference[oaicite:2]index=2.

[52] L. Zhang, R. Senanayake, S. Atapattu, and J. Evans, "Relay assisted underlay cognitive radio networks with multiple users," *arXiv preprint arXiv:2105.03589*, 2021, studies dual-hop DF relaying under PU interference power constraints :contentReference[oaicite:1]index=1.

[53] C. S. Preetham, M. S. G. Prasad, and T. V. Ramakrishna, "Hybrid overlay/underlay transmission with partial and opportunistic relay selection in cognitive radio networks," *Indian Journal of Science and Technology*, vol. 9, no. 39, pp. 1–8, 2016, proposes a hybrid overlay/underlay scheme that uses spectrum sensing and relay selection for adaptive mode switching :contentReference[oaicite:1]index=1.

[54] K. Zheng, X.-Y. Liu, X. Liu, and Y. Zhu, "Hybrid overlay–underlay cognitive radio networks with energy harvesting," *IEEE Transactions on Communications*, vol. 67, no. 7, pp. 4669–4682, 2019, evaluates dynamic underlay/overlay switching with relays and energy detection for mode selection :contentReference[oaicite:2]index=2.

[55] A. Vashistha, S. Sharma, and V. A. Bohara, "Outage analysis of a multiple-antenna cognitive radio system with cooperative decode-and-forward relaying," *IEEE Wireless Communications Letters*, vol. 4, no. 2, pp. 125–128, 2014.

[56] C. K. De and S. Kundu, "Proactive and reactive df relaying for cognitive network with multiple primary users," *Radioengineering*, vol. 25, no. 3, p. 475, 2016.

[57] S. Poornima and A. Babu, "Performance analysis of energy harvesting cognitive relay networks with primary interference," *Telecommunication Systems*, vol. 68, no. 3, pp. 445–459, 2018.

[58] C. K. De and S. Kundu, "Adaptive decode-and-forward protocol based cooperative spectrum sensing in cognitive radio with interference at the secondary users," *Wireless personal communications*, vol. 79, no. 2, pp. 1417–1434, 2014.

[59] A. Saha, S. S. Bhattacherjee, C. K. De, and D. De, "Cooperative spectrum sharing with multi-antenna based adaptive hybrid relay in presence of multiple primary users," *Journal of Information and Optimization Sciences*, vol. 38, no. 6, pp. 857–871, 2017.

[60] Y. Huang, F. Al-Qahtani, C. Zhong, and Q. Wu, "Outage analysis of spectrum sharing relay systems with multi-secondary destinations in the presence of primary user's interference," pp. 1–6, 2013.

[61] D. Arianandа, M. Lakshmanan, and H. Nikookar, "A survey on spectrum sensing techniques for cognitive radio," in *2009 Second International Workshop on Cognitive Radio and Advanced Spectrum Management.* IEEE, 2009, pp. 74–79.

[62] T. Yucek and H. Arslan, "A survey of spectrum sensing algorithms for cognitive radio applications," *IEEE communications surveys & tutorials*, vol. 11, no. 1, pp. 116–130, 2009.

[63] F. Arpanaei, K. Navaie, and S. N. Esfahani, "A hybrid overlay-underlay strategy for ofdm-based cognitive radio systems and its maximum achievable capacity," in *2011 19th Iranian Conference on Electrical Engineering.* IEEE, 2011, pp. 1–6.

[64] B. Prasad, A. Bhowmick, S. Dhar Roy, and S. Kundu, "Performance of cognitive relay network with novel hybrid spectrum access schemes with imperfect

csi," *International Journal of Communication Systems*, vol. 29, no. 11, pp. 1761–1776, 2016.

[65] R. Blasco-Serrano, J. Lv, R. Thobaben, E. Jorswieck, A. Kliks, and M. Skoglund, "Comparison of underlay and overlay spectrum sharing strategies in miso cognitive channels," in *2012 7th International ICST Conference on Cognitive Radio Oriented Wireless Networks and Communications (CROWNCOM)*. IEEE, 2012, pp. 224–229.

[66] R. Rajaganapathi and P. M. Nathan, "Cluster-based spectrum access scheme selection and optimal relay link selection for hybrid overlay/underlay cognitive radio networks," *International Journal of Communication Systems*, p. e4328, 2020.

[67] H. Tran, H.-J. Zepernick, and H. Phan, "Cognitive proactive and reactive df relaying schemes under joint outage and peak transmit power constraints," *IEEE communications letters*, vol. 17, no. 8, pp. 1548–1551, 2013.

[68] T. Zhang, W. Yang, and Y. Cai, "Exact outage performance analysis of multiuser multi-relay spectrum sharing cognitive networks," *RADIOENGINEERING*, vol. 24, no. 1, p. 115, 2015.

[69] A. Saha, C. K. De, A. Nandi, and D. De, "Cooperative spectrum sharing with multi antenna based amplify-and-forward and decode-and-forward relay," in *2016 IEEE Uttar Pradesh Section International Conference on Electrical, Computer and Electronics Engineering (UPCON)*. IEEE, 2016, pp. 224–228.

[70] S. S. Bhattacherjee, A. Saha, C. K. De, and D. De, "Cooperative spectrum sharing with multi-antenna based adaptive hybrid relay," in *2017 International Conference on Wireless Communications, Signal Processing and Networking (WiSPNET)*. IEEE, 2017, pp. 1713–1717.

[71] C. Zhong, T. Ratnarajah, and K.-K. Wong, "Outage analysis of decode-and-forward cognitive dual-hop systems with the interference constraint in

nakagami-m fading channels," *IEEE Transactions on Vehicular Technology*, vol. 60, no. 6, pp. 2875–2879, 2011.

[72] S. Al-Juboori and X. Fernando, "Correlated multichannel spectrum sensing cognitive radio system with selection combining," in *2016 IEEE Global Communications Conference (GLOBECOM)*. IEEE, 2016, pp. 1–6.

[73] Y. Liu, S. A. Mousavifar, Y. Deng, C. Leung, and M. Elkashlan, "Wireless energy harvesting in a cognitive relay network," *IEEE Transactions on Wireless Communications*, vol. 15, no. 4, pp. 2498–2508, 2015.

[74] Y. Yan, J. Huang, and J. Wang, "Dynamic bargaining for relay-based cooperative spectrum sharing," *IEEE Journal on Selected Areas in Communications*, vol. 31, no. 8, pp. 1480–1493, 2012.

[75] V. N. Q. Bao, T. Q. Duong, D. B. da Costa, G. C. Alexandropoulos, and A. Nallanathan, "Cognitive amplify-and-forward relaying with best relay selection in non-identical rayleigh fading," *IEEE Communications Letters*, vol. 17, no. 3, pp. 475–478, 2013.

[76] J. K. Bag, D. Samanta, C. K. De, and A. Chandra, "Outage analysis of joint underlay/overlay cr network," in *Proceedings of the 3rd International Conference on Communication, Devices and Computing*. Springer, 2022, pp. 537–550.

[77] Y. Liao, L. Song, Z. Han, and Y. Li, "Full duplex cognitive radio: a new design paradigm for enhancing spectrum usage," *IEEE Communications Magazine*, vol. 53, no. 5, pp. 138–145, 2015.

[78] Z. Zhang, X. Chai, K. Long, A. V. Vasilakos, and L. Hanzo, "Full duplex techniques for 5g networks: self-interference cancellation, protocol design, and relay selection," *IEEE Communications Magazine*, vol. 53, no. 5, pp. 128–137, 2015.

[79] T. Q. Duong, D. B. Da Costa, T. A. Tsiftsis, C. Zhong, and A. Nallanathan, "Outage and diversity of cognitive relaying systems under spectrum sharing environments in nakagami-m fading," *IEEE Communications Letters*, vol. 16, no. 12, pp. 2075–2078, 2012.

[80] T. Q. Duong, V. N. Q. Bao, and H.-J. Zepernick, "Exact outage probability of cognitive af relaying with underlay spectrum sharing," *Electronics letters*, vol. 47, no. 17, pp. 1001–1002, 2011.

[81] T. Kwon, S. Lim, S. Choi, and D. Hong, "Optimal duplex mode for df relay in terms of the outage probability," *IEEE Transactions on Vehicular Technology*, vol. 59, no. 7, pp. 3628–3634, 2010.

[82] I. Krikidis, H. A. Suraweera, S. Yang, and K. Berberidis, "Full-duplex relaying over block fading channel: A diversity perspective," *IEEE Transactions on Wireless Communications*, vol. 11, no. 12, pp. 4524–4535, 2012.

[83] A. Sabharwal, P. Schniter, D. Guo, D. W. Bliss, S. Rangarajan, and R. Wichman, "In-band full-duplex wireless: Challenges and opportunities," *IEEE Journal on selected areas in communications*, vol. 32, no. 9, pp. 1637–1652, 2014.

[84] T. Riihonen, S. Werner, and R. Wichman, "Mitigation of loopback self-interference in full-duplex mimo relays," *IEEE transactions on signal processing*, vol. 59, no. 12, pp. 5983–5993, 2011.

[85] J. Zhou, T.-H. Chuang, T. Dinc, and H. Krishnaswamy, "Integrated wideband self-interference cancellation in the rf domain for fdd and full-duplex wireless," *IEEE Journal of Solid-State Circuits*, vol. 50, no. 12, pp. 3015–3031, 2015.

[86] H. A. Suraweera, I. Krikidis, G. Zheng, C. Yuen, and P. J. Smith, "Low-complexity end-to-end performance optimization in mimo full-duplex relay systems," *IEEE Transactions on Wireless Communications*, vol. 13, no. 2, pp. 913–927, 2014.

[87] M. Mohammadi, H. A. Suraweera, Y. Cao, I. Krikidis, and C. Tellambura, "Full-duplex radio for uplink/downlink wireless access with spatially random nodes," *IEEE Transactions on Communications*, vol. 63, no. 12, pp. 5250–5266, 2015.

[88] M. Mohammadi, B. K. Chalise, H. A. Suraweera, C. Zhong, G. Zheng, and I. Krikidis, "Throughput analysis and optimization of wireless-powered multiple antenna full-duplex relay systems," *IEEE Transactions on communications*, vol. 64, no. 4, pp. 1769–1785, 2016.

[89] N. H. Tran, L. J. Rodríguez, and T. Le-Ngoc, "Optimal power control and error performance for full-duplex dual-hop af relaying under residual self-interference," *IEEE Communications Letters*, vol. 19, no. 2, pp. 291–294, 2014.

[90] L. J. Rodriguez, N. H. Tran, and T. Le-Ngoc, "Performance of full-duplex af relaying in the presence of residual self-interference," *IEEE Journal on Selected Areas in Communications*, vol. 32, no. 9, pp. 1752–1764, 2014.

[91] M. G. Khafagy, A. Ismail, M.-S. Alouini, and S. Aïssa, "Efficient cooperative protocols for full-duplex relaying over nakagami-m fading channels," *IEEE Transactions on Wireless Communications*, vol. 14, no. 6, pp. 3456–3470, 2015.

[92] V. S. Babu, N. Deepan, and B. Rebekka, "Performance analysis of cooperative full duplex noma system in cognitive radio networks," in *2020 International Conference on Wireless Communications Signal Processing and Networking (WiSPNET)*. IEEE, 2020, pp. 84–87.

[93] X. Xie, Y. Bi, and X. Nie, "Performance analysis of full-duplex spectrum sharing networks under peak interference power and peak transmit power constraints," in *2020 IEEE 20th International Conference on Communication Technology (ICCT)*. IEEE, 2020, pp. 153–156.

[94] D. Bharadia and S. Katti, "Full duplex {MIMO} radios," in *11th {USENIX} Symposium on Networked Systems Design and Implementation ({NSDI} 14)*, 2014, pp. 359–372.

[95] M. Jain, J. I. Choi, T. Kim, D. Bharadia, S. Seth, K. Srinivasan, P. Levis, S. Katti, and P. Sinha, "Practical, real-time, full duplex wireless," in *Proceedings of the 17th annual international conference on Mobile computing and networking*, 2011, pp. 301–312.

[96] 3GPP, "Study on scenarios and requirements for next generation access technologies," *Technical Specification Group Radio Access Network, Technical Report 38.913*, 2016.

[97] M. Series, "Imt vision–framework and overall objectives of the future development of imt for 2020 and beyond," *Recommendation ITU*, vol. 2083, p. 0, 2015.

[98] M. Agiwal, A. Roy, and N. Saxena, "Next generation 5g wireless networks: A comprehensive survey," *IEEE Communications Surveys & Tutorials*, vol. 18, no. 3, pp. 1617–1655, 2016.

[99] X. Wang, M. Jia, Q. Guo, I. W.-H. Ho, and F. C.-M. Lau, "Full-duplex relaying cognitive radio network with cooperative nonorthogonal multiple access," *IEEE Systems Journal*, vol. 13, no. 4, pp. 3897–3908, 2019.

[100] Y. Liu, Z. Ding, M. Elkashlan, and J. Yuan, "Nonorthogonal multiple access in large-scale underlay cognitive radio networks," *IEEE Transactions on Vehicular Technology*, vol. 65, no. 12, pp. 10 152–10 157, 2016.

[101] S. Lee, T. Q. Duong, D. B. da Costa, D.-B. Ha, and S. Q. Nguyen, "Underlay cognitive radio networks with cooperative non-orthogonal multiple access," *IET Communications*, vol. 12, no. 3, pp. 359–366, 2018.

[102] L. Lv, J. Chen, and Q. Ni, "Cooperative non-orthogonal multiple access in cognitive radio," *IEEE Communications Letters*, vol. 20, no. 10, pp. 2059–2062, 2016.

[103] L. Lv, Q. Ni, Z. Ding, and J. Chen, "Application of non-orthogonal multiple access in cooperative spectrum-sharing networks over nakagami-m fading channels," *IEEE Transactions on Vehicular Technology*, vol. 66, no. 6, pp. 5506–5511, 2016.

[104] S. Arzykulov, G. Nauryzbayev, T. A. Tsiftsis, and B. Maham, "Performance analysis of underlay cognitive radio nonorthogonal multiple access networks," *IEEE Transactions on Vehicular Technology*, vol. 68, no. 9, pp. 9318–9322, 2019.

[105] S. Arzykulov, G. Nauryzbayev, T. A. Tsiftsis, B. Maham, and M. Abdallah, "On the outage of underlay cr-noma networks with detect-and-forward relaying," *IEEE Transactions on Cognitive Communications and Networking*, vol. 5, no. 3, pp. 795–804, 2019.

[106] Y. Yu, Z. Yang, Y. Wu, J. A. Hussein, W.-K. Jia, and Z. Dong, "Outage performance of noma in cooperative cognitive radio networks with swipt," *IEEE Access*, vol. 7, pp. 117 308–117 317, 2019.

[107] V. Aswathi and A. Babu, "Performance analysis of nonorthogonal multiple access-based underlay cognitive relay network," *INTERNATIONAL JOURNAL OF COMMUNICATION SYSTEMS*, vol. 32, no. 13, 2019.

[108] S. Arzykulov, T. A. Tsiftsis, G. Nauryzbayev, and M. Abdallah, "Outage performance of cooperative underlay cr-noma with imperfect csi," *IEEE Communications Letters*, vol. 23, no. 1, pp. 176–179, 2018.

[109] Y. Meng, H. Wang, and S. Xu, "Transmission performance analysis of cognitive noma with swipt over nakagami-m fading channels," in *2019 IEEE 19th International Conference on Communication Technology (ICCT)*. IEEE, 2019, pp. 770–775.

[110] D.-T. Do, A.-T. Le, and B. M. Lee, "Noma in cooperative underlay cognitive radio networks under imperfect sic," *IEEE Access*, vol. 8, pp. 86 180–86 195, 2020.

[111] S. Lee, D. B. Da Costa, Q.-T. Vien, T. Q. Duong, and R. T. de Sousa Jr, "Non-orthogonal multiple access schemes with partial relay selection," *IET Communications*, vol. 11, no. 6, pp. 846–854, 2017.

[112] D. Deng, L. Fan, X. Lei, W. Tan, and D. Xie, "Joint user and relay selection for cooperative noma networks," *IEEE Access*, vol. 5, pp. 20 220–20 227, 2017.

[113] Y. Li, Y. Li, X. Chu, Y. Ye, and H. Zhang, "Performance analysis of relay selection in cooperative noma networks," *IEEE Communications Letters*, vol. 23, no. 4, pp. 760–763, 2019.

[114] Z. Yang, Z. Ding, Y. Wu, and P. Fan, "Novel relay selection strategies for cooperative noma," *IEEE Transactions on Vehicular Technology*, vol. 66, no. 11, pp. 10 114–10 123, 2017.

[115] P. Xu, Z. Yang, Z. Ding, and Z. Zhang, "Optimal relay selection schemes for cooperative noma," *IEEE Transactions on Vehicular Technology*, vol. 67, no. 8, pp. 7851–7855, 2018.

[116] T. M. Hoang, N. T. Tan, S.-G. Choi *et al.*, "Analysis of partial relay selection in noma systems with rf energy harvesting," in *2018 2nd International Conference on Recent Advances in Signal Processing, Telecommunications & Computing (SigTelCom)*. IEEE, 2018, pp. 13–18.

[117] A. S. Parihar, P. Swami, V. Bhatia, and Z. Ding, "Performance analysis of swipt enabled cooperative-noma in heterogeneous networks using carrier sensing," *IEEE Transactions on Vehicular Technology*, vol. 70, no. 10, pp. 10 646–10 656, 2021.

[118] A. S. Parihar, P. Swami, and V. Bhatia, "On performance of swipt enabled ppp distributed cooperative noma networks using stochastic geometry," *IEEE Transactions on Vehicular Technology*, vol. 71, no. 5, pp. 5639–5644, 2022.

[119] V. Aswathi and A. Babu, "Performance analysis of noma-based underlay cognitive radio networks with partial relay selection," *IEEE Transactions on Vehicular Technology*, vol. 70, no. 5, pp. 4615–4630, 2021.

[120] D.-T. Do, M.-S. Van Nguyen, F. Jameel, R. Jäntti, and I. S. Ansari, "Performance evaluation of relay-aided cr-noma for beyond 5g communications," *IEEE Access*, vol. 8, pp. 134 838–134 855, 2020.

[121] J. Jose, P. Shaik, and V. Bhatia, "Vfd-noma under imperfect sic and residual inter-relay interference over generalized nakagami-m fading channels," *IEEE Communications Letters*, vol. 25, no. 2, pp. 646–650, 2020.

[122] S. Dhanasekaran and M. Chitra, "Performance analysis of noma in full-duplex cooperative spectrum sharing systems," *IEEE Transactions on Vehicular Technology*, vol. 71, no. 8, pp. 9095–9100, 2022.

[123] E. Björnson, H. Wymeersch, B. Matthiesen, P. Popovski, L. Sanguinetti, and E. De Carvalho, "Reconfigurable intelligent surfaces: A signal processing perspective with wireless applications," *IEEE Signal Processing Magazine*, vol. 39, no. 2, pp. 135–158, 2022.

[124] M. Elhattab, M. A. Arfaoui, C. Assi, and A. Ghrayeb, "Reconfigurable intelligent surface enabled full-duplex/half-duplex cooperative non-orthogonal multiple access," *IEEE Transactions on Wireless Communications*, vol. 21, no. 5, pp. 3349–3364, 2021.

[125] W. Khalid, H. Yu, D.-T. Do, Z. Kaleem, and S. Noh, "Ris-aided physical layer security with full-duplex jamming in underlay d2d networks," *IEEE Access*, vol. 9, pp. 99 667–99 679, 2021.

[126] M. S. Gilan and B. Maham, "Performance analysis of power-efficient irs-assisted full duplex noma systems," *Physical Communication*, vol. 64, p. 102338, 2024.

[127] D. M. M. Plata and Á. G. A. Reátiga, "Evaluation of energy detection for spectrum sensing based on the dynamic selection of detection-threshold," *Procedia Engineering*, vol. 35, pp. 135–143, 2012.

[128] S. P. T. Force, "Spectrum policy task force report et docket no. 02-135," *US Federal Communications Commission*, 2002.

[129] A. Papoulis and S. U. Pillai, *Probability, random variables, and stochastic processes*. Tata McGraw-Hill Education, 2002.

[130] M. M. Molu, P. Xiao, M. Khalily, L. Zhang, and R. Tafazolli, "A novel equivalent definition of modified bessel functions for performance analysis of multihop wireless communication systems," *IEEE Access*, vol. 5, pp. 7594–7605, 2017.

[131] I. S. Gradshteyn and I. M. Ryzhik, *Table of integrals, series, and products*. USA: Academic press, 2014.

[132] X.-T. Doan, N.-P. Nguyen, C. Yin, D. B. Da Costa, and T. Q. Duong, "Cognitive full-duplex relay networks under the peak interference power constraint of multiple primary users," *EURASIP Journal on Wireless Communications and Networking*, vol. 2017, no. 1, pp. 1–10, 2017.

[133] S. Shrestha and K. Chang, "Closed-form solution of outage capacity for cooperative df and af relay network," *Wireless personal communications*, vol. 54, no. 4, pp. 651–665, 2010.

[134] F. R. V. Guimarães, D. B. Da Costa, T. A. Tsiftsis, C. C. Cavalcante, and G. K. Karagiannidis, "Multiuser and multirelay cognitive radio networks under spectrum-sharing constraints," *IEEE Transactions on Vehicular Technology*, vol. 63, no. 1, pp. 433–439, 2013.

[135] G. Chen, Y. Gong, P. Xiao, and J. A. Chambers, "Physical layer network security in the full-duplex relay system," *IEEE transactions on information forensics and security*, vol. 10, no. 3, pp. 574–583, 2015.

[136] A. A. Nasir, X. Zhou, S. Durrani, and R. A. Kennedy, "Relaying protocols for wireless energy harvesting and information processing," *IEEE Transactions on Wireless Communications*, vol. 12, no. 7, pp. 3622–3636, 2013.

[137] H. Saito, "Theoretical analysis of nonlinear energy harvesting from wireless mobile nodes," *IEEE Wireless Communications Letters*, vol. 10, no. 9, pp. 1914–1918, 2021.

[138] A. S. Parihar, P. Swami, K. Choi, P. Brida, and V. Bhatia, "On performance of noma based wireless powered communication networks assisted with power beacons and ppp distributed in," *IEEE Wireless Communications Letters*, 2023.

[139] K. P. Peppas, "Accurate closed-form approximations to generalised-k sum distributions and applications in the performance analysis of equal-gain combining receivers," *IET communications*, vol. 5, no. 7, pp. 982–989, 2011.

[140] M. El Tanab and W. Hamouda, "Resource allocation for underlay cognitive radio networks: A survey," *IEEE Communications Surveys & Tutorials*, vol. 19, no. 2, pp. 1249–1276, 2016.

[141] S. Daoud, D. Haccoun, and C. Cardinal, "On the achievable rate and average sum capacity of spread spectrum underlay cr networks," in *2016 IEEE 84th Vehicular Technology Conference (VTC-Fall)*. IEEE, 2016, pp. 1–5.

[142] A. Abdou, G. Ferré, E. Grivel, and M. Najim, "Interference cancellation in multiuser hybrid overlay cognitive radio," in *21st European Signal Processing Conference (EUSIPCO 2013)*. IEEE, 2013, pp. 1–5.

[143] R. Alhamad, H. Wang, and Y.-D. Yao, "Cooperative spectrum sensing with random access reporting channels in cognitive radio networks," *IEEE Transactions on Vehicular Technology*, vol. 66, no. 8, pp. 7249–7261, 2017.

[144] L. B. Le and E. Hossain, "Resource allocation for spectrum underlay in cognitive radio networks," *IEEE Transactions on Wireless communications*, vol. 7, no. 12, pp. 5306–5315, 2008.

[145] M. Subhedar and G. Birajdar, "Spectrum sensing techniques in cognitive radio networks: A survey," *International Journal of Next-Generation Networks*, vol. 3, no. 2, pp. 37–51, 2011.

[146] H.-V. Khuong, P. C. Sofotasios, V. Q. Son, L. T. Tra, and P. H. Lien, "Analysis of cognitive cooperative networks with best relay selection and diversity reception," in *2015 International Conference on Advanced Technologies for Communications (ATC)*. IEEE, 2015, pp. 651–656.

[147] J. A. Hussein, S. S. Ikki, S. Boussakta, and C. Tsimenidis, "Impact of co-channel interference on an underlay cognitive radio network over nakagami-m fading channels," pp. 1–7, 2017.

[148] K. O. Geddes, S. R. Czapor, and G. Labahn, *Algorithms for Computer Algebra*. Boston: Kluwer, 1992.

[149] M. Broy, "Software engineering—from auxiliary to key technologies," in *Software Pioneers*, M. Broy and E. Denert, Eds. New York: Springer, 1992, pp. 10–13.

[150] R. S. Seymour, Ed., *Conductive Polymers*. New York: Plenum, 1981.

[151] S. E. Smith, "Neuromuscular blocking drugs in man," in *Neuromuscular junction. Handbook of experimental pharmacology*, E. Zaimis, Ed., vol. 42. Heidelberg: Springer, 1976, pp. 593–660.

[152] S. T. Chung and R. L. Morris, "Isolation and characterization of plasmid deoxyribonucleic acid from streptomyces fradiae," 1978, paper presented at the 3rd international symposium on the genetics of industrial microorganisms, University of Wisconsin, Madison, 4–9 June 1978.

[153] Z. Hao, A. AghaKouchak, N. Nakhjiri, and A. Farahmand, "Global integrated drought monitoring and prediction system (gidmaps) data sets," 2014, figshare https://doi.org/10.6084/m9.figshare.853801.

[154] S. A. Babichev, J. Ries, and A. I. Lvovsky, "Quantum scissors: teleportation of single-mode optical states by means of a nonlocal single photon," 2002, preprint at https://arxiv.org/abs/quant-ph/0208066v1.

[155] M. Beneke, G. Buchalla, and I. Dunietz, "Mixing induced CP asymmetries in inclusive B decays," *Phys. Lett.*, vol. B393, pp. 132–142, 1997.

[156] B. Stahl, "deepSIP: deep learning of Supernova Ia Parameters," Astrophysics Source Code Library, p. ascl:2006.023, Jun 2020.

[157] H. V. Nguyen, V.-D. Nguyen, and O.-S. Shin, "In-band full-duplex relaying for swipt-enabled cognitive radio networks," *Electronics*, vol. 9, no. 5, p. 835, 2020.

[158] D. Kim, H. Lee, and D. Hong, "A survey of in-band full-duplex transmission: From the perspective of phy and mac layers," *IEEE Communications Surveys & Tutorials*, vol. 17, no. 4, pp. 2017–2046, 2015.

[159] M. K. Slifka and J. L. Whitton, "Clinical implications of dysregulated cytokine production," *J. Mol. Med.*, vol. 78, pp. 74–80, 2000.

[160] L. J. Rodriguez, N. H. Tran, and T. Le-Ngoc, "Optimal power allocation and capacity of full-duplex af relaying under residual self-interference," *IEEE Wireless Communications Letters*, vol. 3, no. 2, pp. 233–236, 2014.

[161] Z. Ding, I. Krikidis, B. Rong, J. S. Thompson, C. Wang, and S. Yang, "On combating the half-duplex constraint in modern cooperative networks: protocols and techniques," *IEEE Wireless Communications*, vol. 19, no. 6, pp. 20–27, 2012.

[162] R. U. Nabar, H. Bolcskei, and F. W. Kneubuhler, "Fading relay channels: Performance limits and space-time signal design," *IEEE Journal on Selected Areas in communications*, vol. 22, no. 6, pp. 1099–1109, 2004.

[163] K. Azarian, H. El Gamal, and P. Schniter, "On the achievable diversity-multiplexing tradeoff in half-duplex cooperative channels," *IEEE Transactions on information theory*, vol. 51, no. 12, pp. 4152–4172, 2005.

[164] S. Yang and J.-C. Belfiore, "Optimal space–time codes for the mimo amplify-and-forward cooperative channel," *IEEE Transactions on information theory*, vol. 53, no. 2, pp. 647–663, 2007.

[165] Y. Fan, C. Wang, J. Thompson, and H. V. Poor, "Recovering multiplexing loss through successive relaying using repetition coding," *IEEE transactions on wireless communications*, vol. 6, no. 12, pp. 4484–4493, 2007.

[166] C. Wang, Y. Fan, J. S. Thompson, M. Skoglund, and H. V. Poor, "Approaching the optimal diversity-multiplexing tradeoff in a four-node cooperative network," *IEEE Transactions on Wireless Communications*, vol. 9, no. 12, pp. 3690–3700, 2010.

[167] E. G. Larsson and B. R. Vojcic, "Cooperative transmit diversity based on superposition modulation," *IEEE Communications Letters*, vol. 9, no. 9, pp. 778–780, 2005.

[168] S. Narayanan, M. Di Renzo, F. Graziosi, and H. Haas, "Distributed spatial modulation for relay networks," in *2013 IEEE 78th Vehicular Technology Conference (VTC Fall)*. IEEE, 2013, pp. 1–6.

[169] ——, "Distributed spatial modulation: A cooperative diversity protocol for half-duplex relay-aided wireless networks," *IEEE Transactions on Vehicular Technology*, vol. 65, no. 5, pp. 2947–2964, 2015.

[170] S. Hong, J. Brand, J. I. Choi, M. Jain, J. Mehlman, S. Katti, and P. Levis, "Applications of self-interference cancellation in 5g and beyond," *IEEE Communications Magazine*, vol. 52, no. 2, pp. 114–121, 2014.

[171] X. Rui, J. Hou, and L. Zhou, "On the capacity of full-duplex relaying with partial relay selection," *Wireless personal communications*, vol. 75, no. 1, pp. 723–728, 2014.

[172] C. Zhong and Z. Zhang, "Non-orthogonal multiple access with cooperative full-duplex relaying," *IEEE Communications Letters*, vol. 20, no. 12, pp. 2478–2481, 2016.

[173] X. Yue, Y. Liu, S. Kang, A. Nallanathan, and Z. Ding, "Outage performance of full/half-duplex user relaying in noma systems," in *2017 IEEE International Conference on Communications (ICC)*. IEEE, 2017, pp. 1–6.

[174] B. Wang and K. R. Liu, "Advances in cognitive radio networks: A survey," *IEEE Journal of selected topics in signal processing*, vol. 5, no. 1, pp. 5–23, 2010.

[175] C. K. De, R. K. Sinha, and S. Kundu, "Cooperative spectrum sensing with multi antenna based decode-and-forward relay," in *2014 Annual IEEE India Conference (INDICON)*. IEEE, 2014, pp. 1–6.

[176] C. K. De and S. Kundu, "Adaptive decode-and-forward protocol-based cooperative spectrum sensing in cognitive radio," *International Journal of Communication Networks and Distributed Systems*, vol. 14, no. 2, pp. 117–133, 2015.

[177] D. Samanta, J. Kumar Bag, C. Kumar De, and A. Chandra, "A smart spectrum utilization approach using multiantenna-based cognitive relays in cognitive radio network," *International Journal of Communication Systems*, vol. 34, no. 1, p. e4671, 2021.

[178] Y. Meng, H. Wang, and S. Xu, "Transmission performance analysis of cognitive noma with swipt over nakagami-m fading channels," in *2019 IEEE 19th International Conference on Communication Technology (ICCT)*, 2019, pp. 770–775.

[179] D. Datla, A. M. Wyglinski, and G. J. Minden, "A spectrum surveying framework for dynamic spectrum access networks," *IEEE Transactions on Vehicular Technology*, vol. 58, no. 8, pp. 4158–4168, 2009.

[180] H. Islam, Y.-c. Liang, and A. T. Hoang, "Joint power control and beamforming for cognitive radio networks," *IEEE transactions on wireless communications*, vol. 7, no. 7, pp. 2415–2419, 2008.

[181] D. W. K. Ng, E. S. Lo, and R. Schober, "Multiobjective resource allocation for secure communication in cognitive radio networks with wireless information and power transfer," *IEEE transactions on vehicular technology*, vol. 65, no. 5, pp. 3166–3184, 2015.

[182] K. Zheng, W. Sun, X. Liu, D. Zhao, Y. Xu, and J. Liu, "Throughput maximisation for multi-channel energy harvesting cognitive radio networks with hybrid overlay/underlay transmission," *IET Communications*, vol. 16, no. 3, pp. 274–290, 2022.

[183] A. A. Nasir, H. D. Tuan, T. Q. Duong, and H. V. Poor, "Uav-enabled communication using noma," *IEEE Transactions on Communications*, vol. 67, no. 7, pp. 5126–5138, 2019.

[184] D. Samanta, C. K. De, and A. Chandra, "Performance analysis of full-duplex multirelaying energy harvesting scheme in presence of multiuser cognitive radio network," *IEEE Transactions on Green Communications and Networking*, vol. 7, no. 2, pp. 626–634, 2022.

[185] W. Afifi and M. Krunz, "Incorporating self-interference suppression for full-duplex operation in opportunistic spectrum access systems," *IEEE Transactions on Wireless Communications*, vol. 14, no. 4, pp. 2180–2191, 2014.

[186] Y. Sun, D. W. K. Ng, N. Zlatanov, and R. Schober, "Robust resource allocation for full-duplex cognitive radio systems," in *2016 24th European Signal Processing Conference (EUSIPCO)*. IEEE, 2016, pp. 773–777.

[187] G. Zheng, I. Krikidis, and B. orn Ottersten, "Full-duplex cooperative cognitive radio with transmit imperfections," *IEEE Transactions on Wireless Communications*, vol. 12, no. 5, pp. 2498–2511, 2013.

[188] D. Xu, X. Yu, Y. Sun, D. W. K. Ng, and R. Schober, "Resource allocation for irs-assisted full-duplex cognitive radio systems," *IEEE Transactions on Communications*, vol. 68, no. 12, pp. 7376–7394, 2020.

[189] J. Kumar Bag, D. Samanta, C. Kumar De, and A. Chandra, "Outage and throughput performance analysis of smart uav-assisted full-duplex noma-based energy harvesting cognitive radio networks," *International Journal of Communication Systems*, vol. 37, no. 6, p. e5698, 2024.

[190] Y. Yang, J. Xu, G. Shi, and C.-X. Wang, "5g wireless systems," *Wireless Networks*, 2018.

[191] A. Papoulis, *Random variables and stochastic processes*. McGraw Hill, 1965.

[192] D. Samanta, J. Kumar Bag, C. Kumar De, and A. Chandra, "Performance analysis of energy harvesting-based relay-assisted cr network under co-channel interference environment," in *International Conference on Communication, Devices and Computing*. Springer, 2023, pp. 685–705.

[193] D. Samanta, C. K. De, and A. Chandra, "Performance analysis of energy harvesting-based cr network assisted by full-duplex relays under joint underlay/overlay mode," in *International Conference on Communication, Devices and Computing*. Springer, 2023, pp. 617–631.

[194] D. Samanta, J. K. Bag, C. K. De, and A. Chandra, "Performance analysis of full-duplex relay aided multi-primary cr network under non-linear energy-harvesting environment," in *2024 IEEE Calcutta Conference (CALCON)*. IEEE, 2024, pp. 1–6.

[195] D. Samanta, C. K. De, and A. Chandra, "Performance analysis of noma based hybrid cognitive radio network assist by full-duplex relay," *Telecommunication Systems*, vol. 88, no. 1, p. 37, 2025.

Dipak Samanta
05/12/25